D4.4: Experimental validation of IDEALIST network prototypes: results and analysis

Status and Version:	1.0	
Date of issue:	13/11/2015	
Distribution:	Public	
Author(s):	Name	Partner
	Arnaud Dupas	ALBLF
	Patricia Layec	ALBLF
	Sébastien Bigo	ALBLF
	Sergio Belotti	ALU-I
	Filippo Cugini	CNIT
	Gianluca Meloni	CNIT
	Francesco Paolucci	CNIT
	Luca Potì	CNIT
	Nicola Sambo	CNIT
	Antonio Napoli	Coriant DE
	Marc Bohn	Coriant DE
	Ramon Casellas	CTTC
	Ricardo Martinez	CTTC
	Raul Muñoz	CTTC
	Ricard Vilalta	CTTC
	Javier Vílchez	CTTC
	Antonio D'Errico	TEI
	Annachiara Pagano	TI
	Emilio Riccardi	TI
	Roberto Morro	TI
	Talha Raman	TU/e
	Huug de Waardt	TU/e
	Chigo Okonkwo	TU/e
	Juan Pedro Fernández-Palacios	TID
	Óscar González De Dios	TID

	Victor Lopez	TID
	Emilio Hugues-Salas	UNIVBRIS
	Georgios Zervas	UNIVBRIS
	Dimitra Simeonidou	UNIVBRIS
	Shuangyi Yan	UNIVBRIS
	Yi Shu	UNIVBRIS
	Yan Yan	UNIVBRIS
	Reza Nejabati	UNIVBRIS
	Bingli Guo	UNIVBRIS
	Shuping Peng	UNIVBRIS
	Jaume Comellas	UPC
	Lluis Gifre	UPC
	Gabriel Junyent	UPC
	Marc Ruiz	UPC
	Luis Velasco	UPC
	Markus Nölle	HHI
	Pablo Wilke Berenguer	HHI
	Sergio López-Buedo	NAU
	Gabriele Galimberti	CISCO
Checked by:	Óscar González de Dios	TID
	Mike Parker	LEX

Table of Contents

1 Introduction 11

1.1 Purpose and Scope 11

1.2 Reference Material 11
1.2.1 Reference Documents 11
1.2.2 Acronyms 15

1.3 Document History 19

1.4 Document overview 21

2 Description of the Integrated IDEALIST network 21

2.1 Components and DCN addressing 22

3 Experimental IDEALIST Network Prototypes 24

3.1 E1: E2E service provisioning in multi-vendor / multi-domain networking 28
3.1.1 Description of the setup 29
3.1.1.1 Flexgrid Domain 29
3.1.1.2 Multi-vendor Flexgrid domain 30
3.1.1.3 Emulated Flexgrid domain 31
3.1.1.4 Hierarchical Stateful PCE and ABNO Controller 32
3.1.1.5 Planning tool 32
3.1.2 Attained results 32
3.1.2.1 Control plane evaluation 32
3.1.2.2 ALU-UNIVBRIS optical performance 33
3.1.2.3 Multi-vendor flexgrid interoperability performance 33
3.1.3 Analysis of the results 34

3.2 E2: GMPLS/PCE control of National Spanish Flexgrid network with MF-OTPs 34
3.2.1 Description of the setup 35
3.2.2 Obtained results 36
3.2.3 Analysis of the results 37

3.3 E3: Use of front-end and back-end PCE: Defragmentation 38

3.4 E4: Use of front-end and back-end PCE: Modulation format-aware re-optimization 38

3.5 E5. Multi-domain Flexgrid network control based on Hierarchical PCE with BGP-LS 39
3.5.1 Description of the setup 40
3.5.2 Attained results 40
3.5.2.1 Performance evaluation and analysis of SL-E2E 40
3.5.2.2 Performance Evaluation and analysis of SF-PD 42
3.5.3 Analysis of the results 43

3.6 E6-E7. Integrated control with BVT and flexible EXCs 43
3.6.1 Preliminary Test/Integration of the BVT and OTN Controller (in Paris) 44

3.6.2 Final Integration of Metro/Core Border Node (in Bristol) 45
3.6.3 Attained results 46
3.6.4 Analysis of the results 48

3.7 E8. Provisioning multicast connectivity in single-layer and multi-layer networks 48

3.8 E9. Nonlinear pre-distortion of electrical driving signals in optical transmitters 49
3.8.1 Description of the setup 50
3.8.2 Attained results 50
3.8.3 Analysis of the results 52

3.9 E10. Super-channel Provisioning up to 1Tb/s 52
3.9.1 Description of the setup 53
3.9.2 Attained results 54
3.9.3 Analysis of the results 57

3.10 E11. Multi-wavelength sliceable provisioning 57
3.10.1 Description of the setup 57
3.10.2 Attained results 59
3.10.3 Analysis of the results 60

3.11 E12. Differentiated filtering and Super-Filter 61
3.11.1 Description of the setup 61
3.11.2 Attained results 62
3.11.3 Analysis of the results 67

3.12 E13. Elastic Operations and Shifting 67
3.12.1 Description of the setup 68
3.12.2 Attained results 70
3.12.3 Analysis of the results 74

3.13 E14. Monitoring and Modulation Format/Code Rate Adaptation 75
3.13.1 Description of the setup 75
3.13.2 Attained results 76
3.13.3 Analysis of the results 79

3.14 E15. Long Term Channel Overlap 80
3.14.1 Description of the setup 80
3.14.2 Attained results 81
3.14.3 Analysis of the results 82

3.15 E16. CNIT/Ericsson - Coriant Transponder Interoperability 82
3.15.1 Description of the setup 83
3.15.2 Attained results 83
3.15.3 Analysis of the results 84

3.16 E17. Dynamic Bandwidth Allocation 84
3.16.1 Description of the setup 84
3.16.2 Attained results 86

3.17 E18. Fixed-Grid/Flexgrid Data Plane Interoperability Experiment 87
3.17.1 Description of the setup 88
3.17.2 Attained results and analysis 88

3.18 E19. Field trial with Orange Telecom (in collaboration with the EU project SASER) 90
3.18.1 Description of the setup 91

3.18.2 Attained results 91
3.18.3 Analysis of the results 91
3.19 E20. Field trial between Coriant and TeliaSonera International Carrier over Pan-European optical network 92
3.19.1 Description of the setup 92
3.19.2 Attained results 92
3.19.3 Analysis of the results 92
3.20 E21. High capacity high order modulation formats field trials 93
3.20.1 Description of the setup 93
3.20.2 Expected results 95
3.21 E22. Multi-layer use-cases with ANM 96
3.21.1 Description of the setup 96
3.21.2 Attained results 97
3.21.3 Analysis of the results 98
3.22 E23. IPoDWDM Hybrid control plane tests 98
3.22.1 Description of the test setups 99
3.22.2 Test Coverage 101
3.22.2.1 IP and Optical Topology retrieved by MATE 101
3.22.2.2 Service Design (IP + Optical) done by MATE 102
3.22.2.3 Service Deployment (IP + Optical network) done by MATE 102
3.22.2.4 Service Deployment (IP + Optical network) done by MATE with optical path diversity 103
3.22.2.5 Restoration driven by GMPLS 103
3.22.2.6 Circuit/Service re-optimization done my MATE 104
3.22.3 Attained results and Test Matrix 104
4 Conclusions, general analysis and final recommendations 105
4.1 Software-driven flexgrid BVT node 105
4.2 Metro-core border node 106
4.3 Ultra-high capacity flexgrid node 107
4.4 Control and management plane 108
4.5 Network and service interworking 109
4.6 Data Plane Interoperability 109

Executive summary

The key objective behind IDEALIST is to research in detail the most promising technology to meet the demands of the next generation optical transport network. To address this, IDEALIST proposes an Elastic Optical Network (EON) architecture, based on the combination of new technologies such as Sliceable Bandwidth Variable Transponders (S-BVT), flexgrid transmission and switching technologies, capable of fulfilling the requirements in terms of capacity and dynamicity, over both time and direction, of future core networks. The intention is that all the solutions investigated and developed in IDEALIST are easily standardised and industrialised. According to it, the EON architecture of IDEALIST is based on four key elements:

- Data plane: Node architectures and transport systems enabling flexible adaptation on transmission conditions in the network and switching concepts beyond 100 Gbps per channel.
- Control plane: Control plane extensions for multi-vendor EON including multi-domain and multi-layer aspects.
- Network and service interworking: Dynamic network resources allocation at both IP and elastic optical layers according to traffic patterns behaviour.
- Network architecture design: Multilayer network optimization tools enabling both off-line planning and on-line re-optimization in EON.

The work carried out in IDEALIST WP4 is focused on the implementation, validation, and performance analysis of the several solutions proposed through by WP1, WP2 and WP3 in the project. A key factor to achieve this goal is the realization of a suitable testbed where it is possible to perform experiments to validate the concepts studied and designed in IDEALIST. In this sense, IDEALIST WP4 has succeeded at building a pan-European testbed, “the integrated IDEALIST network”, which interconnects all the components developed in the project, both hardware and software. An especial effort, beyond the initial expectancies of the project was made to further integrate the hardware elements. For instance, as a result of this, in the laboratories of Pisa and Bristol the switching elements, S-BVTs, Optical Transport Network (OTN) matrix and control plane were put together to perform the proof of concept of the multi-domain, multi-vendor EON envisioned by IDEALIST. The control and management plane was tested at large, with numerous experiments showing a robust behavior an unprecedented degree, of interoperability, unusual for research projects. This has allowed that some of the extensions developed in WP3 to advance thoroughly in the standardization process, which extremely values interoperability demonstrations.

This deliverable starts with the description of the aforementioned integrated IDEALIST network, resulting from the interconnection of the different WP4 network prototypes. The testbed is physically distributed across Europe, with labs in Madrid, Barcelona, Bristol, Pisa, Vimercate, Paris and Munich, and the locations of all the components and their addressing are presented. The testbed encompasses three flexgrid domains with different capabilities; one Hierarchical Path Computation Element (H-PCE); an Application-Based Network Operations (ABNO) controller for orchestrating all operations in the different domains; and the PLATON planning tool for optical networks that, knowing the network topology as well as the current connection status, is able to run different easily customizable optimization algorithms.

A set of experiments were defined in deliverable D4.3 [58], to be performed in WP4 during the last months of the project (although some results that had been obtained by preliminary tests performed on some of implemented components were also reported), with the aim at validating the IDEALIST technologies and solutions designed in WP2 and WP3, and according to the use-cases and requirements defined in WP1. The reported list was ranging from experiments that involve single partners and/or features up to the final "global" demo that was shown during ECOC'15 (to with experiment E1 refers).

Now, in this D4.4 document, all the experiments (going from E1 to E23) are finally reported by describing, in each case, the details of the experimental setup deployed as a portion of the integrated IDEALIST network, the main objectives proposed, the results obtained, and the performance analysis. At the beginning of each experiment subsection there is a table associating the use-cases that are experimentally covered, with the building-blocks implemented in the project that are used in each use-case. It is then easily deduced that the table in experiment E1 subsection includes all the blocks designed and implemented in IDEALIST project, being hardware or software.

Table 1 summarizes the association between all the experimental use-cases demonstrated, through adding the individual contributions from the experiments (ranging from E1 to E23), and all the IDEALIST building-blocks implemented in WP4. Furthermore, Table 1 is the "experimental version" aligned to the "generic" table of associations (use-cases with building-blocks defined in WP1) of the project presented in D1.6 (see [59], Table 13). So, it has been made a great effort in WP4 to cover the maximum number of use-cases and components experimentally, providing also feedback to WP1.

The experimental use-cases and their reference to the WP1 definition in D1.6 are listed below:

- Resource allocation in EON: It is defined in D1.6, section 3.2.1, and demonstrates algorithmic solution and basic findings for an optical network of known topology (fibres and flexgrid switches are already in place) and traffic that uses flexgrid switches and tunable transponders BVTs. Given the traffic, the network is planned by deciding the placement of transponders and regenerators and their configuration to connections.
- Off-line Planning and Provisioning: It is covered in section 3.2.3. Apart from the use of the flexgrid switches, EONs utilize BVTs that can be configured tuning a number of transmission parameters. Thus network planning, in addition to calculating routes and assigning spectrum to connections, has to decide on configurations of the elastic transponders
- Optical restoration after fibre breaks: It appears in section 3.3.1 and demonstrates EON solution with restoration so that failed demands are re-assigned (if possible) following a fibre cut. As a simple example, following a fibre cut, BVTs can adjust their characteristics to fit the new protection path, enabling higher resource utilization and reducing cost. This section takes these simple
- Optical restoration in IP networks: It is studied in section 3.3.3. EONs are expected to feature not only a flexible channel grid, but also to provide rate-adaptive transceivers. One important use case for such kind of flexrate transceiver technology is the coordinated recovery from optical network failures comprising optical restoration together with packet layer recovery mechanisms.
- OTN over optical grooming: It is explained in section 3.4.2. In wavelength switched optical networks several techniques have been proposed to increase resource utilization by means of traffic grooming. Traffic grooming aims at maximizing switch port

and link capacity utilization by appropriately routing traffic flows to pre-selected points in the network and aggregating them so that they can share common paths. In this use-case, the routing is a combination of OTN grooming assisted by optical bypassing.

- IP over optical planning: It appears in section 3.4.3. Flexgrid technology provides a finer optical spectrum granularity, and allows a new flatter multi-layer approach: IP/MPLS routers equipped with S-BVTs are connected to Bandwidth Variable-Optical Cross Connect (BV-OXC), transforming the multi-layer approach into a single-layer approach where a number of IP/MPLS metro area networks performing aggregation are connected through a flexgrid-based core network.
- IP over optical control: It is presented in section 3.4.4. Elastic data plane solutions proposed in IDEALIST (S-BVTs, elastic OTN/Flexgrid grooming, etc) can be configured by software enabling the following scenarios: dynamic multi-flow and bandwidth allocation, automatic IP link provisioning, automatic IP link provisioning, flexible router interface and multi-layer restoration.
- Dynamic provisioning including DC interconnection: It is described in section 3.5.1. Inter-data centre (DC) traffic highly varies over time as a result of performing elastic DC operations. To improve resource utilization and save costs, dynamic and elastic connectivity is clearly needed. One of the main advantages of flexgrid is the capability to allocate spectrum in a flexible way to fit bandwidth demands. Routing and Spectrum Allocation (RSA) algorithms are needed to find a feasible route and spectrum allocation for a given connection request. In addition, elasticity, i.e., increasing/decreasing the slot width of an existing lightpath e.g., by adding or releasing sub-carriers, according to traffic demands, is also required.
- Dynamic defragmentation and re-optimization: Is in covered in section 3.5.2. We consider an elastic network in which during its operations new connections are established and torn down dynamically. In contrast to traditional Wavelength Division Multiplexing (WDM) networks, where spectrum assignment is uniform (in the form of wavelengths), in EONs the spectrum eventually becomes fragmented, a problem that becomes more severe as time progresses, leading to inefficient spectrum utilization. To address this problem we have developed a Dynamic RSA (D-RSA) algorithm for serving new demands in an elastic optical network that (reactively) de-fragments the spectrum and re-optimizes the network when a new connection cannot be served. The goal is to re-optimize the network, provision the new demand and minimize the changes made in the network.
- Dynamic re-optimization after link failure repairs: It is described in section 3.5.3. We studied the effects of re-optimizing the lightpath connections after a link failure has been repaired (namely, the AFRO problem) as an effective way for both reducing and balancing capacity usage and, by these means, for improving network performance.
- Sliceability in multi-path and Sliceability in multi-cast: These use-cases are covered in section 3.7, in which advantages achievable by adding the sliceability property to a BVT have been proven. In particular, the advantages of deploying S-BVTs under the static traffic assumption in some simple scenarios are analyzed.
- Ultra-high capacity and long-reach transmission. This is a new experimental use-case defined in WP4, in order to demonstrate advanced transmission schemes designed in WP2, enabling ultra-high capacity and long reach: pre-distortion, filtering, Field Trial, and High capacity high order modulation formats.

- Multi-vendor and multi-technology interoperability: Another experimental use-case defined in WP4 to cope with these isssues.

With respect to the definition of the different building-blocks, a detailed explanation is available in section 4.5 of D1.6.

	IDEALIST Building Blocks							
Experimental Use-cases	Algorithm suite (off-line and on-line)	Performance metrics for network modeling and experiments	Planning Tools for EON	BVT and S-BVT	Elastic OTN grooming	Flexgrid ROADM and BV-OXC	GMPLS and OFP extensions for flexgrid	Network Orchestrator (ABNO)
Resource allocation in EON	X	X		X		X	X	X
Off-line Planning and Provisioning	X	X	X		X		X	X
Optical restoration after fibre breaks	X	X		X		X	X	X
Optical restoration in IP networks	X			X		X	X	
OTN over optical grooming	X	X		X	X	X		
IP over optical planning	X		X	X	X	X	X	
IP over optical control	X	X		X	X	X	X	X
Dynamic provisioning including DC interconnection	X	X		X	X	X	X	X
Dynamic defragmentation and re-optimization	X	X	X	X	X	X	X	X
Dynamic re-optimization after link failure repairs	X		X			X	X	X
Sliceability in multi-path	X	X		X		X	X	
Sliceability in multicast	X		X				X	X
Ultra-high capacity and long-reach transmission	X	X		X		X		
Multi-vendor and multi-technology interoperability	X	X		X		X	X	X

Table 1: Experimental Use-cases and IDEALIST Building Blocks

Finally, Table 2 summarizes the association between all the experiments conducted in IDEALIST and the experimental building-blocks required in each experiment:

	IDEALIST Building Blocks							
Experiments	Algorithm suite (off-line and on-line)	Performance metrics for network modeling and experiments	Planning Tools for EON	BVT and S-BVT	Elastic OTN grooming	Flexgrid ROADM and BV-OXC	GMPLS and OFP extensions for flexgrid	Network Orchestrator (ABNO)
E1	X	X	X	X	X	X	X	X
E2	X	X					X	
E3	X		X				X	X
E4	X		X				X	X
E5	X	X					X	X
E6-E7	X	X		X	X	X	X	
E8	X		X				X	X
E9	X	X		X				
E10	X	X		X		X	X	
E11	X	X		X		X	X	
E12	X	X		X		X	X	
E13	X	X		X		X	X	
E14	X	X		X		X	X	
E15	X	X		X			X	
E16	X	X		X		X	X	
E17	X	X						X
E18		X		X		X		
E19	X	X		X		X		
E20	X	X		X		X		
E21	X	X		X		X		
E22	X					X	X	X
E23	X	X	X			X	X	

Table 2: Experiments and IDEALIST Building Blocks

1 Introduction

1.1 Purpose and Scope

The purpose of this deliverable D4.4 is to provide an upgraded description of the experimental prototypes that integrate the IDEALIST testbed that is physically distributed across Europe, providing more specific details on the network locations, connectivity and configuration. In addition, the document reports and analyses the final results attained from the different experiments conducted within the IDEALIST context, integrating the implementations of the adaptive network manager, the multi-domain control plane, and the different node prototypes that in turn provide the integration solutions for the data and control planes, and data plane interoperability.

1.2 Reference Material

1.2.1 Reference Documents

[1] Ll. Gifre, M. Tornatore, L. M. Contreras, B. Mukherjee, L. Velasco, "ABNO-driven Content Distribution in the Telecom Cloud", accepted in Elsevier Optical Switching and Networking, 2016.

[2] A. Castro, Ll. Gifre, C. Chen, J. Yin, Z. Zhu, L. Velasco, S. J. B. Yoo, "Experimental Demonstration of Brokered Orchestration for end-to-end Service Provisioning and Interoperability across Heterogeneous Multi-Operator (Multi-AS) Optical Networks", in Proc. . 41st European Conference on Optical Communication (ECOC), September 2015, Valencia.

[3] L. Velasco, Ll. Gifre, "iONE: A Workflow-Oriented ABNO Implementation", in Photonics in Switching (PS) Conference, September 2015, Florence.

[4] M. Ruiz, L. Velasco, "Serving Multicast Requests on Single Layer and Multilayer Flexgrid Networks", IEEE/OSA Journal of Optical Communications and Networking (JOCN), vol. 7, pp. 146-155, 2015.

[5] Ll. Gifre, F. Paolucci, O. González de Dios, L. Velasco, L. M. Contreras, F. Cugini, P. Castoldi, V. López, "Experimental Assessment of ABNO-driven Multicast Connectivity in Flexgrid Networks", (Invited Paper) IEEE/OSA Journal of Lightwave Technology (JLT), vol. 33, pp. 1549-1556, 2015.

[6] R. Martínez, R. Casellas, R. Vilalta, R. Muñoz, “GMPLS/PCE-controlled Multi-Flow Optical Transponders in Elastic Optical Networks [Invited]”, (Invited Paper) IEEE/OSA Journal of Optical Communications and Networking (JOCN), Vol. 7, Issue 11, pp.B71-B80, 2015.

[7] R. Casellas, R. Martínez, R. Muñoz, R. Vilalta, Lei Liu, “Control and Orchestration of Multi-domain Optical Networks with GMPLS as Inter-SDN Controller Communication”, (Invited Paper) IEEE/OSA Journal of Optical Communications and Networking (JOCN), OFC2015 Special Issue, Vol. 7, Issue 11, pp. B46-B54.

[8] O. González de Dios, R. Casellas, R. Morro, F. Paolucci, V. López, R. Martínez, R.Muñoz, R. Vilalta, P. Castoldi, “Multi-partner Demonstration of BGPLS enabled multi-domain EON control and instantiation with H-PCE”, IEEE/OSA Journal of Optical Communications and Networking (JOCN), OFC2015 Special Issue, Vol. 7, Issue 11.

[9] Ll. Gifre, R. Martínez, R. Casellas, R. Vilalta, R. Muñoz, L. Velasco, “Modulation Format-aware Re-Optimization in Flexgrid Optical Networks: Concept and Experimental Assessment,” in Proc. 41st European Conference on Optical Communication (ECOC),

September 2015, Valencia.

[10] O. González de Dios, R. Casellas, F. Paolucci, A. Napoli, Ll. Gifre, S. Annoni, S. Belotti, U. Feiste, D. Rafique, M. Bohn, S. Bigo, A. Dupas, E. Dutisseuil, F. Fresi, B. Guo, E. Hugues, P. Layec, V. López, G. Meloni, S. Misto, R. Morro, T. Rahman, G. Khanna, R. Martínez, R. Vilalta, F. Cugini, L. Poti, A. D'Errico, R. Muñoz, Y. Shu, S. Yan, Y. Yan, G. Zervas, R. Nejabati, D. Simeonidou, L. Velasco, J. Fernández-Palacios, "First Demonstration of Multi-vendor and Multi-domain EON with S-BVT and Control Interoperability over Pan-European Testbed," in Proc. 41st European Conference on Optical Communications (ECOC), Post-deadline session PDP4.1, September 2015, Valencia.

[11] A. Mayoral, R. Vilalta, R. Casellas, R. Muñoz, R. Martínez, "Traffic Engineering enforcement in multi-domain SDN orchestration of Multi-Layer (packet/optical) networks," in Proc. 41st European Conference on Optical Communication (ECOC), September 2015, Valencia.

[12] R. Casellas, R. Muñoz, R. Vilalta, R. Martínez, "Inter DC orchestration solutions and overarching control: towards a 5G integration," Symposium Optical Communications and Networks for Datacentres within the 41st European Conference on Optical Communication (ECOC), September 2015, Valencia.

[13] Ll. Gifre, M. Ruiz, A. Asensio, L. Velasco, "Comparing Single Layer and Multilayer Approaches to Serve Multicast Requests on Flexgrid Networks," in Proc. IEEE International Conference on Transparent Optical Networks (ICTON), July 2015, Budapest.

[14] Ll. Gifre, N. Navarro, A. Asensio, M. Ruiz, L. Velasco, "iONE: An Environment for Experimentally Assessing In-Operation Network Planning Algorithms," in Proc. IEEE International Conference on Transparent Optical Networks (ICTON), July 2015, Budapest.

[15] R. Casellas, R. Vilalta, R. Muñoz, R. Martínez, "Smart Cities, IoT, SDN, 5G Networks, Cloud Computing…Managing Complexity with SDN Orchestration. Service & Content Provider's Perspective of Smart Cities – How to enrich citizen experience using a pervasive urban SDN connectivity environment," The Software Defined Network – Programmable City Workshop (BiO/ONF), July 2015, Bristol.

[16] R. Casellas, R. Muñoz, R. Martínez, R. Vilalta, A. Mayoral, Lei Liu, T. Tsuritani, I. Morita, "Overarching Control of Flexi Grid Optical Networks: Interworking of GMPLS and OpenFlow Domains," IEEE/OSA Journal of Lightwave Technology, Vol. 33, Issue 5, pp. 1054-1062, 2015.

[17] Ll. Gifre, F. Paolucci, J. Marhuenda, A. Aguado, L. Velasco, F. Cugini, P. Castoldi, O. Gonzalez de Dios, L.M. Contreras, V. López, "Experimental Assessment of Inter-datacentre Multicast Connectivity for Ethernet services in Flexgrid Networks," in Proc. European Conference on Optical Communication (ECOC), September 2014, Cannes.

[18] R. Martínez, Ll. Gifre, R. Casellas, L. Velasco, R. Muñoz, R. Vilalta, "Experimental Validation of Active Frontend - Backend Stateful PCE Operations in Flexgrid Optical Network Re-optimization," in Proc. European Conference on Optical Communication (ECOC), September 2014, Cannes.

[19] Ll. Gifre, L. Velasco, N. Navarro, G. Junyent, "Experimental Assessment of a High Performance Back-end PCE for Flexgrid Optical Network Re-optimization," in Proc. IEEE/OSA Optical Fibre Communication Conference (OFC), March 2014, San Francisco.

[20] Ll. Gifre, F. Paolucci, A. Aguado, R. Casellas, A. Castro, F. Cugini, P. Castoldi, L. Velasco, V. López, "Experimental Assessment of In-Operation Spectrum Defragmentation," (Invited Paper) Springer Photonic Network Communications, vol. 27, pp. 128-140, 2014.

[21] Ll. Gifre, L. Velasco, and N. Navarro, "Architecture of a Specialized Back-end High Performance Computing-based PCE for Flexgrid Networks," in Proc. IEEE International Conference on Transparent Optical Networks (ICTON), June 2013, Cartagena.

[22] P. Wilke Berenguer, T. Rahman, A. Napoli, M. Nölle, C. Schubert, J. K. Fischer, “Nonlinear Digital Pre-Distortion of Transmitter Components“, in Proc. ECOC, September 2015, Valencia.

[23] N. Sambo, G. Meloni, F. Paolucci, F. Cugini, M. Secondini, F. Fresi, L. Potì, and P. Castoldi, "Programmable Transponder, Code and Differentiated Filter Configuration in Elastic Optical Networks," J. Lightwave Technol. 32, 2079-2086 (2014).

[24] N. Sambo, G. Meloni, F. Cugini, A. D'Errico, L. Poti, P. Iovanna, P. Castoldi, "Routing, code, and spectrum assignment (RCSA) in elastic optical networks," in Optical Fibre Communications Conference and Exhibition (OFC), 2015, 22-26 March 2015.

[25] N. Sambo, G. Meloni, F. Paolucci, M. Imran, F. Fresi, F. Cugini, P. Castoldi, L. Poti," First demonstration of SDN-controlled SBVT based on multi-wavelength source with programmable and asymmetric channel spacing", in Proc. ECOC 2014.

[26] F. Paolucci, F. Cugini, F. Fresi, G. Meloni, A. Giorgetti, N. Sambo, L. Potí, A. Castro, L. Velasco, and P. Castoldi, "Superfilter Technique in SDN-Controlled Elastic Optical Networks [Invited]," J. Opt. Commun. Netw. 7, A285-A292 (2015).

[27] F. Paolucci et al. , "Active PCE demonstration performing elastic operations and hitless defragmentation in flexible grid optical networks", Photonic Network Communications, Springer, vol. 29, issue 1, pp 57-66, Feb. 2015.

[28] N. Sambo, F. Paolucci, G. Meloni, F. Fresi, L. Potì, and P. Castoldi, "Control of Frequency Conversion and Defragmentation for Super-Channels [Invited]," J. Opt. Commun. Netw. 7, A126-A134 (2015).

[29] F. Cugini, F. Fresi, F. Paolucci, G. Meloni, N. Sambo, A. Giorgetti, T. Foggi, L. Potí, P. Castoldi, "Active stateful PCE with hitless LDPC code adaptation [Invited]," in Optical Communications and Networking, IEEE/OSA Journal of , vol.7, no.2, pp.A268-A276, February 1 2015.

[30] G. Meloni, T. Foggi, F. Paolucci, F. Fresi, F. Cugini, P. Castoldi, G. Colavolpe, and L. Potí, "First Demonstration of Optical Signal Overlap," post-deadline paper at Photonics in Switching 2014, San Diego (CA, USA), in Advanced Photonics for Communications, OSA Technical Digest (online) (Optical Society of America, 2014), paper NM4D.4.

[31] M. Gunkel, A. Mattheus, A. Napoli, G. Meloni, F. Fresi, T. Rahman, "Elastic Black Link for future vendor independent optical networks," in Optical Fibre Communications Conference and Exhibition (OFC), 2015, 22-26 March 2015.

[32] O. Gonzalez de Dios, R. Casellas, R. Morro, F. Paolucci, V. Lopez, R. Martinez, R. Munoz, R. Vilalta, P. Castoldi, "First multi-partner demonstration of BGP-LS enabled inter-domain EON control with H-PCE," in Optical Fibre Communications Conference and Exhibition (OFC), 2015, 22-26 March 2015.

[33] M. Gunkel, A. Mattheus, F. Wissel, A. Napoli, J. Pedro, N. Costa, T. Rahman, G. Meloni, F. Fresi, F. Cugini, N. Sambo, M. Bohn, “Vendor-Interoperable Elastic Optical Interfaces – standards, experiments and challenges,” OSA J. of Optical and Communication Networking [Invited], to appear on, 2016.

[34] T. Rahman, et al., “Record Field Demonstration of C-band Multi-Terabit 16QAM, 32QAM and

64QAM over 762km of SSMF," Optoelectronics and Communications Conference (OECC), 2015.

[35] http://www.coriant.com/products/hit7300.asp

[36] http://www.coriant.com/solutions/cloudwave-optics.asp

[37] ITU-T recommendation "Spectral grids for WDM applications: DWDM frequency grid", G.694.1, 02/2012, www.itu.int

[38] A. Dupas et al., "Real-time Demonstration of Software-defined Elastic Interface for Flexgrid Networks," OFC2015, Los Angeles USA, March 22-26th 2015.

[39] E. Hugues-Sales et al., "Next Generation Optical Nodes: The Vision of the European Research Project IDEALIST," IEEE Comm. Magazine, February 2015. Pp. 172-181.

[40] O. González de Dios, et al., "First Demonstration of Multi-vendor and Multi-domain EON with S-BVT and Control Interoperability over Pan-European Testbed," IEEE / OSA JLT, 2016.

[41] A. Napoli, et al., "Performance dependence of single-carrier digital back-propagation on fibre types and data rates," Optical Fibre Communications Conference and Exhibition (OFC), 2014. IEEE, 2014.

[42] A. Napoli, et al., "On the next generation bandwidth variable transponders for future flexible optical systems," Networks and 6Communications (EuCNC), 2014 European Conference on. IEEE, 2014.

[43] http://www.coriant.com/company/press_release.asp?id=1233

[44] http://www.coriant.com/company/press_release.asp?id=1232

[45] T. Rahman, et al., "Long-haul terabit transmission (2272km) employing digitally pre-distorted quad-carrier PM-16QAM super-channel," European Conf. on Opt. Comm (ECOC), 2014.

[46] D. Rafique, et al., "9.6 Tb/s CP-QPSK Transmission over 6500km of NZ-DSF with Commercial Hybrid Amplifiers." (2015).

[47] A. Napoli, et al., "Novel digital pre-distortion techniques for low-extinction ratio Mach-Zehnder modulators," Optical Fibre Communication Conference (OFC). Optical Society of America, 2015.

[48] A. Napoli, et al., "Novel DAC digital pre-emphasis algorithm for next-generation flexible optical transponders," Optical Fibre Communication Conference (OFC). Optical Society of America, 2015.

[49] T. Rahman, et al., "Ultralong Haul 1.28-Tb/s PM-16QAM WDM Transmission Employing Hybrid Amplification," Journal of Lightwave Technology (JLT) 33.9 (2015): 1794-1804.

[50] T. Rahman, et al., "Experimental Comparison of 1.28 Tb/s Nyquist WDM vs. Time-Frequency Packing," Photonics in Switching (PS), 2015.

[51] O. González de Dios, R. Casellas, Ed., "Famework and requirements for GMPLS-based control of flexi-grid DWDM networks", IETF Draft draft-ietf-ccamp-flexi-grid-fwk, Aug. 2015.

[52] A. Farrel, D. King, Y. Li, F. Zhang, "Generalized labels for the flexi-grid in lambda switch capable (LSC) label switching routers", IETF Draft draft-ietf-ccamp-flexigrid-lambda-label, Sept. 2015.

[53] F. Zhang, X. Zhang, A. Farrel, O. Gonzalez de Dios, D. Ceccarelli, "RSVP-TE signaling extensions in support of flexible grid", IETF Draft draft-ietf-ccamp-flexible-grid-rsvp-te-ext,

Aug. 2015.

[54] X. Zhang, H. Zheng, R. Casellas, O. Gonzalez de Dios, D. Ceccarelli, “GMPLS OSPF-TE extensions in support of flexi-grid DWDM networks”, IETF Draft draft-ietf-ccamp-flexible-grid-ospf-ext, Oct. 2015.

[55] ICT-IDEALIST deliverable D2.2: “Modelling and experimental work on the chosen flexgrid/flexrate technology options”.

[56] ICT-IDEALIST deliverable D3.2: “Design and Evaluation of the Adaptive Network Manager and Functional Protocol Extensions”.

[57] ICT-IDEALIST deliverable D1.5: “Evaluation of flexgrid technologies”.

[58] ICT-IDEALIST deliverable D4.3: “Node prototypes and adaptive network manager prototype implementation”.

[59] ICT-IDEALIST deliverable D1.6: “Lessons and conclusions from elastic optical networks”.

[60] https://github.com/telefonicaid/netphony-network-protocols

[61] https://github.com/telefonicaid/cne-tnetwork

1.2.2 Acronyms

ABNO	Application-Based Network Operations
AC	Application Code
ADC	Analogue-to-Digital Conversion
ADRENALINE	All-optical Dynamic REliable Network hAndLINg IP/Ethernet Gigabit traffic with QoS
AFRO	After Failure Repair Optimization
ANM	Adaptive Network Manager
AoD	Architecture-on-Demand
API	Application Programming Interface
ASE	Amplified Spontaneous Emission
AWGN	Additive White Gaussian Noise
B2B	Back-To-Back
BBF	BroadBand Forum
BER	Bit-Error-Rate
BER_{th}	BER threshold
BGP-LS	Border Gateway Protocol – Link State
BP	Blocking Probability
BV-OXC	Bandwidth Variable - Optical Cross Connect
BV-WSS	Bandwidth Variable – Wavelength Selective Switch

BVT	Bandwidth Variable Transponder
CD	Chromatic Dispersion
CLI	Command Line Interface
CORBA	Common Object Request Broker Architecture
cPCE	Child-PCE
CRS	Carrier Routing System
CTC	Cisco Transport Controller
CTP	Cisco Transport Planner
DA	Differential Drive Amplifier
DAC	Digital-to-Analog Converter
DC	Data Center
DCN	Data Communications and Networking
DP-nQAM	Dual-Polarization Quadrature Amplitude Modulation of n levels
DP-QPSK	Dual-Polarization Quadrature Phase-Shift-Keying
DSP	Digital Signal Processing
DWDM	Dense Wavelength Division Multiplexing
E2E	End-To-End
ECOC'15	European Conference on Optical Communication 2015
EDFA	Erbium Doped Fibre Amplifier
EMS	Element Management System
ENOB	Effective Number Of Bits
EON	Elastic Optical Network
ERO	Explicit Route Object
EXC	Elastic Cross Connect
FEC	Forward Error Correction
FRR	Fast ReRoute
FS	Frequency Slot
GEF	Gain-Equalizing Filter
GMPLS	Generalized multi-Protocol Label Switching
GPIB	General Purpose Interface Bus
GUI	Graphical User Interface
H-PCE	Hierarchical PCE
HT	Holding Time

HTTP	HyperText Transfer Protocol
IETF	Internet Engineering Task Force
IP	Internet Protocol
IPoDWDM	IP over DWDM
IPSec	IP Security
ITU-T	International Telecommunication Union - Telecommunication Standardization Sector
IQ	Phase-Quadrature
JLT	Journal of Lightwave Technology
JOCN	Journal of Optical Communications and Networking
JSON	JavaScript Object Notation
LDPC	Low Density Parity Check
Ln	Layer n
LO	Local Oscillator
LOGO	Local Optimization/Global Optimization
LSP	Label Switched Path
MATE	Multiprotocol Automation and Traffic Engineering
MF-OTP	Multi-Flow Optical Transponder
MLR	Multi-Layer Restoration
MLR-O	Multi-Layer Optical Restoration
MPLS	MultiProtocol Label Switching
MSE	Mean Squared Error
MW	Multi-Wavelength
NCF	Nominal Centre Frequency
NCS2K	Network Convergence System 2000
NE	Network Element
NETCONF	Network Configuration Protocol
NG	Next Generation
nGE	n Gigabit Ethernet
NMS	Network Management System
OAM	Operation Administration and Maintenance
ODL	OpenDayLight
OFP	OpenFlow Protocol
OH	OverHead

OIF	Optical Internetworking Forum
OMA	Optical Modulation Analyser
OSA	Optical Spectrum Analyser
OSNR	Optical Signal-to-Noise Ratio
OSPF-TE	Open Shortest Path First for Traffic Engineering
OTN	Optical Transport Network
OTU	Optical Transport Unit
OTU2	OTU with 10.70-Gb/s data-rate
PAMW	Programmable and Asymmetric Multi-Wavelength
PBC	Polarization Beam Combiner
PCE	Path Computation Element
PCEP	Path Computation Element Communication Protocol
PLATON	Planning Tool for Optical Networks
PM-nQAM	Polarization-Multiplexed Quadrature Amplitude Modulation of n levels
PM-QPSK	Polarization-Multiplexed Quadrature Phase Shift Keying
pPCE	Parent-PCE
QAM	Quadrature Amplitude Modulation
QoT	Quality of Transmission
REST	Representational State Transfer
RMI	Remote Method Invocation
ROADM	Reconfigurable Optical Add Drop Multiplexer
RRC	Root-Raised-Cosine
RSA	Routing and Spectrum Assignment
RSMA	Routing, Spectrum, Modulation Assignment
RSVP-TE	Resource Reservation Protocol for Traffic Engineering
SASER	SAfe and Secure European Routing
S-BVT	Sliceable BVT
SCC	Spectrum Continuity Constraint
SCgC	Spectrum Contiguity Constraint
SD-FEC	Soft Defined FEC
SDN	Software-Defined Networking
SF-PD	StateFul-H-PCE with Per-Domain instantiation and stitching
SL-E2E	StateLess-H-PCE with e2e signaling and instantiation

SNMP	Simple Network Management Protocol
SNR	Signal-to-Noise Ratio
Soft-FBVT	Software-Driven FlexGrid Bandwidth -Variable Transponder
SPRING	Source Packet Routing in Networking
SRLG	Shared Risk Link Groups
SSMF	Standard Single Mode Fibre
SSS	Spectrum Selective Switch
Sub-TLV	Subtype/Length/Value
SW	Software
TC	Transponder Class
TCP	Transmission Control Protocol
TE	Traffic Engineering
TED	Traffic Engineering Database
TFP	Time Frequency Packing
TL-1	Transaction Language 1
TLS	Tunable Laser Source
TLV	Type/Length/Value
UNI	User Network Interface
URL	Uniform Resource Locator
USB	Universal Serial Bus
VNT	Virtual Network Topology
VOA	Variable optical attenuator
WAE	WAN Automation Engine
WSS	Wavelength selective switch
XML	eXtensible Markup Language
XRO	Exclude Route Object
YANG	Yet Another Next Generation

1.3 Document History

Version	Date	Authors	Comment

0.001	22/06/2015	WP4 team, template and ToC prepared by Javier Vílchez	Table of contents and section editors and reviewers.
0.002	26/06/2015	WP4 team, ToC upgraded by Javier Vílchez	ToC upgraded as agreed during the last conf.call
0.003	06/10/2015	UPC, TI, Coriant, CTTC	Contributions to Sections 1.1, 1.3, 1.5, 2 (figures 1,2,3), 3 (table 1), 3.2, 3.3, 3.4, 3.7, 3.8, 3.21
0.004	08/10/2015	CTTC, TID	Tables in Executive Summary (Use cases-Building Blocks, Experiments-Building Blocks) to be completed by all partners. Tables of Use cases-Building Blocks associated to each experiment (each Section 3.x)
0.005	18/10/2015	UPC, TID, UNIVBRIS, HHI, CTTC, CNIT, TEI	Contributions to tables of BB in Executive Summary. Contributions to 1.3.1, 3, 3.x (E2, E3, E4, E7, E8, E9, E10, E11, E12, E13, E14, E15, E18, E22) and 4.1 sections
0.006	24/10/2015	CTTC, Coriant, ALBLF, UNIVBRIS, TI, NAUDIT	Contributions to tables of Exec. Summary, to 1.3, 1.5, 3, 3.x (E6-E7, E16, E17, E19, E20), and 4.2, 4.3, 4.4 sections
0.007	02/11/2015	LEX	Proof-read (English grammar etc.) of v0.006
0.008	12/11/2015	CTTC, Cisco, TID, TI	Contributions to Tables 1&2, Sections 1, 2, 3, 3.1, 3.5, 3.22 (new for experiment E23), 4 and 4.5

1.0	13/11/2015	CTTC	Contributions to Exec. Summary and Acronyms

1.4 Document overview

Following this first section of the document, the deliverable D4.4 is structured as follows:

Section 2 describes the integrated IDEALIST testbed, based on hierarchical module composition ranging from network planning tools to data plane prototypes with interoperability. For the integrated demonstration, details on the testbed locations and connectivity across Europe are given, with the components forming part of the pan-European network at each location also listed. The IDEALIST testbed is divided into multiple domains, which are also presented.

Section 3 reports the set of experiments carried out on the different network prototypes implemented, as introduced previously in the reference [58] (sections 3 and 4). For each experiment that involved a single partner and/or featured in the final "global" demo that was shown during the recent ECOC'15 conference (Valencia, Spain), the main objectives, and recently attained results and analyses are all provided.

Finally, Section 4 provides analyses and general conclusions of the results gained from the experiments, in the context of the overall history of the project. The conclusions are also linked to WP1, as a means to confirm how well the expected results of the project have indeed been achieved through all the various experiments. Finally, recommendations are also provided for each of the main topics of the integrated IDEALIST network.

2 Description of the Integrated IDEALIST network

In order to demonstrate the IDEALIST data and control architecture, an integrated testbed (shown in Figure 1) is built by the interconnection of the different WP4 components, both hardware and software, physically distributed within labs. The testbed encompasses three flexgrid domains with different capabilities, one hierarchical PCE, an ABNO controller and the PLATON planning tool. The domains are interconnected resulting in the inter-domain topology shown in Figure 2.

The planning tool and ABNO controller are used to demonstrate the in-operation network planning concepts. The data components have been deployed in two different labs, one in Bristol and the other in Pisa, integrating components from Paris and Vimercate. The nodes and S-BVT components are aimed at demonstrating the control and data plane Integration, as well as data plane interoperability. Extended information on the integrated testbed components is detailed in section 3.1, where the integrated experiment is explained.

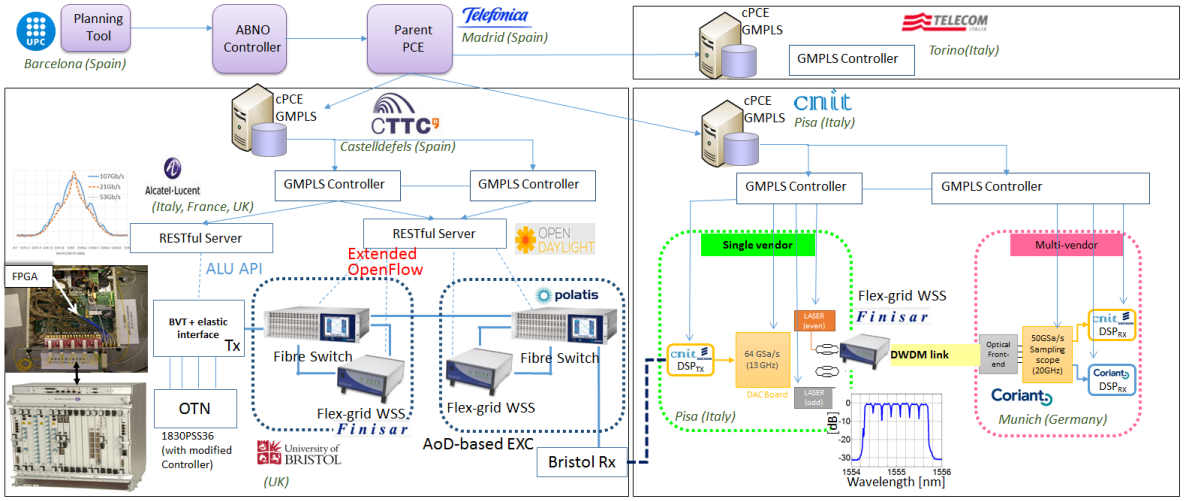

Figure 1: IDEALIST Multi-partner Pan-European Testbed integrating control and data

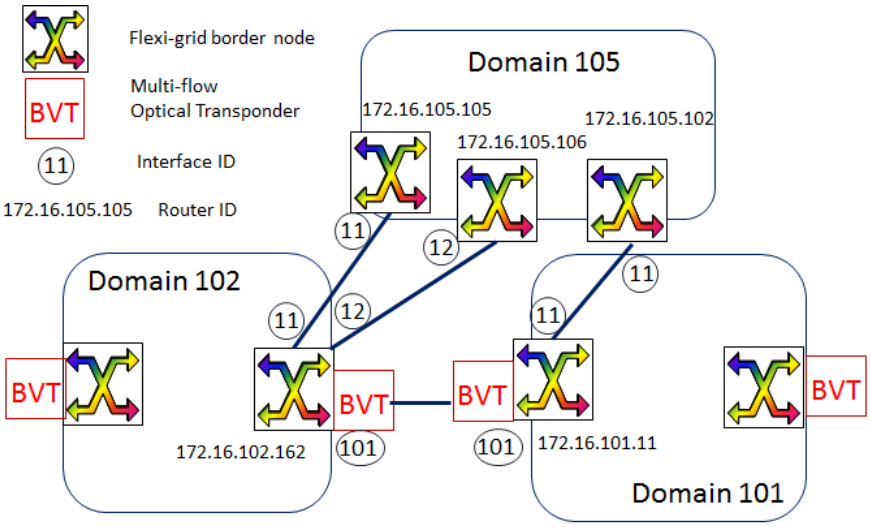

Figure 2: Inter-domain topology

2.1 Components and DCN addressing

The testbed is physically distributed across Europe, with labs in Madrid, Barcelona, Bristol, Pisa, Vimercate, Paris and Munich. All of the locations are connected via IPSec tunnels. For the integrated demonstration, components from Paris have been moved to Bristol, and components from Munich have been moved to Pisa.

The Idealist DCN addressing is as follows:

- CNIT: 172.16.101.0/24
- CTTC: 172.16.102.0/24
- UPC: 172.16.103.0/24
- TID: 172.16.104.0/24
- TI: 172.16.105.0/24

The components of the testbed, with the address and physical location are shown in the table below:

Component	Address	Port	Physical Location	Description
Parent PCE	172.16.104.201	4189 (TCP)	Madrid	Stateful Active parent PCE
Parent PCE BGP-LS speaker	172.16.104.201		Madrid	BGP-LS Speaker attached to the parent PCE
ABNO Controller	172.16.104.203		Madrid	SDN Controller
OAM Handler	172.16.104.203		Madrid	Monitors bandwidth use
Topology Module	172.16.104.203		Madrid	Topology module with TED details
Provisioning Manager	172.16.104.203		Madrid	ABNO Provisioning manager
IDEALIST Testbed GUI	172.16.104.199	80	Madrid	Graphical User Interface URL: http://172.16.104.199/GUI_Platon/frontend.php
PLATON GUI	172.16.104.199	80	Madrid	Graphical User Interface of the Planning tool thttp://172.16.104.199/GUI_Id/frontend.php
Redis	172.16.104.199	6380	Madrid	Redis DataBase
TI Domain Child PCE	172.16.105.103	4189 (TCP)	Turin	Path Computation Element
TI Emulated Node (Roma)	172.16.105.102		Turin	Emulated Control Plane Node
TI Emulated Node (Genova)	172.16.105.105		Turin	Emulated Control Plane Node
TI Emulated Node (Torino)	172.16.105.106		Turin	Emulated Control Plane Node
CTTC Domain PCE	172.16.102.161	4189 (TCP)	Barcelona	Path Computation Element
BGP-LS Speaker of CTTC child PCE	172.16.102.161		Barcelona	BGP-LS Speaker
GMPLS node controller of Bristol Node (1)	172.16.102.161		Barcelona	GMPLS controller remotely connected to Bristol
GMPLS node controller of Bristol	172.16.102.162		Barcelona	GMPLS controller remotely connected to

Node (2)				Bristol
Bristol node 1 (optical switching)		8080 (TCP)	Bristol	REST API to configure switching
Bristol node 2 (optical switching)		8080 (TCP)	Bristol	REST API to configure switching
BVT	-	-	Paris (moved to Bristol)	Sliceable Bandwidth (controlled via REST server)
OTN Matrix	-	-	Paris(moved to Bristol)	(controlled via REST server)
Controller of BVT and OTN Matrix		8080 (TCP)	Vimercate (Italy) (moved to Bristol)	REST Server
CNIT Child PCE	172.16.101.1	4189	Pisa	Pisa
CNIT/Ericsson S-BVT				
Coriant S-BVT			Munich (moved to Pisa)	
PLATON	172.16.103.4	8080	Barcelona	PLATON Planning tool

Table 3: Components and DCN addressing for the integrated demonstration

3 Experimental IDEALIST Network Prototypes

In this section, we detail the set of prototypes and experiments conducted in IDEALIST, and present a table specifying experiment, objectives (link back to D4.3), with brief comments on the results and achievements: validation or performance evaluation.

Experiment	Main Objectives	Results	Section
E1. E2E service provisioning in multi-vendor / multi-domain networking	This experiment aims at setting up an E2E service in the integrated IDEALIST testbed, which includes all the components developed in WP4, in order to demonstrate the feasibility of the overall IDEALIST architecture as defined in WP1.	Experimental proof of concept of IDEALIST data and control architecture. Interoperability between S-BVT implementations.	A demo was shown at ECOC'15 and complete results are reported in Section 3.1
E2. GMPLS/PCE control of National Spanish Flexgrid network with MF-OTPs	Validation of the implemented extensions for GMPLS routing and signaling protocols, and experimental evaluation of the proposed RSMA algorithm in the	Numerical results obtained at the GMPLS control plane of ADRENALINE testbed: experimental Delay and BP results for *partial* and *full* MF-	Preliminary results were reported in [56]. Final results are reported in Section 3.2

	ADRENALINE testbed.	OTPs information models	
E3. Use of front-end and back-end PCE: Defragmentation	Assess the ability of the ABNO architecture to deal with the defragmentation use-case.	Experimental Proof of Concept	Complete results reported in [58]
E4. Use of front-end and back-end PCE: Modulation format-aware re-optimization	Evaluate a modulation format-aware algorithm to re-optimize resource utilization after a link repair	Experimental Proof of Concept	Complete results reported in [58]
E5. Multi-domain Flexgrid network control based on Hierarchical PCE with BGP-LS	Demonstrate multi-domain control plane for EONs.	Control plane interoperability.	Preliminary results reported in [58]. Final results are reported in Section 3.5
E6-E7. Integrated control with BVT and flexible EXCs	Demonstrate B2B and 175-km transmission through 2 nodes within domain 102, using the elastic S-BVT	Performance evaluation using the metro/core border node prototype with integrated control	Results are reported in Section 3.6
E8. Provisioning multicast connectivity in single-layer and multi-layer networks	Demonstrate multicast provisioning on single-layer and multilayer networks.	Experimental Proof of Concept	Complete results reported in [58]
E9. Nonlinear pre-distortion of electrical driving signals in optical transmitters	Demonstrate the possibilities of increasing transponder performance by using pre-distortion techniques.	Implemented pre-distortion techniques are able to significantly increase system performance, especially when using nonlinear pre-distortion algorithms.	Preliminary results reported in [58]. Final results are reported in Section 3.8
E10. Superchannel provisioning up to 1 Tb/s	Soft-FBVT provisioning of configurable superchannel	Performance evaluation, validation, joint control and data plane	Preliminary description in [58] (testbed). Complete description and results in Section 3.9
E11. Multi-wavelength sliceable provisioning	Soft-FBVT provisioning with configurable multi-wavelength source with asymmetric spacing	Performance evaluation, validation, joint control and data plane	Preliminary description in [58] (testbed). Complete description and results in Section 3.10
E12. Differentiated filtering and Super-Filter	Optimization methods for Soft-FBVT-generated channel and superchannel	Performance evaluation, validation, joint control and data plane	Preliminary description in [58] (testbed). Complete description and results in Section

	occupancy in the EON		3.11
E13. Elastic Operations and Shifting	Soft-FBVT capability to perform multi-action re-optimizations, elastic operations and hitless defragmentation of superchannels in both E2E and source-independent fashion	Performance evaluation, validation, joint control and data plane	Preliminary description in [58] (testbed). Complete description and results in Section 3.12
E14. Monitoring and Modulation Format / Code rate adaptation	Soft-FBVT capability to perform monitoring QoT-aware proactive restoration by adapting physical parameters (e.g., modulation format and code rate)	Performance evaluation, validation, joint control and data plane	Preliminary description in [58] (testbed). Complete description and results in section 3.13
E15. Long Term Channel Overlap	Long term scenario experiment with complete overlap of independent signals in the frequency domains	Performance evaluation, validation, joint control and data plane	Preliminary description in [58] (testbed). Complete description and results in section 3.14
E16. CNIT/Ericsson - Coriant Transponder Interoperability	Integrate data and control planes demonstrating an automatic configuration of DSP for interoperability between transponders of different vendors	Joint control and data plane. Transmission performance of the single-vendor (CNIT / Ericsson) & cross-vendor (CNIT / Ericsson & Coriant) solution as BER vs. distance.	Preliminary results reported in [58]. Final results are reported in Section 3.15
E17. Dynamic Bandwidth Allocation	To show that the ABNO architecture is capable of detecting variations in traffic patterns, and to reconfigure links according to these traffic variations.	Experimental evaluation on how the appropriate bandwidth for links is calculated, according to the monitoring information. The experiment also shows how the ABNO controller can reconfigure the network	Preliminary results reported in [58]. Final results are reported in Section 3.16
E18. Fixed-Grid/Flexgrid Data Plane Interoperability Experiment	Interoperability demonstration between a Flexgrid network domain and a legacy Fixed-Grid network domain, leveraging the availability of real-time BVTs and EXCs to enable compatibility between these types of	Experimental validation and performance evaluation of data plane transmission in a flexgrid and fixed grid optical testbed	Preliminary results reported in [58]. Final results are reported in Section 3.17

	networks.		
E19. Field trial with Orange Telecom (in collaboration with the EU project SASER)	The field trial (carried out in France at the premises of Orange Telecom in Lyon) tests in the field the analyses previously carried out in the lab.	Completed multi-terabit field trial showcasing the latest advances in ultra-high-capacity optical communications technologies being investigated. First-ever demonstration of terabit super-channel transmission across a live network in France, as well as the first-ever field demonstration of full flexi-rate and flexgrid transmission	Results are reported in Section 3.18
E20. Field trial between Coriant and TeliaSonera International Carrier over Pan-European optical network	Evaluate high-order modulation formats jointly with advanced DSP techniques (at both sides of the transponder) to achieve record transmission	Industry-first demonstration of cutting-edge flexi-rate technology for advancing the state of optical layer flexibility. High order modulation formats for metro, regional and long-haul optical systems with real-time BVT are showcased	Preliminary results reported in [58]. Final results are reported in Section 3.19
E21. High capacity high order modulation formats field trials	Validate in a field trial environment the investigations described in E20. The field trial has the goal of testing the IDEALIST high-order modulation format solutions in a real DWDM system configuration, focusing on interoperability of existing and commercially available coherent 40-Gb/s and 100-Gb/s channels with photonic integrated high capacity channels provided by the project.	We expect to show ultra-high capacity transmission by employing a wide range of high-order modulation formats. Moreover, typical upgrade scenarios will be tested by varying symbol rate, modulation formats, and FEC overhead. We plan transmission over the entire C-band, thus achieving or improving upon the results obtained in Section 3.18	The planned date is within the last two weeks of November 2015. Results will be available only for the final audit.
E22. Multi-layer use-cases with ANM	First experimental demonstration based on two multi-layer use-cases with ANM: the Automatic IP Link Provisioning use-case,	Experimental demonstration obtaining PCEP and HTTP messages exchange and traces for the IP Link	Results are reported in Section 3.21

	and the MPLS Service use-case.	provisioning use–case, and for MPLS service workflow. This validates the capability for ANM to support not only flexgrid scenarios, but also multi-layer use-cases.	
E23. IPoDWDM Hybrid control plane tests	To prove the IPoDWDM network solution based on Hybrid Control plane, covering function from a simple circuit set-up to a complex service provisioning with re-optimization.	Several tests for validation of the new Hybrid control plane, by using the CTP planner, and experimental tests through a 3-node DWDM network.	Results are reported in Section 3.22

Table 4: List of experiments, main objectives and results

3.1 E1: E2E service provisioning in multi-vendor / multi-domain networking

The operation of multi-domain and multi-vendor EONs can be achieved by interoperable S-BVTs, a GMPLS / BGP-LS-based control plane and a planning tool. E1 experiment aims at demonstrating and validating the IDEALIST end-to-end data and control architecture. The IDEALIST control plane, which has been extended in WP3 to include the control of S-BVTs and EXCs enables the end-to-end provisioning and recovery of network services. The IDEALIST multi-partner testbed is built by interconnecting all the building blocks of IDEALIST, including the data-plane components. The interoperability between different S-BVT implementations of IDEALIST is experimentally tested. In this case, transponders/S-BVTs are configured using only the information distributed by WP3 control plane. The performance, in terms of BER, is compared against the single-vendor implementation case, where the information used by the S-BVTs is not restricted to the one disseminated by the control plane and proprietary FEC and DSP algorithms can be employed. E1 can be considered as the proof-of-concept of the IDEALIST project, as all components developed in WP4 participate in the experiment.

Use-cases	**Building Blocks**							
	Algorithm suite (off-line and on-line)	Performance metrics for network modeling and experiments	Planning Tools for EON	BVT and S-BVT	Elastic OTN grooming	Flexgrid ROADM and BV-OXC	GMPLS and OFP extensions for flexgrid	Network orchestrator (ABNO)
Resource allocation in EON	X	X		X		X	X	X
Offline Planning and Provisioning	X	X	X		X		X	X
Optical restoration after fibre breaks	X	X		X		X	X	X
Dynamic provisioning including DC interconnection	X	X		X	X	X	X	X

Ultra-high capacity and long-reach transmission	X	X		X		X		
Multi-vendor and multi-technology interoperability	X	X		X		X	X	

Table 5: Use-cases and Building Blocks associated with E1

3.1.1 Description of the setup

In order to demonstrate the feasibility and performance of a multi-domain multi-vendor EON network, WP4 components have been interconnected to build a pan-European test-bed with both control and data. This testbed, illustrated and explained in section 2, is built by the interconnection of different components, both hardware and software, physically distributed within labs. The testbed encompasses three flexgrid domains with different capabilities, one hierarchical PCE, an ABNO controller and the PLATON planning tool. The domains are interconnected resulting in the inter-domain topology shown in Figure 2. Two kinds of domain interconnections are envisioned. In the first one, S-BVTs are attached to the border nodes of each domain and both transponders are back-to-back connected. In the second one, the border nodes are transparently interconnected by a fibre, allowing end-to-end media channels to be set up. Note that, for practical reasons, real data plane connectivity only happens inside the domains, while the interconnection is logical. In addition, it is worth mentioning that the data plane domains are multi-partner, and equipment developed by multiple parties was integrated in the same laboratories.

3.1.1.1 Flexgrid Domain

The flexgrid domain defined as 102 in Figure 2 includes two nodes (Figure 3). Each node includes:

- A flexible and configurable digital cross-connect (OTN switching fabric) for client mapping and centralized control of S-BVT. To this end, the hardware controller has been modified to adapt the commands from the RESTful server to the registers of the FPGA-based S-BVT;
- Real-time S-BVT modules carrying multiple OTU2 tributaries into a single flexible OTU container (which follows the “beyond 100G” OTN standards recommendation) thanks to programmable FPGAs and a multi-flow optical front end that can adapt its symbol rate such as 107 Gb/s or 53.5Gb/s per carrier and its number of carriers according to the reach, physical impairments or capacity demand. The FPGA platform is a Xilinx Virtex 7 580HT with high speed output serializer/deserializer GTZ interfaces up to 28 Gb/s;
- An all-optical matrix that provides flexibility through AoD in terms of synthesis of fibre switching cross-connections (~1dB/cross-connection, 192x192 Polatis switch series 6000), optical bandwidth switching with bandwidth-variable WSSs (4x16 Finisar WaveShaper);
- An off-line coherent receiver, able to recover the transmitted signals using an all-optical coherent front-end (polarization beam splitters, 90°-optical hybrid and balanced receivers) and an off-line DSP (OMA Keysight N4391A).

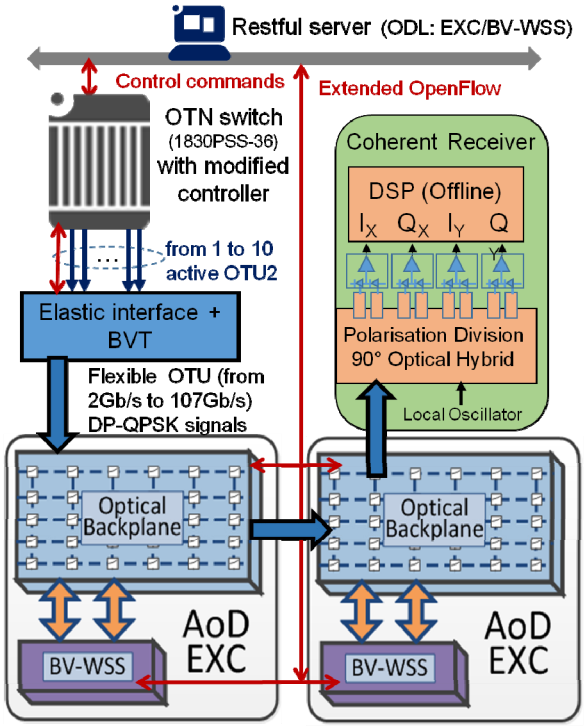

Figure 3: Flexgrid Domain (102)

The GMPLS control plane is thus able to configure the underlying hardware (via the connection control interface) by using dedicated REST interfaces, as mandated by the signaling process. This covers the cross-connection configuration, the WSS filters and the S-BVT. A deployed middleware translates the high-level REST interfaces to the actual low-level hardware interface. In particular, it can configure the number of physical OTU2 tributaries/lanes interfaced to the elastic BVT, and the required symbol-rate. So if there are five OTU2 lanes to be carried, the BVT is configured at 13 GBd PM-QPSK. The middleware contains RESTful Servers e.g. running as a northbound interface on top of a SDN ODL controller with their southbound interface based on extended OFP. The transport equipment (e.g., Fibre Switch and BV-WSS) has an OFP agent capable to translate the received OFP commands to specific equipment APIs (e.g., TL1).

3.1.1.2 Multi-vendor Flexgrid domain

The second domain (101) (Figure 1, bottom-right) includes integrated data and control plane.

The data plane setup consists of four-nodes flexgrid network (based on configurable SSSs), a CNIT/Ericsson DSP unit at the transmitter, and two different ones (CNIT/Ericsson and Coriant) at the receiver, as part of an optical coherent testbed. The transmitter is able to provide a super-channel with different configurable number of carriers and capacity (i.e. 1 carrier for 100G, 3 carriers for 400G and 7 carriers for 1T). At 1 Tb/s, we adopted PM-16QAM Nyquist-shaped signals shaped by a roll-off = 0.05 and symbol rate = 23 GBd.

A 64-GSa/s DAC was used with 3 dB bandwidth of 13 GHz and ENOB 5.5. In order to mitigate DAC bandwidth limitations, digital pre-emphasis was applied to ensure proper rectangular shape. Two single polarization IQ-modulators were used to modulate the even and odd sub-carriers of the super-channel. Subcarrier spacing was set to 25 GHz. Next, the single polarization signals went through the polarization multiplex emulation stage

where they were first split into two orthogonal polarizations, delayed with respect to each other for de-correlation and finally combined by a PBC resulting in a polarization multiplexed signal. The even and odd sub-carriers were multiplexed via 3 dB coupler resulting in a multiple sub-carrier super-channel. The testbed was equipped with an optical re-circulating loop consisting of 2×80 km SSMF spans, EDFAs to compensate for span losses, and a wave-shaper acting as a loop filter to perform gain equalization and suppress accumulated out-of-band ASE noise. In addition, a polarization scrambler was also employed to evenly distribute polarization dependent loop effects. After the loop circulation, the desired sub-carrier was selected via a tunable band-pass filter, then demodulated by employing coherent phase- and polarization-diversity detection, and finally setting the LO at the nominal central frequency of the selected sub-carrier. The received optical signal is mixed with the LO through a polarization-diversity 90°-hybrid optical coupler, whose outputs are sent to four couples of balanced photo-diodes. The four photo-detected signals are sampled and digitized through a 20-GHz 50-GSa/s real-time oscilloscope. The sampled signals were saved for off-line receiver DSP. The line-rate of 1.28 Tb/s allows us to assume a 23% FEC-OH plus 5% framing OH. Such value would guarantee proprietary soft-decision FEC with 23% OH and a pre-FEC BER of 3.37×10^{-2}.

The control plane is performed via Linux-based C++ GMPLS controllers located at each physical node of the network. Controllers run PCEP establishing session with the domain active stateful cPCE and RSVP-TE to perform signaling. Controllers are connected with the data plane test-bed (i.e., SSS, transmitter and receiver) by means of USB, serial and GPIB interfaces. Based on RSVP-TE messages, controllers are able to automatically configure SSSs (i.e., filter shape as the reserved frequency slot), transponders parameters (i.e., symbol-rate, number of carriers, sub-carrier central frequencies) and DSP parameters (i.e., modulation format, FEC).

Domain active stateful cPCE, developed in C++ in a Linux box, performs intra-domain topology export advertisement by means of BGP-LS, impairment-aware path computation, multi-action re-optimization, adaptation and instantiation by means of PCEP.

Multi-vendor interoperability between CNIT/Ericsson and Coriant DSPs was achieved by the exchange of novel AC and TC attributes in BGP-LS and PCEP/RSVP-TE protocols, in line with ITU recommendations. The AC attribute, exported by BGP-LS within the TE link attribute extensions, defines the whole network scenario of application (i.e., in terms of wavelength range, type of fiber, dispersion compensation, presence of amplifiers, system rate, etc). The TC attribute identifies the transponder features and compatibility by implicitly defining a large set of available and allowed physical transmitter/receiver parameters values and ranges. In particular, the TC has been encoded as a novel Sub-TLV specification inside the MF-OTP extensions of PCEP and RSVP-TE, specifying the super-channel description (i.e., in terms of sub-carriers nominal central frequencies and width, modulation, FEC). Path computation allows transponder-transponder end point assignment only if they both belong to the same TC or to compatible TCs. The same policy is enforced in the RSVP-TE signaling at the endpoint nodes, during the actual transponder selection and configuration.

3.1.1.3 Emulated Flexgrid domain

The third domain, defined as 105, is composed of six nodes running a GMPLS control plane on dedicated Linux boxes. No data plane is employed: therefore, media layer devices (i.e. SSS) are emulated within the same boxes running the GMPLS controllers. An active stateful cPCE, enhanced with BGP-LS speaker features, collects local topology information and coordinates with the pPCE for path calculations and LSPs provisioning

inside the domain. Persistent PCEP sessions between the cPCE and all the border nodes are configured to accomplish this.

3.1.1.4 Hierarchical Stateful PCE and ABNO Controller

The pPCE is built using the open source Netphony Hierarchical Stateful PCE suite, developed in Java, and is deployed in a virtual machine that is connected to the control plane network. The pPCE uses the Netphony BGP-LS speaker and TED to obtain the domain interconnection and the TE details of both border nodes and inter-domain links. Thus, when the pPCE is used for end to-end computations, runs an algorithm to select the domains and performs a distributed RSA when end-to-end media channel is requested. When the inter-domain links are a transponder interconnection, the pPCE does not need to perform the RSA. A Redis database is used to store persistently the LSP and Traffic Engineering databases. The ABNO controller, built with the Netphony Open Source ABNO suite, runs in the same virtual machine as the pPCE. A workflow is implemented that defines the interactions with the pPCE and can be triggered either from the Planning tool or from the Network Management System. A web server with the GUI is also deployed to facilitate the operation of the network.

3.1.1.5 Planning tool

Upon the reception of a bundle of connections to be served, the PLATON planning tool solves an optimization problem so as to minimize the resources used for the whole bundle. To that end, the planning tool explores a fixed number of solutions by randomly sorting the bundle set. For each individual connection request, the planning tool solves the RSMA problem (an extension of the RSA problem, where the modulation format is as well assigned).

3.1.2 Attained results

To demonstrate the architecture, an end-to-end connection of 107 Gb/s, with one segment in domain 102, and a second segment with a cross-vendor connection between S-BVTs in domain 101, is setup.

3.1.2.1 Control plane evaluation

A Wireshark capture of the PCEP messages flow of the computation and instantiation is shown in Figure 4 with a total set-up time of 6.12 seconds. In the trace, it can be seen that the instantiation time is dominated by the hardware configuration, 2.29 seconds in domain 101 and 5.96 seconds in domain 102.

Computation

REF	SDN_CONTROLLER	SDN_CONTROLLER	Path Computation Request (PCReq)
0.002892	TID_PARENT_PCE	172.16.102.161	Path Computation Request (PCReq)
0.003051	TID_PARENT_PCE	CNIT_CHILD_PCE	Path Computation Request (PCReq)
0.067978	172.16.102.161	TID_PARENT_PCE	Path Computation Reply (PCRep)
0.119092	CNIT_CHILD_PCE	TID_PARENT_PCE	Path Computation Reply (PCRep)
0.122653	SDN_CONTROLLER	SDN_CONTROLLER	Path Computation Reply (PCRep)

Provisioning

0.153279	SDN_CONTROLLER	SDN_CONTROLLER	Path Computation LSP Initiate (PCInitiate)
0.160785	TID_PARENT_PCE	CNIT_CHILD_PCE	Path Computation LSP Initiate (PCInitiate)
0.161159	TID_PARENT_PCE	172.16.102.161	Path Computation LSP Initiate (PCInitiate)
2.245301	CNIT_CHILD_PCE	TID_PARENT_PCE	Path Computation LSP State Report (PCRpt)
6.119321	172.16.102.161	TID_PARENT_PCE	Path Computation LSP State Report (PCRpt)
6.123022	SDN_CONTROLLER	SDN_CONTROLLER	Path Computation LSP State Report (PCRpt)

Figure 4: Message Capture at pPCE

3.1.2.2 ALU-UNIVBRIS optical performance

The flexgrid domain (102) has been characterized in terms of optical performance for both S-BVTs and off-line processing from Alcatel-Lucent (ALU) and University of Bristol (UNIVBRIS). The results are shown in detail in experiments E6-E7.

3.1.2.3 Multi-vendor flexgrid interoperability performance

Figure 5 reports the transmission performance of the single-vendor ($CNIT_{TX} \rightarrow CNIT_{RX}$) and cross-vendor ($CNIT_{TX} \rightarrow Coriant_{RX}$). Both solutions are deployed in the (101) domain at the maximum capacity (i.e., 1 Tb/s per super-channel). The aforementioned pre-FEC BER threshold of 3.37×10^{-2} will be considered only for the single-vendor scenario (i.e., a proprietary and more powerful SD-FEC can be adopted). In both cases we used blind-DSP algorithms, because an interoperability scenario would not allow the usage of algorithms that require knowledge of the link or of training sequences.

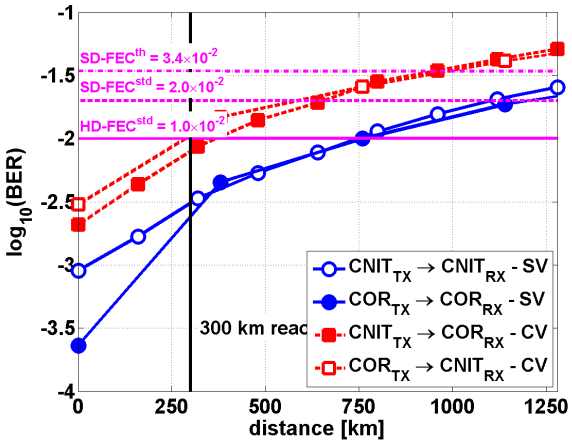

Figure 5: Single- and cross-vendor transmission reach

In the case that we opt for the cross-vendor solution, we can only rely on already standardized FEC. For example, the ITU standard G975.1, appendix I.7 hard-decision super-FECstd (HD-FECstd) with 20% could use a pre-FEC BER threshold = 1×10^{-2}. This value could increase, in the case that new SD-FEC becomes standard, up to a reasonable pre-FEC BER threshold = 2×10^{-2}. Based on the pre-FEC thresholds, we can draw the following conclusions concerning the experiment carried out by employing the testbed

depicted in Figure 1. In the case that we assume the usage of already standardized HD-FECstd a transmission up to ~750 km is guaranteed when performing single-vendor transmission. This is halved when we operate in cross-vendor mode. Though the system performance has been significantly reduced, such a scenario (with cross-vendor transmission) would still guarantee the error-free transmission over the majority of European links. Moreover, if we could adopt a standardized FEC (SD-FECstd), the reach would approach 1100 km for single-vendor case, and ~600 km for cross-vendor transmission. Finally, in the case of proprietary FEC, the transmission distances would be ~1800 km, and once again about half in case of cross-vendor transmission. These values are summarized in Table 6:

	Reach [km]		
Case	**HD-FEC^{std}**	**SD-FEC^{std}**	**SD-FECth**
Single-vendor	750	1100	1800
Cross-vendor	300	600	900

Table 6: Performance results

3.1.3 Analysis of the results

The experiment has demonstrated a fully end-to-end interoperable EON network at control and data plane levels, following IDEALIST WP1, WP2 and WP3 solutions. The interoperability of several implementations of S-BVTs, with Hard-decision and Soft-decision FECs, is evaluated. The control architecture is able to configure the S-BVTs so the multi-vendor transmission reach is failure-free up to 300 km with current FEC standards.

3.2 E2: GMPLS/PCE control of National Spanish Flexgrid network with MF-OTPs

Experiment E2 aims at validating and evaluating the GMPLS protocol (routing and signaling) extensions for managing a flexgrid network, especially considering the capabilities and available resources arising from S-BVT technology. The main motivation is to demonstrate the feasibility of implementing GMPLS extensions under dynamic traffic scenarios. The following table summarizes the targeted IDEALIST use-case, along with the key building blocks being considered.

Use-case	**Building Blocks**		
	Algorithm suite (off-line and on-line)	Performance metrics for network modeling and experiments	GMPLS and OFP extensions for flexgrid
Resource allocation in EON	X	X	X

Table 7: Use-case and Building Blocks associated with E2

3.2.1 Description of the setup

This experiment evaluates the performance of the implemented extensions for GMPLS routing and signaling protocols, and also the novel on-line RSMA algorithm to dynamically configure flexgrid paths between two remote MF-OTPs/S-BVTs, serving LSP demands (i.e., allocation of both MF-OTP and optical spectrum resources). RSMA relies on a distance-adaptive mechanism to attain efficient use of those resources.

The experimental performance evaluation [6] is conducted using the GMPLS control plane of the ADRENALINE testbed where flexgrid optical hardware (i.e., MF-OTPs and BV-OXCs) is emulated. The GMPLS control plane of the ADRENALINE testbed is an experimental platform providing full and real implementation of the involved processes and control protocols (routing and signaling) as well as the active PCE. Every network node has a GMPLS control plane instance enabling control communications with other nodes using a dedicated data communication (control plane) network. Nevertheless control plane decisions when setting up a flexgrid LSP do not result in a real configuration of the underlying optical hardware since ADRENALINE lacks such optical infrastructure.

The network topology follows a Spanish EON formed by 22 links and 14 BV-OXCs (see Figure 6). Each optical link has its own distance (in km) and supports 128 NCFs (*n: 0..127*) with a channel spacing of 6.25 GHz. As the control links (used for exchanging routing and signaling messages) are considered in fibre, link propagation delays are also taken into account to deliver control messages. This is used for computing the setup delay for establishing LSPs. Every network node is controlled by a GMPLS control plane implemented on a Linux-based router with an Intel Xeon 3 GHz processor. The active PCE is co-located with N1. As depicted in Figure 6, 11 nodes are equipped with MF-OTPs. Such a pool of nodes constitutes the possible pair of source and destination nodes for any *req*. The rest of the nodes (a total 3) are intermediate optical switches. The number of sub-carriers equipped in each MF-OTP is varied: 5, 10, 15 and 20. The supported modulation formats by the sub-carriers are: DP-QPSK, DP-8QAM and DP-16QAM.

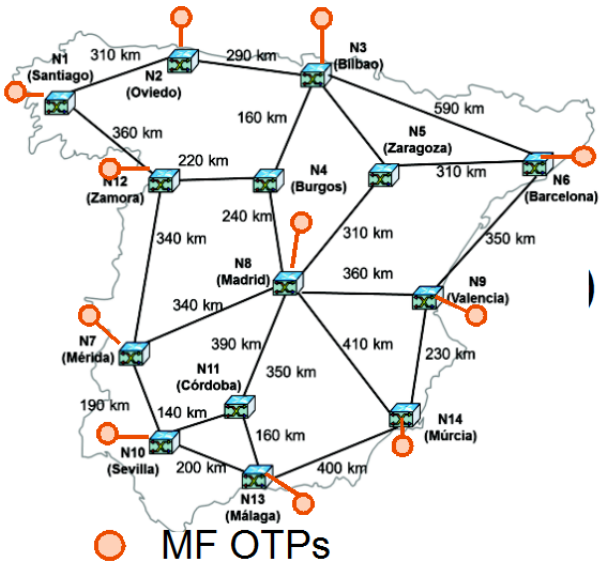

Figure 6: Transport network topology with MF-OTPs

Table 8 depicts the bits/symbol, the Gb/s (assuming a fixed symbol rate of 25 Gbauds/s) and the maximum supported path distance (i.e., *MaxDmf*) for each of the supported modulation formats (*mf*). The requested bandwidth (*R*) for each *req* is uniformly distributed

as multiples of 100 Gb/s up to 500 Gb/s. Table 8 shows the number of required sub-carriers for each possible *R* bit rate.

mf	DP-QPSK	DP-8QAM	DP-16QAM
bits/symbol	4	6	8
bit rate (Gb/s)	100	150	200
MaxDmf (km)	3000	1000	650
R (Gb/s)	n_{sc}		
100	1	-	-
200	2	-	1
300	3	2	-
400	4	-	2
500	5	-	-

Table 8: Number of sub-carriers & *MaxDmf* per *mf* and bit rate (*R*)

We assume uniform traffic between all the nodes equipped with MF-OTPs. The arrival process of the LSP demands is assumed to be Poisson with a mean inter-arrival time of 10s. The HT of the LSPs is modeled as a negative exponential, whose mean is varied to obtain different network loads.

Each sub-carrier has a fixed FS width of $m = 2$ (i.e., 25 GHz), so that a 400 Gb/s LSP using 2 sub-carriers at DP-16QAM uses a FS width of 50 GHz, whilst the same LSP using 4 sub-carriers with DP-QPSK requires a FS of 100 GHz.

3.2.2 Obtained results

Two figures of merit are used for the performance evaluation: the connection BP, and the delay (in ms) for both the connection setup and the RSMA computation. In particular, BP allows an indication of the efficiency of the RSMA algorithm when operating with either *partial* or *full* MF-OTP model at the time of handling the network resources when dynamically setting up flexgrid LSPs.

Table 9 gathers the obtained numerical results from varying the HT (i.e., 25, 50, 75 and 100 s) when the RSMA algorithm adopts either a *partial* or *full* model. These results are presented as: the time required by the RSMA algorithm to be executed; the average setup time (computed as the elapsed time between when the LSP request is received and when the LSP is actually set up); the RSMA errors (i.e., path computation failures); the signaling errors; and the BP.

		Delay (ms)		Error		
HT (s)	Model	RSMA	Setup	RSMA	Sign.	BP (%)
25	Partial	11.2	51.4	1	225	22.6
	Full	12.3	50.9	6	12	1.8
50	Partial	11.5	51.8	9	278	28.7
	Full	11.3	50.9	24	3	2.7
75	Partial	10.7	51.7	23	322	34.5
	Full	10.9	50.4	34	18	5.2
100	Partial	10.5	50.9	26	331	35.7
	Full	11.4	50.8	60	8	6.8

Table 9: Experimental Delay and BP results

Figure 7 depicts the BP when the number of sub-carriers per MF-OTP is varied (i.e., 5, 10, 15 and 20) and the HT is fixed to 100s:

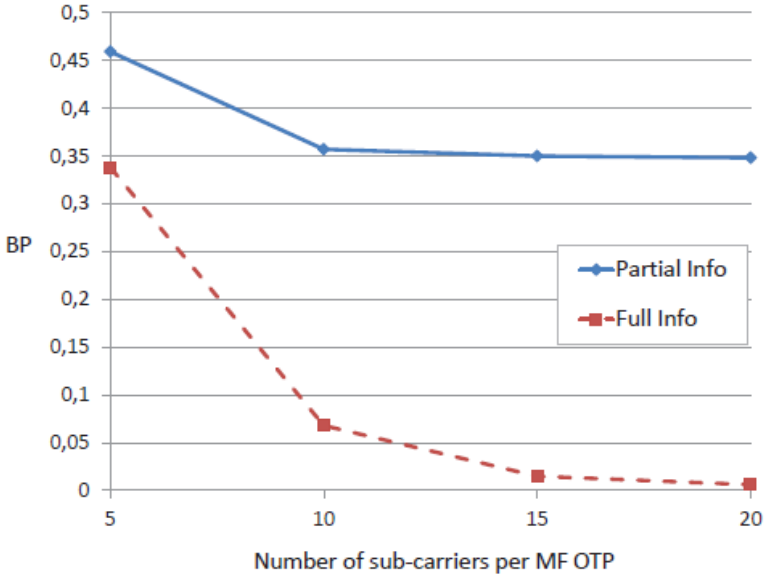

Figure 7: BP vs. number of sub-carriers per MF-OTP for *partial* and *full* models.

3.2.3 Analysis of the results

In general for all HT values, the use of the *full* model lowers the BP as compared to the *partial* model. This is attained at the expense of a slight increase in the complexity of the RSMA algorithm as well as the generated control plane overhead (MF-OTP spectrum status information). LSP failures are divided into path computation (i.e., RSMA failures) and signaling errors. In both models, we observe that the RSMA errors are mainly caused by the lack of available sub-carriers at the time that the route is computed. That is, an insufficient number of sub-carriers are available at either the source or destination nodes for *req*. On the other hand, signaling errors occur when the computed LSPs are being actually set up. The main difference between both models (*partial* and *full*) lies with the signaling errors. In the *partial* model, these errors principally happen due to the difficulties of dealing with either the SCC or the SCgC constraints. Thus contention on the MF-OTP interfaces with existing LSP is likely to occur. Applying the *full* model reduces these problems. Indeed, the RSMA algorithm is aware of the optical spectrum status of the MF-OTP interfaces, which in turn facilitates dealing with the required end-to-end spectrum restrictions (SCC and SCgC). Signaling errors appearing in the *full* model could be due to either concurrent LSPs being signaled, or that the RSMA algorithm is operating with outdated PCE's TED. We observe that the differences with respect to the setup and RSMA delays are negligible, since both models use (practically) the same RSMA algorithm.

From Figure 7, we can see that as the number of subcarriers is increased the BP attained by the *full* model is enhanced since the lack of sub-carriers is less of a troublesome factor for the RSMA computation. In the *partial* model, the increase in the number of sub-carriers also allows an improvement in the BP, but only up to a certain value (10) of sub-carriers. Above this value, the achieved improvement becomes negligible, since the errors are not

due to the lack of available sub-carriers during the path computation, but rather due to the spectrum restriction problems that the signaling encounters. Consequently, regardless of whether the number ensuring both SCC and SCgC is increased when the *partial* model is used, the establishment of LSPs is greatly complicated.

In the light of these results, we conclude that the use of a *full* model attains a better performance in terms of connection blocking (BP) as compared to the *partial* strategy. This enhancement is, however, achieved at the expense of increasing the control overhead, since a greater number of MF-OTP capabilities and attributes need to be employed within the *full* model.

3.3 E3: Use of front-end and back-end PCE: Defragmentation

This use-case assesses the SPRING algorithm in dealing with the issue of defragmentation. In particular, with the PLATON tool configured as a back-end PCE.

Use-case	Building Blocks			
	Algorithm suite (off-line and on-line)	Planning Tools for EON	GMPLS and OFP extensions for flexgrid	Network Orchestrator (ABNO)
Dynamic defragmentation and re-optimization	X	X	X	X

Table 10: Use-case and Building Blocks associated with E3

Figure 8 describes the distributed field trial, with the results of this experiment reported in reference [58].

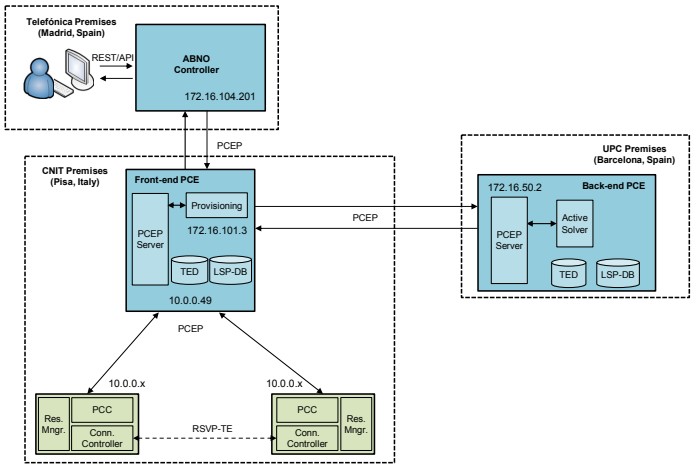

Figure 8: Distributed testbed set-up

3.4 E4: Use of front-end and back-end PCE: Modulation format-aware re-optimization

This use-case evaluates the AFRO algorithm to re-optimize resource utilization after a link repair is proposed.

Use-case	Building Blocks			
	Algorithm suite (off-line and on-line)	Planning Tools for EON	GMPLS and OFP extensions for flexgrid	Network Orchestrator (ABNO)
Dynamic defragmentation and re-optimization	X	X	X	X

Table 11: Use-case and Building Blocks associated with E4

The proposed workflow was implemented using the ABNO architecture and was experimentally assessed in the distributed testbed as depicted in Figure 9. The results of this experiment were reported in the reference [58].

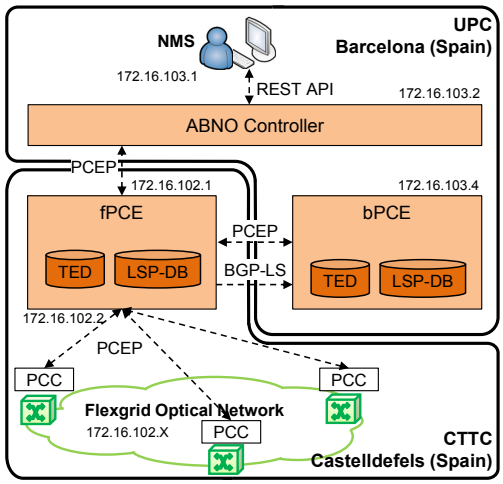

Figure 9: Control and management architecture

3.5 E5. Multi-domain Flexgrid network control based on Hierarchical PCE with BGP-LS

The control of multi-domain EON is possible by combining H-PCE based computation, BGP-LS topology discovery, remote instantiation via PCEP, and signaling via RSVP-TE. Two evolutionary architectures are considered, one based in stateless H-PCE, PCEP instantiation and end-to-end RSVP-TE signaling (SL-E2E), and a second one based on stateful active H-PCE with per-domain instantiation and stitching. The experiment aims at performing protocol interoperability and demonstrating the two possible control architectures.

Use-cases	Building Blocks			
	Algorithm suite (off-line and on-line)	Performance metrics for network modeling and experiments	GMPLS and OFP extensions for flexgrid	Network Orchestrator (ABNO)
Resource allocation in EON	X		X	X

Dynamic provisioning including DC interconnection	X	X	X	X
Multi-vendor and multi-technology interoperability	X	X	X	X

Table 12: Use-cases and Building Blocks associated with E5

3.5.1 Description of the setup

The IDEALIST multi-partner control plane testbed interconnects four European research institutions, located in Madrid (Telefónica I+D), Barcelona (CTTC), Torino (TI) and Pisa (CNIT). The testbed physical topology is depicted in Figure 10. Partners' premises are connected (at the control plane level) by means of dedicated IPSec tunnels. The resulting low level connectivity layout is a hub, centered at CTTC. Static routing entries provide full connectivity between partners' private addresses, secured and isolated from the rest of Internet traffic. On top of this distributed control plane connectivity network, logical relationships between PCEs are established, in particular between Telefónica I+D PCE, acting as pPCE, and the other PCEs, acting as cPCE, as shown in Figure 10. The PCEs of the test-bed have been independently developed by each partner. BGP-LS speakers are implanted by each partner.

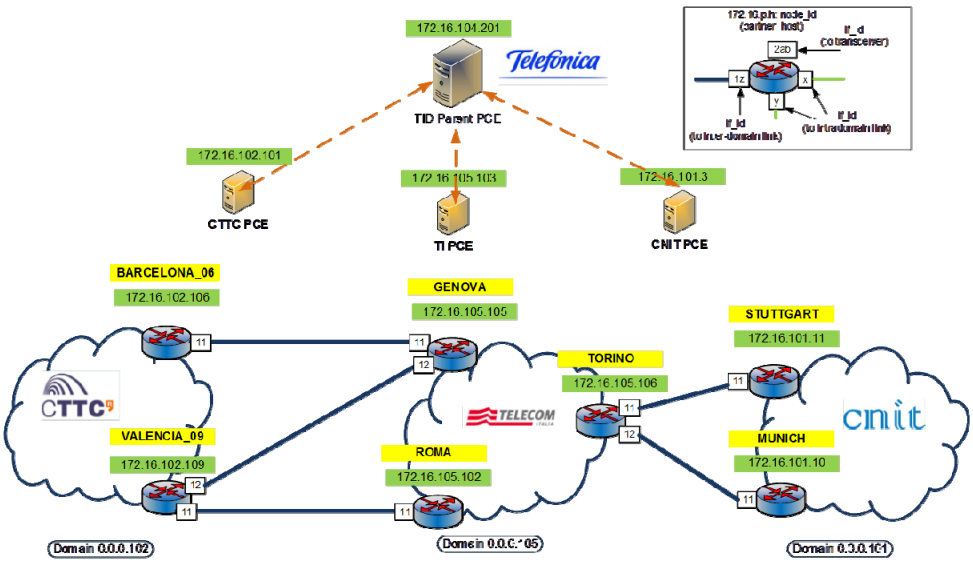

Figure 10: topology of Multi-partner IDEALIST testbed

3.5.2 Attained results

The proposed architectures and control extensions are evaluated. The results are published in detail in the JOCN paper [8] .

3.5.2.1 Performance evaluation and analysis of SL-E2E

First of all, the architecture has been fully validated functionally, and the interoperability of four PCEP implementations has been achieved. Figure 11 shows a Wireshark capture in the parent PCE machine, showing the path computation interactions and the later initiation procedure when architecture SL-E2E is used:

REF	SDN_CONTROLLER	SDN_CONTROLLER	PCEP	140	Path Computation Request (PCReq)
0.030268	TID_PARENT_PCE	CTTC_CHILD_PCE	PCEP	132	Path Computation Request (PCReq)
0.030695	TID_PARENT_PCE	CNIT_CHILD_PCE	PCEP	132	Path Computation Request (PCReq)
0.031230	TID_PARENT_PCE	TI_CHILD_PCE	PCEP	132	Path Computation Request (PCReq)
0.054446	CTTC_CHILD_PCE	TID_PARENT_PCE	PCEP	268	Path Computation Reply (PCRep)
0.094012	CNIT_CHILD_PCE	TID_PARENT_PCE	PCEP	204	Path Computation Reply (PCRep)
0.094972	TI_CHILD_PCE	TID_PARENT_PCE	PCEP	152	Path Computation Reply (PCRep)
0.110598	SDN_CONTROLLER	SDN_CONTROLLER	PCEP	328	Path Computation Reply (PCRep)
4.144313	TID_PARENT_PCE	CTTC_CHILD_PCE	PCEP	380	Path Computation LSP Initiate (PCInitiate)
24.898735	CTTC_CHILD_PCE	TID_PARENT_PCE	PCEP	376	Path Computation LSP State Report (PCRpt)

Figure 11: Capture of PCEP message flow in SL-E2E

In the example, a media channel with m = 2 is requested from node 172.16.102.101 interface 1000, in CTTC domain, to node 172.16.101.16 interface 100 in CNIT domain. Figure 12 shows the RSVP-TE interactions that are triggered by the PCEP instantiation message:

0.000000	172.16.102.106	172.16.105.105	RSVP	358	PATH Message. SESSION: IPv4-LSP, Destination 172.16.101.16, Short Call ID 0, Tu
0.002783	172.16.105.105	172.16.102.106	RSVP	54	ACK Message.
0.002818	172.16.105.105	172.16.105.106	RSVP	298	PATH Message. SESSION: IPv4-LSP, Destination 172.16.101.16, Short Call ID 0, Tu
0.005953	172.16.105.106	172.16.105.105	RSVP	60	ACK Message.
0.009747	172.16.105.106	172.16.101.11	RSVP	274	PATH Message. SESSION: IPv4-LSP, Destination 172.16.101.16, Short Call ID 0, Tu
15.006515	172.16.105.105	172.16.105.106	RSVP	298	PATH Message. SESSION: IPv4-LSP, Destination 172.16.101.16, Short Call ID 0, Tu
15.007658	172.16.105.106	172.16.101.11	RSVP	274	PATH Message. SESSION: IPv4-LSP, Destination 172.16.101.16, Short Call ID 0, Tu
15.123490	172.16.101.11	172.16.105.106	RSVP	60	ACK Message.
20.640682	172.16.101.11	172.16.105.106	RSVP	142	RESV Message. SESSION: IPv4-LSP, Destination 172.16.101.16, Short Call ID 0, Tu
20.644463	172.16.105.106	172.16.105.105	RSVP	142	RESV Message. SESSION: IPv4-LSP, Destination 172.16.101.16, Short Call ID 0, Tu
20.645651	172.16.105.105	172.16.105.106	RSVP	54	ACK Message.
20.646162	172.16.105.105	172.16.102.106	RSVP	142	RESV Message. SESSION: IPv4-LSP, Destination 172.16.101.16, Short Call ID 0, Tu
20.698241	172.16.102.106	172.16.105.105	RSVP	60	ACK Message.

Figure 12: RSVP-TE capture at Telecom Italia border node "Torino"

The experiment shows that the total computation time, including all the interactions between parent and child PCEs is 68 ms. In the example, three domains are involved in the computation and instantiation. The initiation time is 5.7 seconds. Most of the time of the initiation is due to the configuration of the real OXC WSS-based flexgrid nodes in CNIT testbed. The total initiation time is shown in Eq. 1, which includes the time to reach the parent PCE (in both ways, $RTT_{ANM\text{-}PPCE}$), the computing time of the parent PCE (T_{COMP_PPCE}), the maximum of the queries to the child PCEs ($T_{PPCE\text{-}X\text{-}CPCE}$, where X is CNIT, CTTC or TI, and includes the time to reach the child PCE and the computing time of the child PCE), the time to query (and get and answer) the head end node ($RTT_{ANM\text{-}HEAD\text{-}NODE}$), and the end-to-end signaling time (sum of the RSVP times per domain and the RTT of the inter-domain links). In this architecture, the computing time is dominated by the slowest response time of a child PCE, as the requests are in parallel, but the setup time increases with the number of domain, as there is an end-to-end signaling session.

$$T_{ini-SL-E2E} = RTT_{ANM-PPCE} + T_{COMP\_PPCE} + \max\left(T_{PPCE-CNIT-CPCE}, T_{PPCE-CTTC-CPCE}, T_{PPCE-TI-CPCE}\right) + RTT_{ANM-HEAD-NODE} + \sum_{each\_domain} T_{RSVP} + \sum_{each\_id\_link} RTT_i$$

Eq. 1: Total Initiation time in SL-E2E

It has to be taken into account that both CTTC and TI test-beds run on emulated nodes, and thus set-up time is faster. The latencies between the different components is shown in Figure 13, that shows the mean times of the important steps as well.

Ping times	
	avg/mdev
TID-CTTC	14.3/1.454 ms
TID-TI	65.228/3.600 ms
TID-CNIT	63.768/8.397 ms
CTTC-TI	51.31/1.997 ms
TI-CNIT	100.11/3.502 ms

Computing times (same in SL-E2E and SF-PD)	
	avg/mdev
TOTAL Comp	70,4/1,3 ms
TID-CTTC	24,3254/0,41 ms
TID-TI	65,31/1,87 ms
TID-CNIT	66,57/2,93 ms

setup time (SL-E2E vs SF-PD)	
	avg/mdev
SL-E2E CTTC-TI-CNIT	5,6/0,32 sec
SF-PD CTTC-TI-CNIT	5,04/0,16 sec

Figure 13: Experimental results

3.5.2.2 Performance Evaluation and analysis of SF-PD

Figure 14 shows the message flow (Wireshark capture) in the parent PCE machine, including the path computation interactions and the later initiation procedure using the SF-PD architecture. The same end-points as in the previous example are used. In this experiment, the total computation time, including all the interactions between parent and child PCEs is similar to the SL-E2E case, as the computation procedure remains unchanged. However, the total initiation time, 5.25 seconds, is lower than in the SL-E2E case, as the per-domain initiations are performed in parallel.

REF	TID_PARENT_PCE	TID_PARENT_PCE	PCEP	152	Path Computation LSP Initiate (PCInitiate)
0.029259	TID_PARENT_PCE	TI_CHILD_PCE	PCEP	132	Path Computation Request (PCReq)
0.029923	TID_PARENT_PCE	CNIT_CHILD_PCE	PCEP	132	Path Computation Request (PCReq)
0.030393	TID_PARENT_PCE	CTTC_CHILD_PCE	PCEP	132	Path Computation Request (PCReq)
0.093511	CNIT_CHILD_PCE	TID_PARENT_PCE	PCEP	204	Path Computation Reply (PCRep)
0.093578	CTTC_CHILD_PCE	TID_PARENT_PCE	PCEP	268	Path Computation Reply (PCRep)
0.190464	TI_CHILD_PCE	TID_PARENT_PCE	PCEP	152	Path Computation Reply (PCRep)
0.200313	TID_PARENT_PCE	CTTC_CHILD_PCE	PCEP	292	Path Computation LSP Initiate (PCInitiate)
0.201983	TID_PARENT_PCE	CNIT_CHILD_PCE	PCEP	244	Path Computation LSP Initiate (PCInitiate)
0.203277	TID_PARENT_PCE	TI_CHILD_PCE	PCEP	220	Path Computation LSP Initiate (PCInitiate)
0.249590	CTTC_CHILD_PCE	TID_PARENT_PCE	PCEP	272	Path Computation LSP State Report (PCRpt)
0.449333	TI_CHILD_PCE	TID_PARENT_PCE	PCEP	192	Path Computation LSP State Report (PCRpt)
5.240077	CNIT_CHILD_PCE	TID_PARENT_PCE	PCEP	204	Path Computation LSP State Report (PCRpt)
5.244234	TID_PARENT_PCE	TID_PARENT_PCE	PCEP	348	Path Computation LSP State Report (PCRpt)

Figure 14: Capture of message flow in SF-PD

The total initiation time is shown in Eq. 2, which includes the time to reach the parent PCE (in both ways, $RTT_{ANM\text{-}PPCE}$), the computing time of the parent PCE (T_{COMP_PPCE}), the maximum of the queries to the child PCEs ($T_{PPCE\text{-}X\text{-}CPCE}$, where X is CNIT, CTTC or TI, and includes the time to reach the child PCE and the computing time of the child PCE), and the maximum of the times to provision in each domain (summing the round trip time from parent PCE to the child PCE, and the signaling time in the domain). As there is no end-to-end signaling, no messages are exchanged between domains. The time of the initiation in this case is dominated by the longer setup time, which corresponds to the real OXC WSS based flexgrid nodes in CNIT testbed.

$$T_{ini-SF-PD} = RTT_{ANM-PPCE} + T_{COMP\_PPCE}$$
$$\max\left(T_{PPCE-CNIT-CPCE}, T_{PPCE-CTTC-CPCE}, T_{PPCE-TI-CPCE}\right)$$
$$+\max\begin{pmatrix}\left(RTT_{PPCE-CTTC} + T_{RSVP-CTTC}\right),\\ \left(RTT_{PPCE-TI} + T_{RSVP-TI}\right),\\ \left(RTT_{PPCE-CNIT} + T_{RSVP-CNIT}\right)\end{pmatrix}$$

Eq. 2: Total Initiation time in SF-PD

3.5.3 Analysis of the results

In this experiment an extended demonstration of the multi-domain EON control plane based on H-PCE architecture was implemented and evaluated. High degree of interoperability in the multi-partner multi-platform distributed control plane EON test-bed was achieved by employing the most recent PCEP, OSPF-TE, BGP-LS and RSVP-TE protocol extensions. Two architectural scenarios, based on stateless PCE performing end-to-end instantiation and stateful PCE performing per-domain instantiation and stitching were implemented and fully tested, respectively. Experimental results showed path computation, including all protocol interactions and LSP setup times. Moreover, extended control plane messages and operation for each scenario were detailed, highlighting the extensions conceived for EON and multi-domain scenario. The adoption of BGP-LS extensions fully enabled multi-domain TE and was demonstrated in a limited number of domains. The results provided in this work aim at representing the current state-of-the-art of the research in EON control plane and the reference benchmark for future research activities and extensions in the context of multi domain optical networks

3.6 E6-E7. Integrated control with BVT and flexible EXCs

The aim of the experiment **E7** is to validate the whole system architecture of the metro/core border node encompassing both data and control plane interactions. The motivation is thus to assess the feasibility of the integrated prototyped subsystems, enabling the automatic configuration of the optical network elements (i.e., S-BVT, flexgrid optical switches, and OTN switch) as a result of the control plane (GMPLS/PCE) decisions for a new established flexgrid LSP.

Different use-cases are applicable to the node architecture developed for the metro/core border node. In this experiment, the targeted use-cases are: Resource allocation in EON; OTN over optical grooming; and Dynamic provisioning of a connection requiring the setup of optical cross-connects and a new data rate from the S-BVT/OTN node. However, the following use-cases were also showcase possibilities.

Use-cases	**Building Blocks**					
	Algorithm suite (off-line and on-line)	Performance metrics for network modeling and experiments	BVT and S-BVT	Elastic OTN grooming	Flexgrid ROADM and BV-OXC	GMPLS and OFP extensions for flexgrid
Resource allocation in EON	X		X		X	X
Optical restoration after fibre breaks			X		X	
OTN over optical grooming		X	X	X	X	
IP over Optical planning	X		X	X	X	X
IP over Optical control	X		X	X	X	X

Dynamic provisioning including DC interconnection	X	X	X	X	X	X
Dynamic defragmentation and re-optimization			X	X	X	

Table 13: Use-cases and Building Blocks associated with E7

The first step focused on the integration of the elastic interface with the commercial 1830PSS OTN switch from Alcatel-Lucent and centralized control (formerly experiment **E6** in [58]). This is described in subsection 3.6.1.

A second step was the final setup located in Bristol, for which all the various Alcatel-Lucent equipment had to be moved to Bristol University, see subsections 3.6.2 and next.

3.6.1 Preliminary Test/Integration of the BVT and OTN Controller (in Paris)

Before moving to Bristol, we had to integrate the different software and hardware elements developed in Paris and Vimercate and run initial experiments to check the first phase of integration. The Paris setup is depicted in Figure 15 and involves a RESTful server translating commands from the GMPLS control plane from CTTC towards the OTN switch; a modification of the first level controller was embedded inside the Alcatel-Lucent 1830PSS OTN switch in order to support and control the FPGA-based prototyped elastic interface.

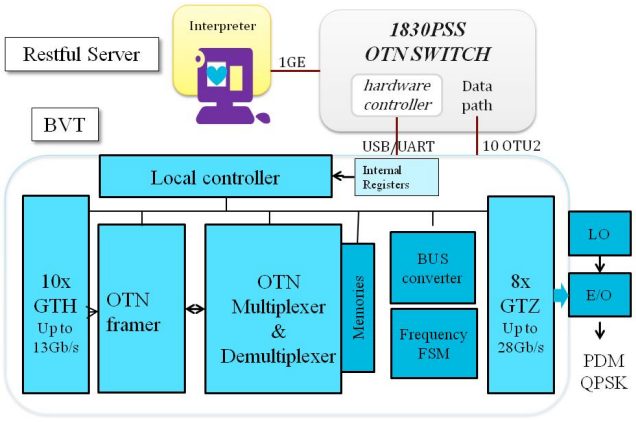

Figure 15: Experimental setup with Restful server, OTN switch and elastic interface

In terms of providing a more detailed description of the experiments, the incoming signaling messages are in http/json format and include the information related to the central frequency *n* and number of flexgrid slots *m* of 12.5-GHz as defined in [37] to be occupied by the elastic optical signal. The restful server has knowledge of the hardware state composition of the OTN switch and elastic transmitter. When a new frequency demand has been interpreted and is compatible with transmitter capabilities, low-level commands are sent via a 1GE link to the hardware controller of the OTN switch matrix 1830PSS-36. The linux kernel of this hardware controller has been modified to adapt the commands coming from the restful server into register access orders with hand-checking. Inside the BVT box (Figure 15), a register map is programmed and used by a local controller to perform all the switching, memories and finite state machine control. It is able also to manage the number

L of OTU2 lanes at 10.7Gb/s that have to be multiplexed and demultiplexed, and to control the baud rate of the high speed interfaces in order to generate the appropriate multiplexed flow. As the output baud rate can vary from 5.3 Gbd to 26.7 Gbd to generate a multiplexed optical PM-QPSK signal from 21.4 Gb/s to 107 Gb/s, the Restful server sends the corresponding number of slots *m*, with *m*=1, 2 or 3. Thus the maximum spectral occupancy in term of flexgrid slots is 37.5GHz for this experiment and granularity. This can be easily adapted to higher bit rates and finer granularities.

3.6.2 Final Integration of Metro/Core Border Node (in Bristol)

This section is the follow-up of the previous subsection 3.6.1 and shows the final setup with both data plane and full control plane experiments. The partners involved were Alcatel-Lucent Bell Labs France, Alcatel-Lucent Italy, CTTC and the University of Bristol. The data plane hardware and software elements were installed in the Bristol facilities. To this end, Alcatel-Lucent Bell Labs sent its commercial OTN Switch matrix, FPGA-based elastic interface and Restful server to Bristol.

For the demonstration, two nodes were set up. Each node included: (I) a flexible and configurable digital cross connect (OTN fabric) for client mapping and centralized control of S-BVT; (II) real-time S-BVT modules carrying multiple OTU2 tributaries thanks to programmable FPGAs and a (multi-flow) optical front-end that can adapt its symbol rate such as 107Gb/s, 53.5Gb/s per carrier [38] and its number of carriers according to the reach, physical impairments or capacity demand; (III) an optical matrix that provides flexibility through AoD in terms of synthesis of fibre switching cross-connections, optical bandwidth switching with bandwidth variable WSS [39]; and (IV) an offline coherent receiver, able to recover the transmitted signals. Figure 16 shows the schematic setup of the demonstration (the coherent receiver is not included in Figure 16).

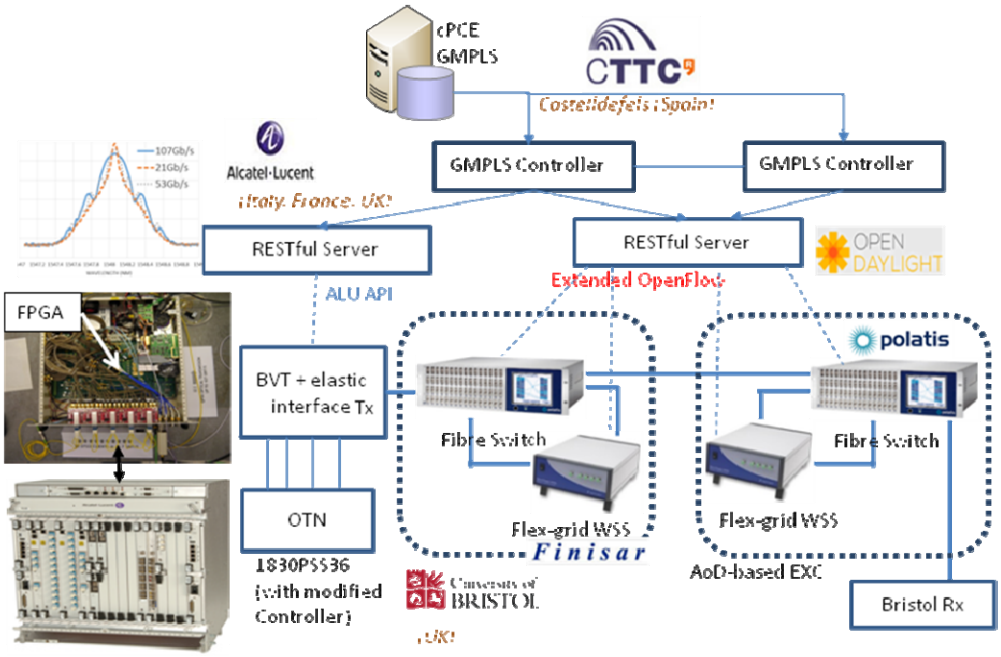

Figure 16: Schematic of the border node and the elastic network based on EXCs

Figure 16 shows that the GMPLS control plane is able to configure the underlying hardware (via the connection control interface) by using dedicated REST API interfaces, as mandated by the signaling process. This covers the cross-connection configuration, the WSS filters and the S-BVT. Middleware translates the high-level REST interfaces to the actual low-level hardware interface, so that it can, in particular, configure the number of physical OTU2 tributaries/lanes interfaced to the elastic BVT, and the required symbol-rate. If there are five OTU2 lanes to be carried, the BVT is configured at 13-GBd PM-QPSK. The middleware contains RESTful Servers, e.g. running as a northbound interface on top of a SDN ODL controller with their southbound interface based on extended OFP. The transport equipment (e.g., Fibre Switch and BV-WSS) has an OFP agent capable of translating the received OFP commands to specific equipment APIs (e.g., TL-1) [10].

Figure 17 shows a photograph of one part of the setup previously presented in Figure 16. In Figure 17, we can clearly see the commercial Alcatel-Lucent OTN switch together with its RESTful server and the FPGA-based real-time elastic BVT. Figure 17 also shows the AoD EXC with the optical fibre patchcords required for connectivity to the fibre links, amplifiers, BV-WSS, real-time BVT and coherent detector. In addition, Figure 17 shows the RESTFUL server used for the EXC/BV-WSS, where Open Day Light software is implemented and the off-the-shelf BV-WSS. The elements on the upper part of Figure 17 were brought from Paris to Bristol (BVT RESTFUL server, OTN Switch and BVT) so as to perform the collaborative data plane measurements.

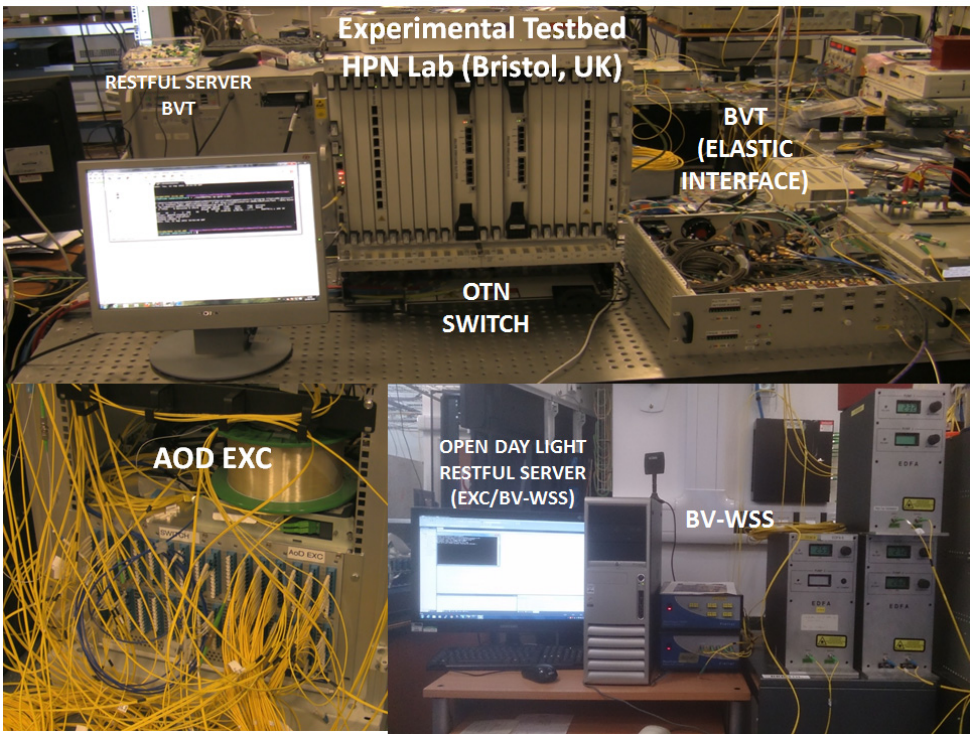

Figure 17: Photo of experimental setup at the University of Bristol

3.6.3 Attained results

Several tests from GMPLS controllers to the remote REST interfaces were performed successfully. Figure 18 shows the resulting BER vs. OSNR curves of the elastic S-BVT interfaces and DSP receivers from Alcatel-Lucent and University of Bristol. For ALU→UNIVBRIS, ALU's transmitter is used as well as the DSP of UNIVBRIS at the

receiver. Conversely, for UNIVBRIS→ALU, the S-BVT transmitter of UNIVBRIS is used and the DSP design of ALU. The figure shows constellations for the back-to-back and after-transmission cases including 175 km of SSMF and two AoD nodes.

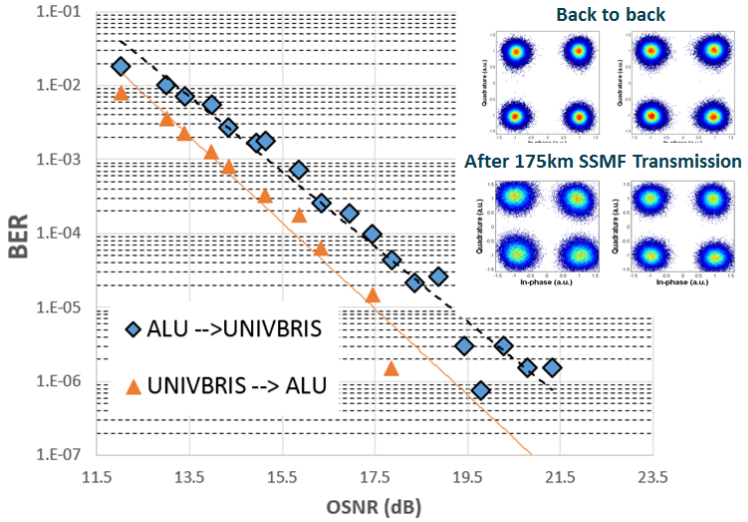

Figure 18: Back-to-back BER vs OSNR performance (ALU/UNIVBRIS), constellations for B2B/175-km transmission through 2 nodes using the elastic S-BVT

The total setup time for a new connection was also measured, such that including optical cross-connects, OTN switch and elastic interface a total setup of 6.12 seconds was measured for an end-to-end configuration of a 107-Gb/s connection. Further tests show that end-to-end reconfiguration restricted to elements between the RESTful server and S-BVT real-time transmitter (with no optical cross-connect reconfiguration here) only needs 0.89 seconds.

Figure 19 shows the GMPLS (RSVP-TE and OSPF-TE) and PCEP protocol messages used to set up the flexgrid connection within the flexgrid domain. The PCE receives a Path Computation Req message to compute a connection between the two end-points of the network (172.16.102.161 and 172.16.102.162) where the requested bandwidth is specified (107.1 Gb/s or 53.5 Gb/s). The PCE computes the explicit route in terms of nodes and links, the frequency slot (central frequency and slot width), as well as the modulation format to be used in the BVT in order to accommodate the requested flexgrid optical connection. This computed route is then passed to the ingress node (172.16.102.161) to trigger the connection via the RSVP-TE Path message. Once the egress node (172.16.102.162) receives the Path message, it responds with the RSVP-TE Resv message to confirm that the connection is established. During the exchange of the RSVP-TE messages, the configuration of the underlying optical network hardware is performed by means of the corresponding REST APIs. Last but not least, once the connection is successfully established, the OSPF-TE updates the status of the allocated resources at the control plane within the entire domain. For the sake of completeness. Figure 20 shows the REST API commands sent by the control plane in order to configure the flexgrid connection in the optical transport network elements formed by the fibre switch and the WSS.

Filter: pcep or rsvp or ospf — Expression... Clear Apply Save

Time	Source	Destination	Protocol	Info
2.037156	172.16.102.161	172.16.102.162	RSVP	HELLO Message.
2.037187	172.16.102.161	172.16.102.170	RSVP	HELLO Message.
3.971072	172.16.102.161	172.16.102.162	RSVP	PATH Message. SESSION: IPv4-LSP, Destinatio
3.971366	172.16.102.162	172.16.102.161	RSVP	ACK Message.
3.817040	172.16.104.201	172.16.102.161	PCEP	PATH COMPUTATION REQUEST MESSAGE
3.825789	172.16.102.161	172.16.104.201	PCEP	PATH COMPUTATION REPLY MESSAGE
3.905427	172.16.102.161	172.16.104.201	PCEP	NOTIFICATION MESSAGE
3.905460	172.16.102.161	172.16.104.201	PCEP	NOTIFICATION MESSAGE
3.963600	172.16.104.201	172.16.102.161	PCEP	Unknown Message (12).
4.021692	172.16.104.201	172.16.102.161	PCEP	KEEPALIVE MESSAGE
3.984380	10.0.5.2	224.0.0.5	OSPF	LS Update
3.987271	10.0.5.2	224.0.0.5	OSPF	LS Update
5.036006	172.16.102.160	172.16.102.161	ICMP	Destination unreachable (Host unreachable)
5.988291	10.0.5.1	224.0.0.5	OSPF	LS Acknowledge
6.806259	10.0.5.1	224.0.0.5	OSPF	Hello Packet
6.806593	10.0.5.2	224.0.0.5	OSPF	Hello Packet
7.039864	172.16.102.161	172.16.102.170	RSVP	HELLO Message.
7.039890	172.16.102.161	172.16.102.162	RSVP	HELLO Message.
8.236721	172.16.102.162	172.16.102.161	RSVP	RESV Message. SESSION: IPv4-LSP, Destinatio

Figure 19: Protocol captures (PCEP, GMPLS RSVP-TE and OSPF-TE) for establishing the flexgrid connection

Time	Source	Destination	Protocol	Info
.000000	84.88.62.99	137.222.177.97	HTTP	PUT /controller/nb/v2/flowprogrammer/default/node/OF/00:00:00:00:00:00:6c:56/staticCFlow/wss HTTP/1.1 (application/json)
.061439	137.222.177.97	84.88.62.99	TCP	[TCP segment of a reassembled PDU]
.061451	137.222.177.97	84.88.62.99	HTTP	HTTP/1.1 201 Created (application/json)
.114616	84.88.62.99	137.222.177.97	HTTP	PUT /controller/nb/v2/flowprogrammer/default/node/OF/00:00:00:00:00:00:05:1e/staticCFlow/backplane2 HTTP/1.1 (application/json)
.176321	137.222.177.97	84.88.62.99	TCP	[TCP segment of a reassembled PDU]
.176339	137.222.177.97	84.88.62.99	HTTP	HTTP/1.1 201 Created (application/json)
.253597	84.88.62.99	137.222.177.98	HTTP	PUT /Idealist/Test HTTP/1.1 (application/json)
.197579	137.222.177.98	84.88.62.99	HTTP	HTTP/1.1 200 OK
.249602	84.88.62.99	137.222.177.97	HTTP	PUT /controller/nb/v2/flowprogrammer/default/node/OF/00:00:00:00:00:01:28:2f/staticCFlow/wss HTTP/1.1 (application/json)
.310477	137.222.177.97	84.88.62.99	TCP	[TCP segment of a reassembled PDU]
.310696	137.222.177.97	84.88.62.99	HTTP	HTTP/1.1 201 Created (application/json)
.363769	84.88.62.99	137.222.177.97	HTTP	PUT /controller/nb/v2/flowprogrammer/default/node/OF/00:00:00:00:00:00:05:1e/staticCFlow/backplane1 HTTP/1.1 (application/json)
.425349	137.222.177.97	84.88.62.99	TCP	[TCP segment of a reassembled PDU]
.425362	137.222.177.97	84.88.62.99	HTTP	HTTP/1.1 201 Created (application/json)

Figure 20: REST API interfaces for configuring the flexgrid optical network elements (Fibre Switch and WSS)

3.6.4 Analysis of the results

From the curves depicted in Figure 18, a minimum penalty of <2 dB is observed, showing the effectiveness of interoperability between different elastic S-BVTs. The figure shows constellations for the back-to-back and after transmission cases, including 175 km of SSMF and two AoD nodes. With respect to the constellations in Figure 18, the results show the interoperability between the Alcatel-Lucent S-BVT transmitter and UNIVBRIS S-BVT receiver. These results are based on real-time FPGA devices and an oscilloscope for off-line processing. To our knowledge, this is the first experiment that involves control plane and data plane with real-time FPGA-based BVTs in a networking scenario considering an AoD structure. This control plane configures S-BVTs to adapt the transmission baud-rate and spectra to different conditions. More details of this application are shown in Section 3.17, experiment E18.

3.7 E8. Provisioning multicast connectivity in single-layer and multi-layer networks

Two approaches were proposed in [57] to provide large capacity (e.g. 100 Gb/s) multicast connectivity services in a multi-layer scenario, where a set of federated DCs are connected

through a flexgrid optical network. In the first approach, a VNT was created for each multicast request by establishing light-trees in the flexgrid network. In the second approach, multicast services were served on a multi-purpose VNT supported by 400-Gb/s lightpaths, thus favouring resource utilization. The feasibility of implementing both approaches using standardized control plane protocols was studied in WP4.

Use-case	Building Blocks			
	Algorithm suite (off-line and on-line)	Planning Tools for EON	GMPLS and OFP extensions for flexgrid	Network Orchestrator (ABNO)
Sliceability in multicast	X	X	X	X

Table 14: Use-case and Building Blocks associated with E8

Experimental assessment was carried out in the distributed field trial set-up depicted in Figure 21. The results of this experiment were reported in [58].

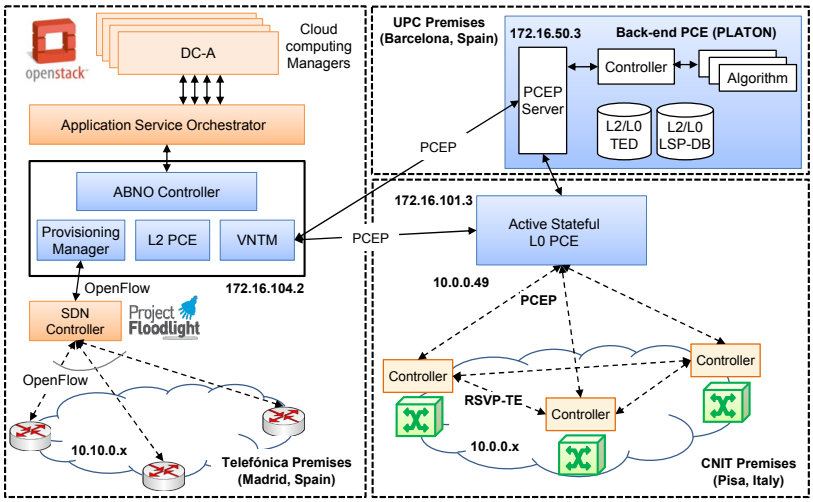

Figure 21: Distributed testbed set-up. IP addresses are shown

3.8 E9. Nonlinear pre-distortion of electrical driving signals in optical transmitters

The goal of this experiment was the validation of a nonlinear pre-distortion approach to compensate for nonlinearities introduced by the components in the optical transmitter. This nonlinear pre-distortion approach was able to significantly improve the back-to-back performance of the system. It is therefore very likely, that the maximum transmission distance for the particular systems can also be made to be substantially larger.

Use-cases	Building Blocks		
	Algorithm suite (off-line and on-line)	Performance metrics for network modeling and experiments	BVT and S-BVT

OTN over optical grooming	X	X	X
Ultra-high capacity and long-reach transmission	X	X	X

Table 15: Use-cases and Building Blocks associated with E9

3.8.1 Description of the setup

The transmitter considered in this work was composed of a 4-channel DAC with a nominal resolution of 8 bits, a 4-channel differential drive amplifier (DA) and a dual-polarization IQ-modulator. DAC and DA were modeled jointly by a Volterra series, whose coefficients were obtained from a least-squares fit to an input/output measurement. Each channel of the DP-IQ modulator was modeled independently as a dynamic linear response introduced by the electrode's frequency response and walk-off between the electrical and optical waves, followed by a static nonlinear response given by the sinusoidal electro-optical transfer function of the Mach-Zehnder interferometers. The frequency response and the sinusoidal transfer function were obtained from measurements. Based on the models of the transmitter shown in the setup, a pre-distorting filter for the electrical components and the modulators was derived independent of each other.

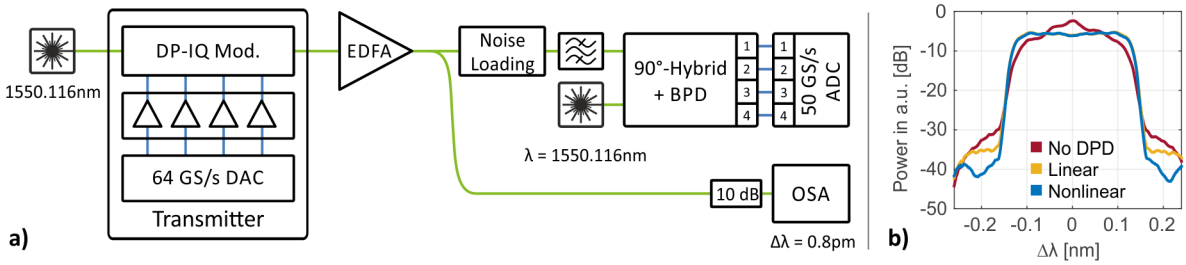

Figure 22: a) Experimental setup used to measure the optical back-to-back performance of a 32 GBd PDM-16-QAM single channel. b) Measured spectra show reduced out-of-band frequency components when nonlinear DPD is applied. Figure taken from [22]

The full nonlinear pre-distortion chain was as follows: application of inverse sinusoidal transfer function, compensation of the linear frequency response of the modulators, nonlinear Volterra filter to compensate for the electrical components.

In a first validation step, the electrical components seen in Figure 22(a) were first characterized without the electro-optical conversion, and our approach was then compared to a purely linear one by evaluating the BER as the SNR was varied.

In a second step, the setup in Figure 22(a) was used to evaluate the optical back-to-back performance for the case not only of a nonlinear and linear pre-distortion, but also for no pre-distortion of any of the transmitter devices.

3.8.2 Attained results

In this first step, the influence of a nonlinear pre-distortion of just the electrical components was investigated for a 28 GBd signal with a RRC pulse shape and several higher-order

QAM formats, namely 16-, 32-, 64- and 128-QAM. The results obtained for nonlinear and linear pre-distortion are compared to the AWGN channel in Figure 23.

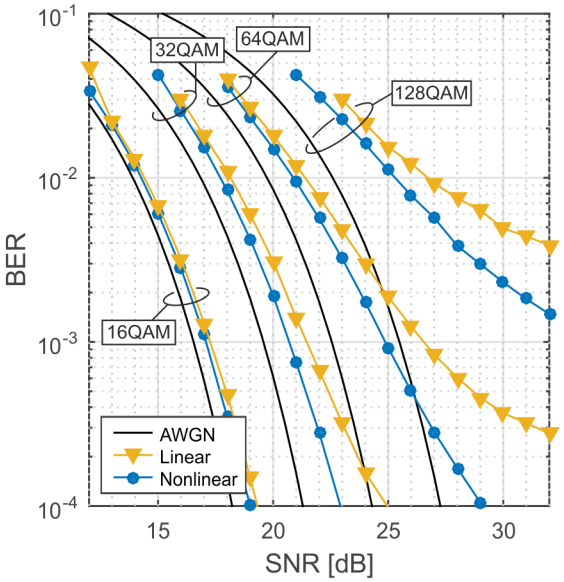

Figure 23: Electrical BER measurement of 28 GBd 16-, 32-, 64-, and 128-QAM signals with a RRC pulse shape for linear and nonlinear pre-distortion. Figure taken from [22]

For clarity, the penalties in required SNR for a BER of 10^{-2} are shown below in Table 16.

	Linear DPD	Nonlinear DPD
16-QAM	0.6	0.5
32-QAM	1.3	0.9
64-QAM	1.7	1.2
128-QAM	4.1	2.7

Table 16: SNR penalties to AWGN theory at BER=1E-2 in dB

In a second step, the pre-distortion approaches were compared in an optical back-to-back measurement, with 32 GBd polarization-division multiplexed 16-QAM modulated onto a single carrier. The first result is shown as a spectrum in Figure 22(b), which shows reduced nonlinear mixing products when using nonlinear pre-distortion. In Figure 24 the resulting waterfall curves are shown when nonlinear, linear and no pre-distortion are applied.

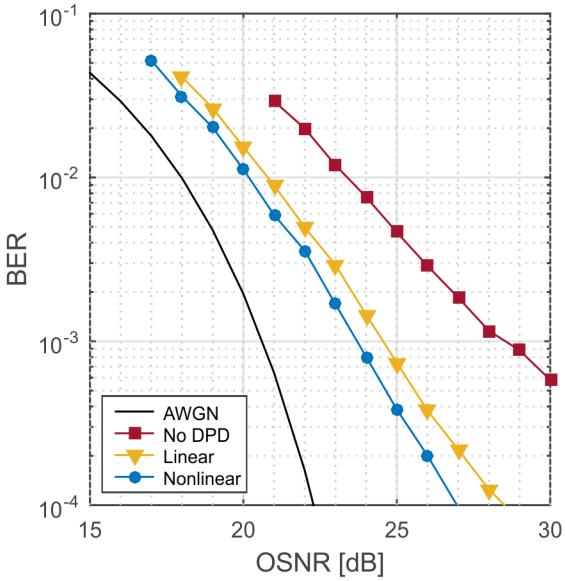

Figure 24: Optical back-to-back BER measurement of 32 GBd PDM-16-QAM for linear, nonlinear and no pre-distortion. Figure taken from [22]

3.8.3 Analysis of the results

The results obtained from the first investigation indicate greater improvement due to the use of nonlinear pre-distortion with higher cardinalities of the modulation format. The second investigation shows that compared to no pre-distortion the benefits of either linear or non-linear pre-distortion is very large. Therefore, nonlinear pre-distortion is seen to be of particular interest for format-variable transceivers, especially in the case of higher order modulation formats. These results and also the figure of this section were reported in [22].

3.9 E10. Super-channel Provisioning up to 1Tb/s

The goal of this experiment is to show the flexibility of the flexgrid S-BVT, hereafter referred to as Soft-FBVT provided by CNIT and TEI in terms of provisioning of different configurable superchannels at different bitrates, whose general architecture was defined in WP2. Different numbers of subcarriers and transmission parameters (e.g., modulation format, LDPC code rate) are considered. Performance in terms of optical reach, bit-error-rate and spectral efficiency are provided. Provisioning is driven by two alternative control planes: PCE/GMPLS and SDN. Extensions are used to properly configure the transmitter and receiver, and also the transit BV-WSS filters.

The WP4 components (as defined in [58]) of the experiment are the CNIT and TEI Soft-FBVT, the CNIT PCE/GMPLS controllers and the CNIT SDN controller. The experiment has also been reported in [23] and [24].

Use-cases	**Building Blocks**				
	Algorithm suite (off-line and on-line)	Performance metrics for network modeling and experiments	BVT and S-BVT	Flexgrid ROADM and BV-OXC	GMPLS and OFP extensions for flexgrid

IP over Optical control	X		X	X	X
Dynamic provisioning including DC interconnection	X	X	X	X	X
Ultra-high capacity and long-reach transmission	X	X	X	X	

Table 17: Use-cases and Building Blocks associated with E10

3.9.1 Description of the setup

Two sub-experiments are hereafter described: sub-experiment 1 shows the ability to generate different types of superchannel (i.e., at 400 Gb/s and 1 Tb/s) by means of the CNIT control plane, whereas sub-experiment 2 evaluates the detailed performance of a 1-Tb/s superchannel as a function of the code rate and the number of traversed filters.

Sub-experiment 1

Super-channels with R = 1.12 Tb/s, N = 3 (480 Gb/s) and 7 (1.12 Tb/s), S = 28 GHz, and B = 200 GHz have been generated. The testbed of the data plane is shown in Figure 25. A recirculating loop is exploited to vary the all-optical reach. N = 3 (7) optical carriers are generated by means of 100-kHz linewidth tunable laser sources. In particular, the odd and even channels are modulated separately by means of two integrated double-nested Mach-Zehnder modulators (IQ-MZM). 40-Gb/s LDPC-coded electrical signals are applied to the in-phase (I) and the quadrature (Q) ports of the modulators. This way, 80 Gb/s QPSK channels are obtained. The bit-rate is then further doubled up to 160 Gb/s per channel, by emulating polarization multiplexing through a 50/50 beam splitter, an optical delay, and a polarization beam combiner. A first programmable SSS (SSS1) is used to separately filter and multiplex the odd and even channels.

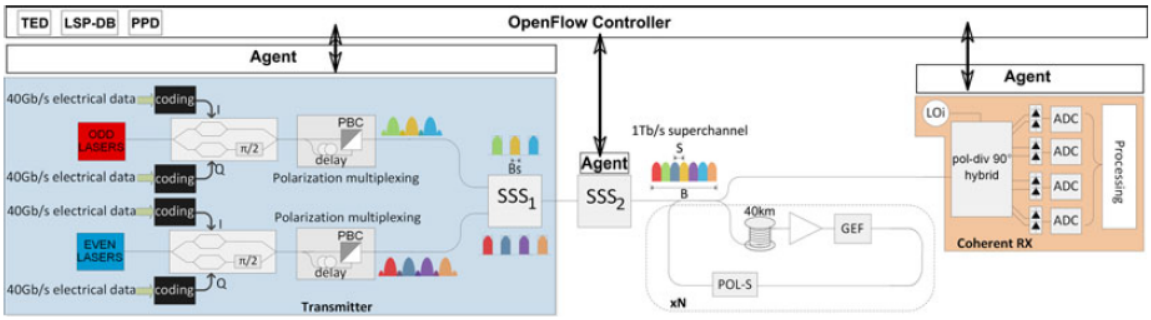

Figure 25: SuperChannel provisioning. Sub-Experiment 1 testbed

The generated signal enters the ingress node, which is emulated by the second SSS (SSS2), and it is then transmitted through a recirculating fibre loop (used to emulate the signal transmission over a real link) by means of a 50/50 optical beam splitter. The recirculating loop is composed by a 40-km-long standard single mode fibre spool followed by an EDFA and a GEF. A polarization scrambler in the loop emulates random signal polarization variation. The whole testbed is handled and configured by the CNIT SDN control plane, extensively described in [58].

Sub-experiment 2

The second experimental testbed is shown in Figure 26. N optical carriers are generated by means of 100-kHz linewidth TLSs. The odd and even channels are modulated separately by means of two integrated double-nested Mach-Zehnder modulators (IQ-MZM). 40-Gb/s LDPC-coded electrical signals are applied to the in-phase (I) and the quadrature (Q) ports of the modulators. In this way, 80 Gb/s QPSK channels are obtained. The bit rate Rs is then further doubled up to 160 Gb/s per channel, by emulating polarization multiplexing through a 50/50 beam splitter, an optical delay, and a PBC. Thus, in this experiment, the bit rate Rs of each sub-carrier is fixed. Electrical 9th-order 10-GHz low-pass filters are used in order to limit the sub-carriers bandwidth and allow a sub-carrier spacing of 20 GHz. Thus a spectral occupation lower than the Nyquist bandwidth is obtained. A simple beam combiner is used as the multiplexer for the odd and even channels. A recirculating loop structure is used to emulate the signal transmission along different network nodes. The recirculating loop is composed of a Finisar SSS and two 40-km-long standard single mode fibre spools, each one followed by an EDFA. A GEF is used to balance the distortions due to the amplifier profile, and a polarization scrambler is included in the loop to emulate random signal polarization variation. The Finisar SSS emulates intermediate nodes. A broadcast-&-select node architecture is assumed, so that traversing a node implies a single filter stage as in each loop. With such a re-circulating loop configuration, filtering effects are emphasized, since a filter is traversed after just 80 km, while a link in a backbone is composed of several 80-km spans. Coherent detection is applied with offline processing.

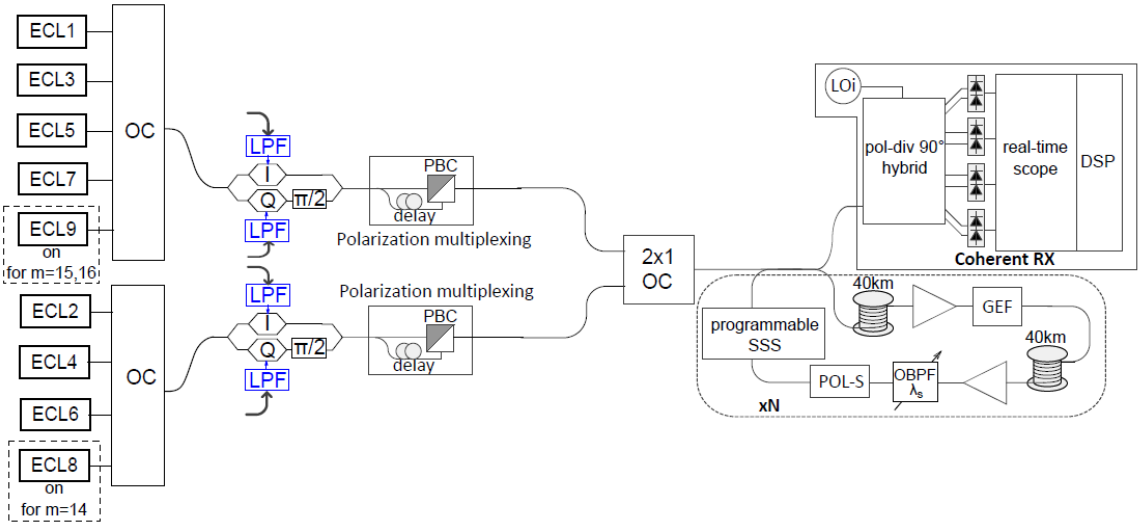

Figure 26: SuperChannel provisioning. Sub-Experiment 2 testbed

3.9.2 Attained results

Sub-experiment 1

Given the path length, the highest code rate (i.e., lowest redundancy) guaranteeing error-free transmission after forward-error-correction is selected. Based on the code rate and the fixed R, m, the information rate RI is derived. Figure 27 shows the information rate versus the path length. Thus, each path length in the plot is associated with the suitable code rate. Then, given the selected code rate, the information rate is shown. As an example, for a path length of 3000 km, a code rate of 9/10 assures error-free transmission. With a 9/10 code rate, an information rate of around 1 Tb/s is achieved. Figure 27 shows that the

redundancy of the code increases with the path length because more robustness to the impairments is required. Consequently, the information rate decreases with the path length, if R is fixed. For example, an information rate of 1 Tb/s can be assured for a path length of 3000 km, while for a length of 5250 km the information rate is reduced by around 17% with respect to 1 Tb/s.

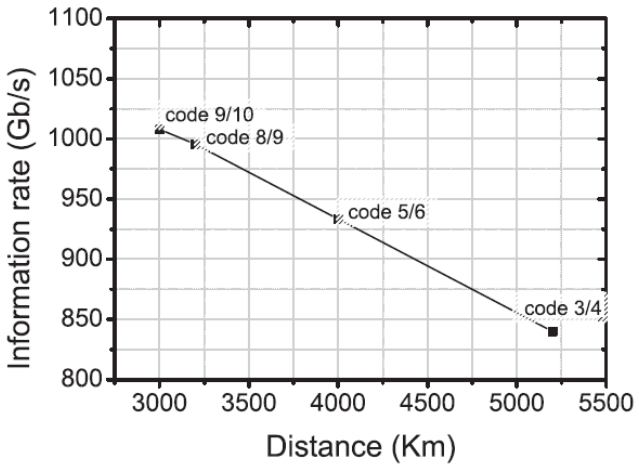

Figure 27: Information rate vs optical reach for gross Terabit

For 400-Gb/s transmission (480 Gb/s gross rate, 3 subcarriers instead of 7), the same behaviour is obtained, with a properly scaled Y axis. In particular, at 3000 km we obtained an information rate of about 400 Gb/s with 8/9 code rate. Similarly, code 3/4 achieves 5250 km with a 350-Gb/s net information rate (17% of reduction).

The transmission parameters information derived from such experiments has been uploaded in the PPD exploited by the implemented OF-controller, in order to select the proper transmission parameters upon connection request. The OF-controller performs path computation, then, by exploiting PPD, selects the proper transmission parameters (e.g., code rate) to guarantee error-free transmission along the computed path. First, a request of RI = 1 Tb/s is considered in a flexgrid scenario, with OF messages exchanged in the control plane. The OF-controller processes the request, computing a path of 3250 km. Based on measurements in Figure 27, the OF-Controller computes the proper transmission parameters (e.g., RC =5/6, N = 8). Figure 28 shows the OF messages exchanged within the control plane between the OF Controller (IP 10.0.0.49) and the OF switch agents (IP 10.0.0.x, x ∈[1], [4]) that are co-located within the four testbed nodes and are responsible of configuring the transmitter/receiver physical parameters and the SSS filter shapes. In particular, Figure 28 shows a capture of the OFPT_FLOW_MOD message sent to the ingress node. The OFPT_FLOW_MOD message includes the proposed OFPT_OCH_SPEC OF struct for time frequency packing. As shown in the figure the struct includes: 1) type of channel: multicarrier; 2) N = 8; 3) Rs = 160 Gb/s; 4) sub-carrier modulation format: PM-QPSK each; 5) sub-carrier central frequency (e.g., 192.894 GHz); 6) Bs = 28GHz; 7) Nyquist flag: time frequency packing; 8) the type of adopted code: LDPC; 9) RC = 5/6 for a path length of 3250 km. Moreover, the SSS2 is set to n = −22 and m = 18 for the super-channel pass-through.

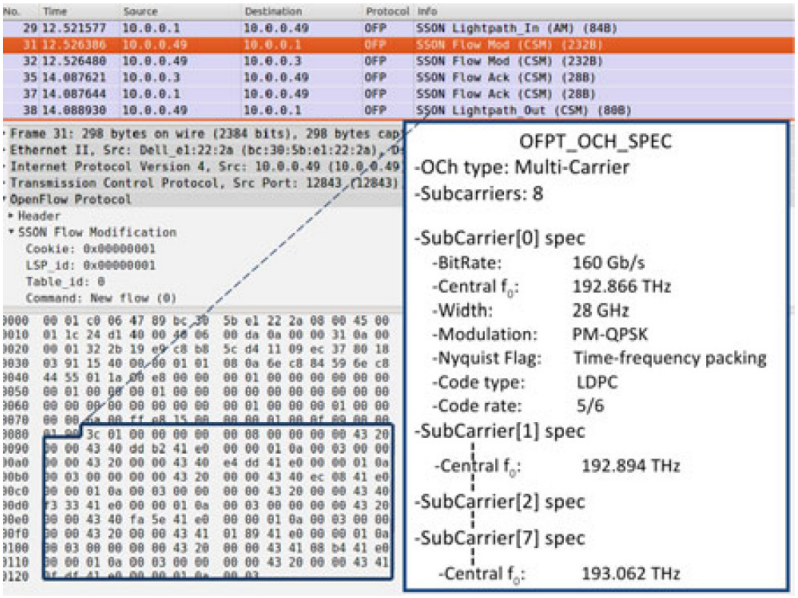

Figure 28: Control plane messages for Soft-FBVT provisioning (1 Tb/s)

Sub-experiment 2

Figure 29 shows the relation between the code rate, the optical reach, and the number of traversed nodes (thus, including filtering), the number of sub-carriers N, and m for a 1-Tb/s superchannel. Reported values satisfy the criteria for error free transmission. Such relations have been identified through measurements on a 1-Tb/s information-rate super-channel considering the re-circulating loop, by adding a SSS Finisar waveshaper inside the 80-km loop. Bi and Ri were set to 20 GHz and 160 Gb/s, respectively. For example, it is possible to see that a ci = 8/9 guarantees QoT for a path of four nodes when m = 12 (150 GHz is larger than B = 140 GHz). If five nodes instead of four have to be traversed, the same redundancy can be kept, but the filters have to be enlarged, thus m = 13. If six nodes have to be traversed more redundancy is required (ci = 4/5) enabling up to eight nodes in the path. Finally, we clarify that the QoT is mainly affected by filtering effects; indeed, without filters in the loop, 5000 km is able to be reached. Regarding the complexity of code-adaptive TFP, PM-QPSK TFP requires a transponder that only supports PM-QPSK; thus a DAC at the transmitter is not required. At the receiver, TFP requires a sequence detector. Conversely, format-adaptive NWDM requires a DAC at the transmitter (e.g., to support 16QAM), with symbol-by-symbol detection at the receiver. From the figure we can deduce that the achieved spectral efficiency is equal to 6.1 bit/s/Hz.

c_i	Reach [km]	Traversed nodes	N	B [GHz]	*m* and width [GHz]
8/9	320	4	7	140	m=12; 150
8/9	400	5	7	140	m=13; 162.5
4/5	640	8	8	160	m=14; 175
3/4	720	9	9	180	m=15; 187.5
3/4	1500	12	9	180	m=16; 200

Figure 29: Relation between code rates, reach and superchannel features (1 Tb/s)

3.9.3 Analysis of the results

Distance-adaptive-Tb/s transmission has been demonstrated for the Soft-FBVT. The first experiments reported a control plane configuration of 400 Gb/s and 1 Tb/s superchannels, with different number of sub-carriers, and the evaluation of the optical reach. In the second experiment, detailed results for 1 Tb/s with different configurations of subcarriers, spectrum and occupied frequency slots determining different optical reach values with different code rates have been provided. The Soft-FBVT can be configured with a different set of code rates, number of carriers in order to fit a desired frequency slot and achieve a desired optical reach. Results show that PM-QPSK-based Terabit can be conveyed in a (140, 180) GHz range, corresponding to a (150, 200 GHz) flexgrid frequency slot width, depending on the desired optical reach. The maximum obtained optical reach is 1500 km and 12 traversed nodes (up to 5000 km if intermediate nodes are not considered), with 3/4 code rate. The achieved spectral frequency is very high, at about 6 bit/s/Hz.

3.10 E11. Multi-wavelength sliceable provisioning

The goal of this experiment is to show the capability of the Soft-FBVT for provisioning optical channels with the same laser source with configurable asymmetric spacing and routing them to different output ports of the transmitter, thus enabling sliceability functionality. The multi-wavelength source is evaluated in terms of stability and bit-error-rate measurements at the receivers. SDN control plane extensions are used to configure the transmitter multi-wavelength source and to enforce sliceability.

The WP4 components (as defined in [58]) of the experiment are the CNIT and TEI Soft-FBVT and the CNIT SDN controller. The experiment has been also reported in [25].

Use-cases	**Building Blocks**				
	Algorithm suite (off-line and on-line)	Performance metrics for network modeling and experiments	BVT and S-BVT	Flexgrid ROADM and BV-OXC	GMPLS and OFP extensions for flexgrid
Resource allocation in EON	X		X	X	X
IP over Optical control	X		X	X	X
Dynamic provisioning including DC interconnection	X	X	X	X	X
Sliceability in multi-path	X	X	X	X	X

Table 18: Use-cases and Building Blocks associated with E11

3.10.1 Description of the setup

The testbed is depicted in Figure 30, where 480-Gb/s optical signals are considered. The Soft-FBVT at the transmitter side is based on a PAMW source generating three sub-carriers. It includes a LDPC encoder, three PM-QPSK transmitters, each one modulating a

sub-carrier and achieving 160 Gb/s PM-QPSK, and a coupler to multiplex the modulated sub-carriers. Sliceability is supported thanks to SSSs, i.e. the sub-carriers are selected by a specific port through the proper configuration of the SSS passband, while they are blocked by the other SSSs. At the receiver side, the transponder is composed of three coherent receivers, one for each possible sub-carrier. For each coherent receiver, a tunable laser used as a LO must be tuned in order to match the proper sub-carrier. As a result, two optical signals beat into the opto/electronic conversion module providing four analog electrical signals. ADC conversion is performed and DSP is used. Each receiver includes an LDPC decoder.

The PAMW architecture generating three sub-carriers is shown in Figure 30(d). The architecture is based on IQ modulators driven by radio frequency (RF) clocks and configured as single side-band suppressed carrier modulation generation (SSBG). A TLS provides the central subcarrier at a frequency f0. The sub-carrier at f0 is split into three branches, to create three sub-carrier copies. One is kept at f0, while the other two are shifted in frequency, exploiting the SSBG. RF clocks f1 and f2 determine the sub-carrier spacing. In particular, SSB is achieved as follows. A relative phase difference of π/2 is introduced into the RF signals while entering into the inputs of the IQ modulator. The shift towards higher or lower frequencies (e.g., ±f1) is achieved with a proper configuration of the IQ bias by introducing a phase difference of +π/2 or −π/2. Both symmetric and asymmetric carrier spacing can therefore be achieved by choosing the appropriate RF clocks. Three sub-carriers are therefore obtained at f0, f0 − f1, and f0 + f2.

Control plane extensions are proposed to enable path computation and node configuration (e.g., S-BVT), aware of the constraints imposed by the use of different source types (e.g., PAMW, and MW generating contiguous and symmetric sub-carriers). The SDN control plane is assumed to have OpenFlow protocol and proper extensions. The physical parameters of the computed optical signal (i.e., single or multi-carrier) are carried by the OCH SPEC subobject enclosed within the FLOW MOD message sent by the OpenFlow controller to the OpenFlow agent co-located within the source node. Three fields of the OCH SPEC are therefore proposed, associated with each single generated signal: the related source type field, specifying: 1) the kind of source, e.g. S-BVT composed of tunable lasers, MW source generating contiguous/symmetric sub-carriers (with constraints), or PAMW source; 2) the laser id (belonging to an S-BVT), i.e. the identifier of the physical laser source; 3) the tone id, i.e. the identifier of the frequency tone generated by the indicated source and associated with the signal through its central frequency (as an example, PAMW may hold multiple tone ids; i.e. three in our implementation).

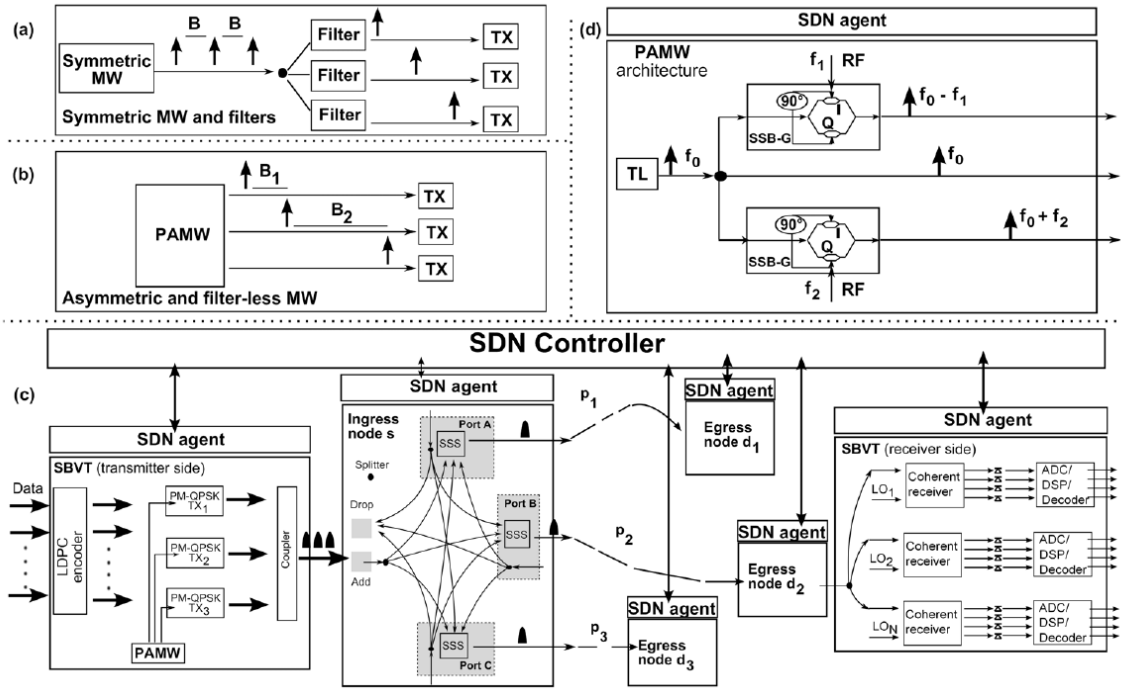

Figure 30: Multi-wavelength CNIT Soft-FBVT testbed

3.10.2 Attained results

A first set of results demonstrates the sliceability of the Soft-FBVT and the asymmetry of the channels generated by PAMW. Three 160-Gb/s PM-QPSK channels are generated. Two channels are spaced by 25 GHz, while the third one is spaced out by the central channel of 37.5 GHz. Figure 31(a) and Figure 31(b) show the spectrum at the output of the PAMW source, before modulation, for the sub-carriers f0 − f1 (with f1 = 37.5 GHz), and f0 + f2 (with f2 = 25 GHz), when f0 = 192.8125 THz. Figure 31(c) shows the spectrum of the modulated sub-carriers with asymmetric spacing, after the coupler. Such sub-carriers are then filtered and sliced by the SSSs with a ITU-T flexgrid bandwidth of 25 GHz. Figure 31(d) shows BER measurements vs. OSNR for the three sub-carriers, named ch1, ch2, and ch3, after transmission along different paths of 80, 70 and 70 km.

In a second set of results, superchannel functionality is demonstrated: the S-BVT and MW are programmed to generate a 480 Gb/s super-channel, composed of 3 × 160-Gb/s sub-carriers spaced by 20 GHz (total 60 GHz), within an ITU-T flexgrid frequency slot of 62.5 GHz. Figure 31(e) shows the spectrum of the modulated super-channel after the coupler. Figure 31(f) shows BER measurements vs. OSNR for the three sub-carriers, after transmission along 80 km of fibre.

Finally, Figure 32 shows a capture of the control plane messages at the OpenFlow controller (IP 10.0.0.49) related to the third experiment. Open-Flow packets trigger the three channels setup in sequential and independent fashion. The FLOW MOD message to the source OpenFlow Agent (10.0.0.1) referred to the left side channel of Figure 31(c) is expanded, showing the SSS assigned frequency slots (n,m) (6.25 GHz channel spacing is assumed) and the OCH SPEC fields including the selected source specifications.

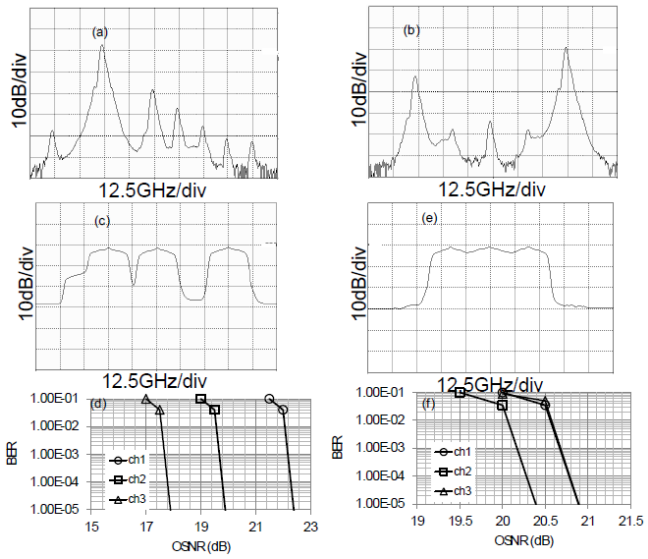

Figure 31: Soft-FBVT sliceability experimental results with PAMW

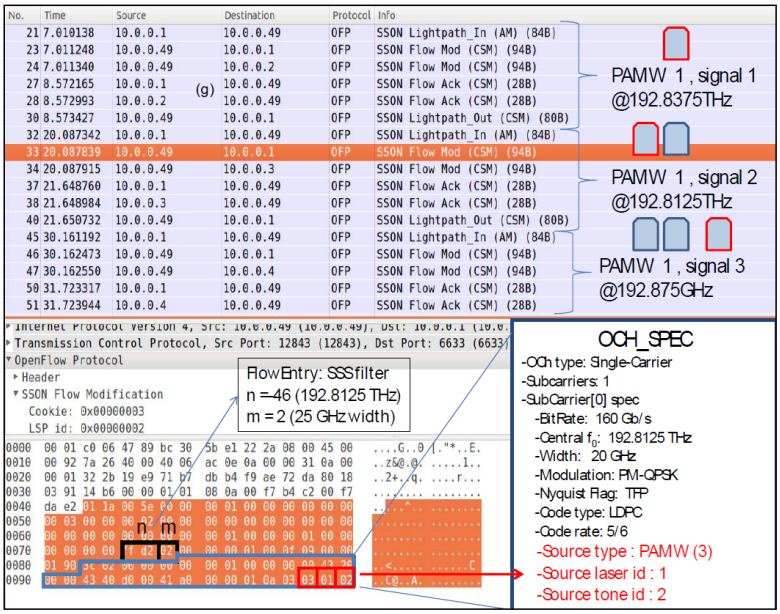

Figure 32: Control plane capture showing PAMW OpenFlow extensions

3.10.3 Analysis of the results

In the first experiment, we obtained a side-band suppression of about 15 dB for f0 + f2 (Figure 31b) and more than 20 dB for f0 − f1 (Figure 31a). In both cases f0 was suppressed by more than 20 dB (Figure 31a,b).

For all the tree connections (i.e., ch1, ch2, ch3), a BER lower than 10^{-5} is achieved for the OSNR of the paths (i.e., the maximum OSNR).

In the second set of results, we can observe that a BER lower than 10^{-5} is achieved on the path. The adoption of such extensions within the FLOW MOD message may be achieved by providing the information of the number and the type of sources installed at a source node during the node discovery phase. In particular, for the PAMW sources, additional

information such as the maximum number of programmable frequency tones, the maximum frequency offset, the maximum all-optical reach (or the required OSNR to achieve a given BER) may help to improve path computation effectiveness. The proposed OpenFlow extensions are able to select a single PAMW source with the same laser id and different incremental tone identifiers, thus fully enabling sliceable Soft-FBVT provisioning with PAMW.

3.11 E12. Differentiated filtering and Super-Filter

The goal of this experiment is to validate optimization methods for the occupancy of channel and superchannels in EONs. Differentiated filter configuration (DFC) and Super Filter techniques proposed in WP2 and WP3 are enforced to signals generated and received by the Soft-FBVT. DFC allows a lightpath to be configured with different filter widths at each intermediate node. Super Filter allows co-routed segments of different lightpaths to share a unique filter configuration. Extensions implemented at the SDN controller enable the two methods to be driven and controlled by the control plane. DFC is evaluated in both a pure EON scenario and a hybrid EON/DWDM scenario. SuperFilter is evaluated in an ad-hoc testbed employing a recirculating loop in order to evaluate the feasibility of the technique as a function of the number of traversed BV-WSSs.

The WP4 components (as defined in [58]) of the experiment are the CNIT and TEI Soft-FBVT and the CNIT SDN controller. The experiment has been also reported in [23] and [26].

Use-cases	**Building Blocks**				
	Algorithm suite (off-line and on-line)	Performance metrics for network modeling and experiments	BVT and S-BVT	Flexgrid ROADM and BV-OXC	GMPLS and OFP extensions for flexgrid
Resource allocation in EON	X		X	X	X
Dynamic provisioning including DC interconnection	X	X	X	X	X
Ultra-high capacity and long-reach transmission	X	X	X	X	

Table 19: Use-cases and Building Blocks associated with E12

3.11.1 Description of the setup

Sub-experiment 1: DFC

The testbed utilized for the DFC experiment is derived from the one described in Section 3.9.1 (experiment E10, sub-experiment 1). In particular, a 50-GHz fixed-grid WSS is inserted between the EDFA and the GEF of the recirculating loop. To fit the fixed-grid, a 1-Tb/s super-channel is designed as in sub-experiment 1 of E10. In this case, the super-channel is deployed with N = 8. Sub-carrier spacing is designed such that two sub-carriers can be accommodated within the 50-GHz fixed grid. This means that the super-channel can occupy 4 × 50 GHz = 200 GHz. The baud rate of each sub-carrier is set to 35 or 40 Gbaud.

Sub-experiment 2: Super-Filter

The data plane experimental setup is shown in Figure 33. The Soft-FBVT employs the TFP technique, with LDPC coding and off-line coherent detection adopted. Three carriers are generated by means of a 100-kHz linewidth TLS. In particular, the central carrier and the other two side-carriers are separately modulated by using two integrated double-nested Mach-Zehnder modulators (IQ-MZM). LDPC code is inserted by the encoder module shown in the figure. In addition, 30-Gb/s coded electrical data are applied to the in-phase (I) and quadrature (Q) ports of the modulators. In this way, QPSK channels with a gross bit-rate of 60 Gb/s are obtained. The bit-rate is then further doubled up to 120 Gb/s per channel by utilizing polarization multiplexing via a 50/50 beam splitter, an optical delay, and a PBC. The rate of the LDPC code used is equal to 9/10. A further 4% of redundancy is considered in order to allow error-free operation (after decoding, since the LDPC code has an intrinsic floor), thus providing a net bit-rate of 103.8 Gb/s. A programmable BV-OXC is used to separately filter and multiplex the channels. A recirculating loop is used to reproduce the transmission of the channels through a cascade of nodes. The recirculating loop is comprised of two spans of 40-km-long standard single-mode fibre spools followed by an EDFA amplifier. A second programmable BV-OXC is used in the loop in order to specifically reproduce the cascading of several filters. A polarization scrambler in the loop emulates random polarization variation. All channels enter into the common port of the BV-OXC. The channels are then filtered and separated, and then coupled again together at the BV-OXC output.

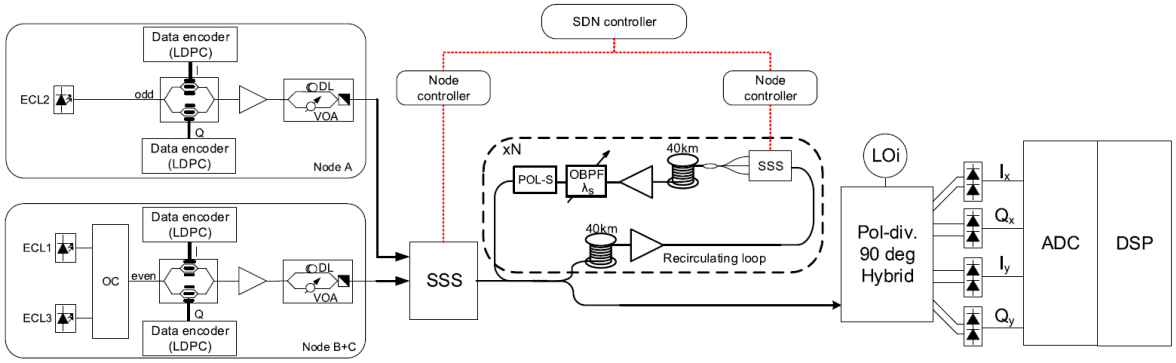

Figure 33: SuperFIlter data plane setup

3.11.2 Attained results

Sub-experiment: DFC

Figure 34 shows the Terabit spectrum to fit the fixed grid, the WSS filter shape, the spectrum of the generated superchannel, and its spectrum after 15 recirculating loops.

Figure 35 shows the information rate vs. the number of crossed WSSs for different values of carrier baud rate. During the experiment, the passband of SSS2 at the ingress node was set to 225 GHz (i.e., larger than 200 GHz) thus allowing filtering to operate in the flat region and resulting in negligible SSS filtering effects. The maximum number of WSSs experimentally crossed is 15 at 4.2 b/s/Hz and 35 Gbaud (RC = 3/4, RI = 0.84 Tb/s). On the other hand, at a spectral efficiency of 5.69 b/s/Hz and 40 Gbaud (RC = 8/9, RI = 1.138 Tb/s) up to five WSSs could be traversed.

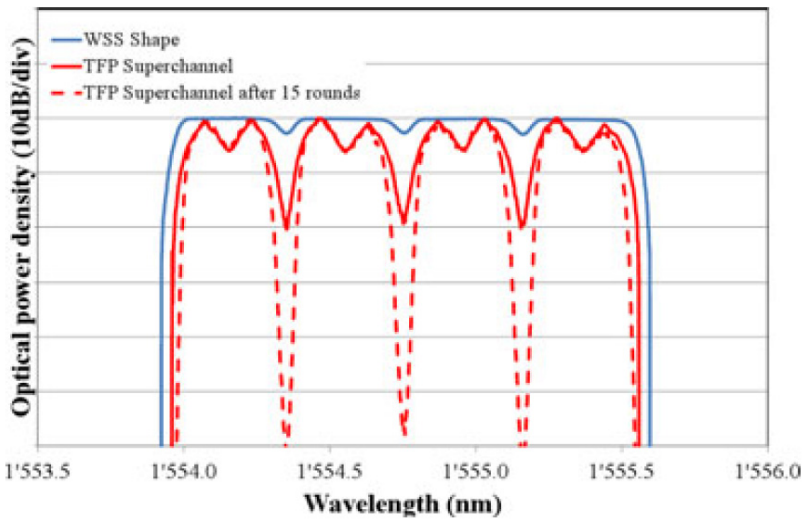

Figure 34: Terabit spectrum in presence of BV-WSS

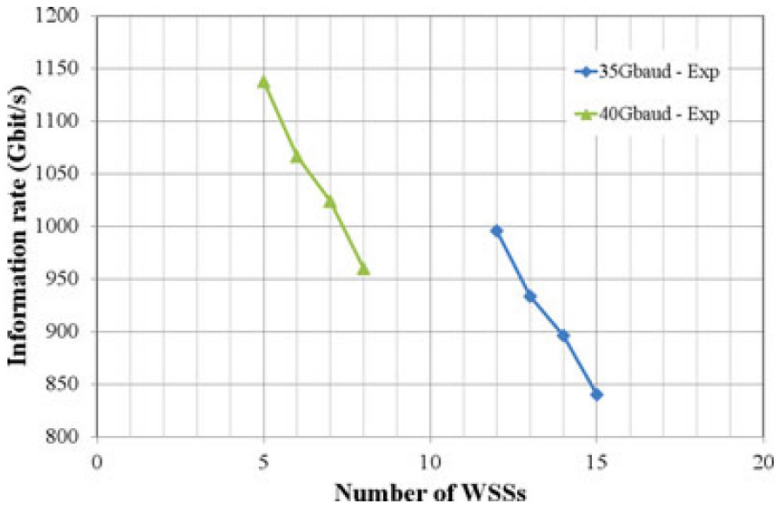

Figure 35: Information rate vs crossed WSSs in mixed fixed-flexgrid scenario

Control plane message capture is also performed in the mixed fixed/flexgrid scenario to demonstrate the effectiveness of SDN-based DFC. A request of RI = 1 Tb/s is assumed. The OF-controller processes the request, computing a path of thirteen nodes, thus including SSS2 at the ingress and twelve WSSs in the other nodes (each one emulated in the recirculating loop). Transmission parameters are selected (e.g., 35 Gbaud corresponding to Rs = 140 Gb/s and RC = 8/9) based on measurements in Figure 35, obtained with a SSS2 passband of 225 GHz and WSS passbands of 4 × 50 GHz (as in Figure 34). Figure 36 shows two OFPT_FLOW_MOD messages sent to the ingress node equipped with a SSS (packet 99) and to an intermediate node equipped with a 50-GHz fixed grid WSS (packet 100), respectively. The recirculating loop is emulated within the control plane closed around node 2 (IP 10.0.0.2). The former message shows the spectrum label sent to SSS2 , employing flexible grid with m = 18 resulting in B = 225 GHz. The latter message shows the extended DWDM label simultaneously activating at the WSS four adjacent 50 GHz standard channels in order to shape the super-channel properly (as in Figure 34). The extended label version specifies the edges of the superchannel (expressed

as n values with 50 GHz channel spacing, in this case from n = −7 to n = −4) to be activated. The experiment demonstrated that SDN can easily handle DFC, thus differentiating the configuration of filters along the path (SSS to 225 GHz and WSSs to 50 GHz).

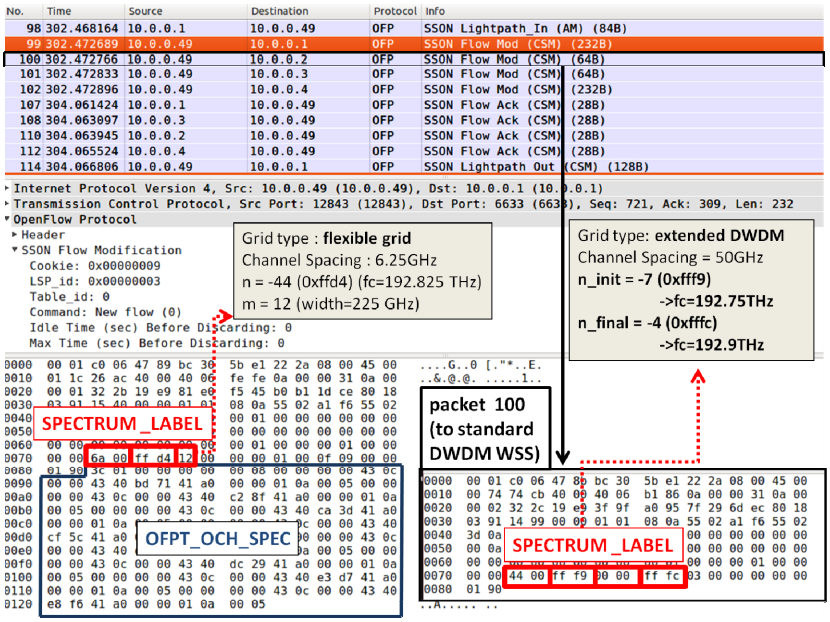

Figure 36: OpenFlow messages in DFC fixed/flexgrid scenario

Sub-experiment: Super-Filter

The scenarios considered for comparing experimental results are the following (where a 100-Gb/s single carrier signal is considered):

1) scenario 1: edge lightpaths are configured with 37.5 GHz filter, central lightpath is configured with 25 GHz. Spectral efficiency is greater; however the central lightpath may experience detrimental filtering effects.
2) scenario 2: all lightpaths are configured with 37.5 GHz filter, QoT is guaranteed, while spectral efficiency is reduced.
3) scenario 3: Super-filter, a unique filter is applied to the 3 lightpaths, with the same spectral efficiency of scenario 1; however the central lightpath experiences a flat region of the filter and QoT is preserved.

Figure 37 shows BER performances for the back-to-back configuration (BTB) and the aforementioned scenarios. The reported measures are performed by averaging over 10 blocks of samples, each containing eight randomly selected code words per quadrature per polarization (with code rate equal to 9/10). BER values below 10^{-6} could not be reliably measured, such that the LDPC error floor (expected to be below 10^{-6}) was not observed in the experimental setup. The system performance is also evaluated for all the scenarios, measuring the required OSNR to obtain error-free operation after a configured number of circulations in the fibre loop (i.e., number of traversed nodes). The OSNR penalty with respect to the signal at the transmitter is depicted in Figure 38. Considering the first scenario, an increasing penalty is measured when the number of traversed nodes increases. Error-free operation cannot be achieved for more than five traversed nodes, and a penalty of 7.5 dB is measured after five nodes (in agreement with the simulation results

reporting a penalty of 8 dB after five nodes). The optical spectrum of the channels at the transmitter and after five nodes (i.e., five fibre loop circulations) is reported in Figure 39, showing a clear filtering effect for the central channel. In Figure 38, the measurements for the second scenario are also reported. In this case, a minor penalty after only 10 nodes is experienced. Due to hardware constraints (only two BV-OXCs are employed in the testbed), the super-filter scenario is reported, focusing only on the cascade of super-filters. In particular, only one filter is traversed before the signal enters the recirculating loop. Results show a penalty of about 1 dB after 10 traversed nodes, thus confirming the successful behaviour of the proposed super-filter technique.

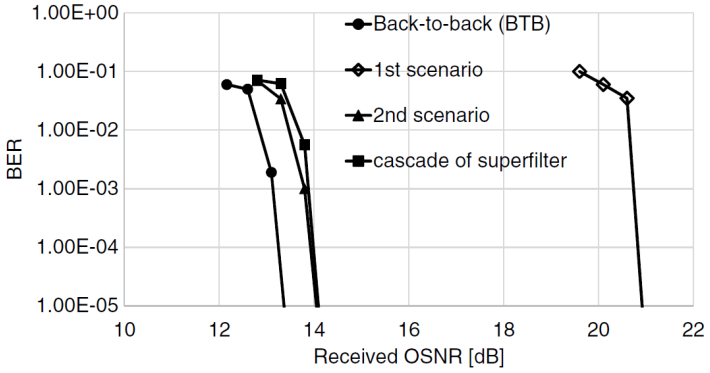

Figure 37: Super-Filter: BER

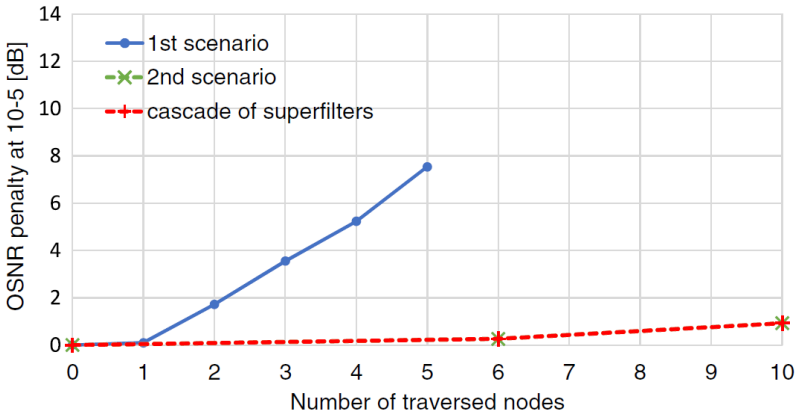

Figure 38: Super-Filter: OSNR penalties

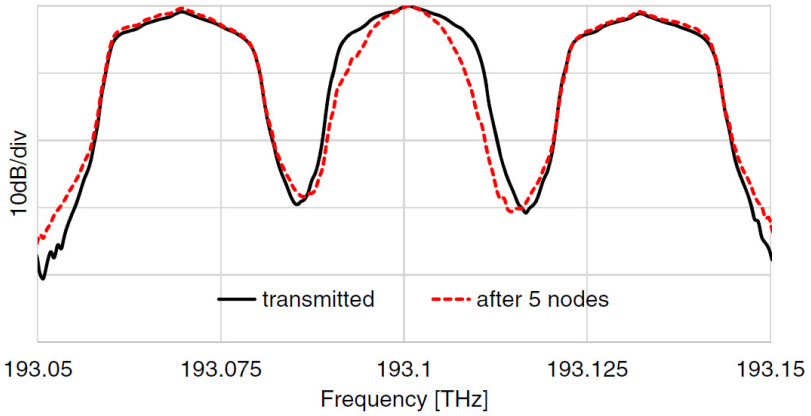

Figure 39: Super-Filter: optical spectrum for scenario 1

Extended SDN control plane is employed to configure the super-filters. The OF-controller exploits a physical parameter database (PPD) to gain knowledge of the expected QoT experienced by the lightpath along the network for the considered modulation format (PM-QPSK in this case). The stateful OF-controller also exploits a LSPDB storing the attributes of existing active lightpaths, including their routes and related BV-OXC filtering configurations. In this way, the OF-controller is able to account for filtering cascade effects as well as QoT parameters (e.g., OSNR) during the path computation. The nominal central frequency does not mean the actual central frequency of a specific signal, but means the central value of the frequency filter to be enforced at the BV-OXC. As shown in the Wireshark captures of Figure 40 and Figure 41, a spectrum reservation of 25 GHz is sent by the OF-controller (IP: 10.0.0.49) to different source and destination nodes. Then, common co-routed segment nodes are configured with S = 8, i.e., 100 GHz. In the latter case shown in Figure 41, the novel flag SUPERFILTER is enclosed within the FLOW_MOD to bypass local filter contention and admission control and allow the filter overlap on the existing filters. In this way, the path is successfully activated. Note that, as shown in the data plane results, no detrimental effects are induced onto the adjacent lightpaths during filter adaptations since the LCoS configuration is not modified at those frequencies. If the edge lightpath is torn down, the OF-controller will not completely release its resources. In particular, a slice of 12.5 GHz contiguous to the A-W resources will be maintained along E-P. To this extent, the FLOW_MOD of type “delete” includes the SUPERFILTER flag and encloses the (n) and (m) values (different from those installed within the flow entry) corresponding to the portion of the filter to be released.

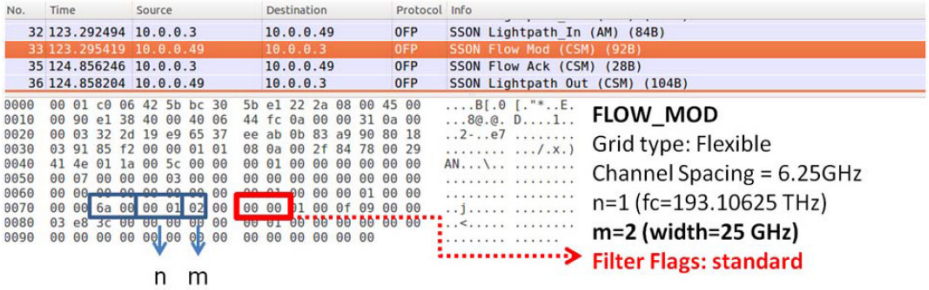

Figure 40: OpenFlow capture at ingress node (standard filtering)

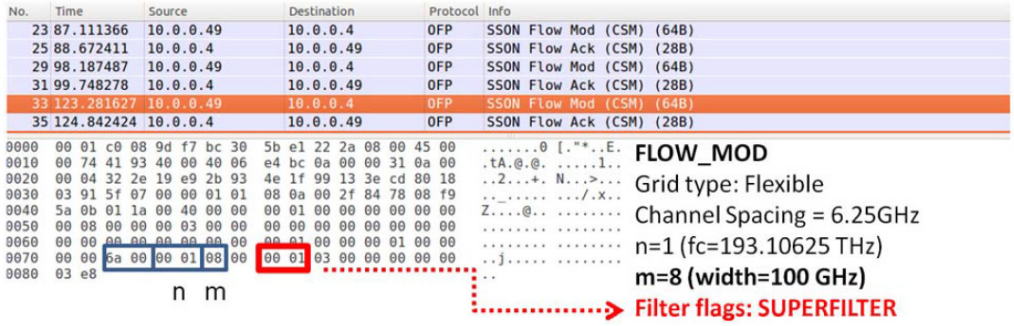

Figure 41: OpenFlow capture at intermediate node (Super-filter)

3.11.3 Analysis of the results

DFC

According to the DFC, the passband of the filters traversed by the same connection can be configured to different values. This can be easily done thanks to exploiting the possibilities of SDN, which, differently from RSVP-TE, does not require that the passband value is unique for the whole connection. DFC can be particularly effective in the case where a network is equipped with filters based on different technologies (e.g., WSSs and SSSs) or experiences the presence of detrimental filtering effects. As a result, spectrum reservation can be minimized on a per node basis according to the expected QoT of each single lightpath, thus improving the overall spectrum utilization. Such a technique can be applied to both a single carrier and a super-channel.

Super-Filter

The experimental results confirm that the Super-Filter technique achieves a better performance for a channel experiencing a flat region of the filter with respect to standard filtering. Results with the proposed technique show a penalty of about 1 dB for the filtering cascade effect after 10 traversed nodes with respect to the standard filtering scenario, where error-free operation is not achieved for more than 5 traversed nodes.

The proposed Super-Filter technique opens the way for a new family of efficient impairment-aware routing and spectrum-assignment solutions and re-optimization procedures, where lightpaths are routed to try to maximize the spectrum contiguity along common network segments.

3.12 E13. Elastic Operations and Shifting

The goal of this experiment is to validate the Soft-FBVT capability to perform elastic operations and defragmentation, driven in a combined way by the control plane. In particular, requests to increase the bitrate of a given connection trigger the CP to move adjacent channels in order to make space for the spectrum occupancy modification. The experiment considers the Push-Pull hitless-shifting procedure for defragmentation, evaluated in both E2E (for a 400-Gb/s superchannel) and source-independent configuration exploiting a PPLN (for a 200-Gb/s superchannel). The combined multi-action optimization procedure is driven by an extended active stateful PCE. SDN controller is exploited in order to consider the source-independent defragmentation scenario.

The WP4 components (as defined in [58]) of the experiment are the CNIT and TEI Soft-FBVT, the CNIT PCE/GMPLS control plane and the CNIT SDN controller. The experiment has been also reported in [27] and [28].

Use-cases	Building Blocks				
	Algorithm suite (off-line and on-line)	Performance metrics for network modeling and experiments	BVT and S-BVT	Flexgrid ROADM and BV-OXC	GMPLS and OFP extensions for flexgrid
Resource allocation in EON	X		X	X	X
Dynamic defragmentation and re-optimization	X	X	X	X	X

Table 20: Use-cases and Building Blocks associated with E13

3.12.1 Description of the setup

End-to-end shifting

The description of the setup is divided into two parts. In the first part, the key data plane aspect of Soft-FBVT controlled shifting tunability is described. Then in the second part, the whole testbed including control plane is described.

The main goal of the data plane part of this experiment is to assess the key building block of the considered defragmentation method. The technique, called Push-Pull, has been proposed and evaluated from an implementation and data plane point of view, mainly focused on single carrier channels. In this experiment, we extend the applicability of the push–pull technique to superchannels. In order to validate the proposed solution, a tunable 400-Gb/s superchannel has been generated through PM-DQPSK modulation of a four-lines 25-GHz-spaced optical comb occupying a 100GHz slot. The optical comb was generated by using two cascaded Mach-Zehnder modulators (MZM), as shown in Figure 42. In a first stage (MZM-1), two 50-GHz spaced optical carriers are obtained from a continuous wave at a wavelength of 1,554.30 nm, provided by a TLS with a linewidth of about 100 kHz. In particular, MZM-1 is driven by a 25-GHz RF clock, which provides as a result two new optical carriers 50 GHz apart at the output, while suppressing the original carrier frequency. The two newly generated lines are then directly fed into the second stage MZM-2 driven by a 12.5-GHz RF clock. By using standard SMF, data decorrelation among the carriers is obtained after 10 km). At the receiver, intradyne coherent detection is employed for each sub-carrier by using an additional ECL as a local oscillator. A real-time oscilloscope (50 GS/s, 20 GHz bandwidth, 8 bit resolution) is used as an analogue-to-digital converter. Digital samples are then resampled at two samples per symbol and processed by an adaptive two-dimensional fractionally-spaced feed forward equalizer, followed by an asynchronous detection strategy. A frequency estimation algorithm is included in the recursive computation of the phase reference symbol, in order to compensate for phase rotation over a symbol time due to carrier frequency offset.

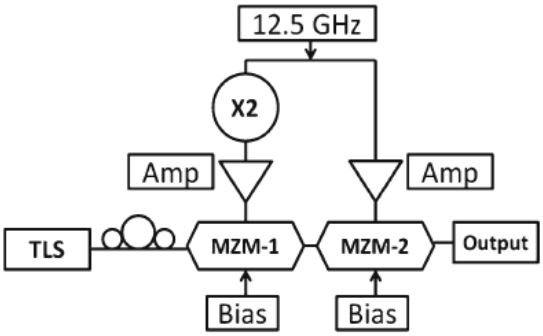

Figure 42: Soft-FBVT shifting: tunable comb laser scheme

To experimentally assess elastic operation and defragmentation driven by the CNIT stateful PCE controlling, the joint data-control testbed as shown in Figure 43 has been setup. CNIT PCE runs dedicated joint path computation/re-optimization algorithms developed in collaboration with UPC. In particular, the EL-SPRESSO algorithm has been implemented in the CNIT PCE. GMPLS controllers are able to send shifting commands to the Soft-FBVT by means of dedicated hardware commands through USB and serial interfaces.

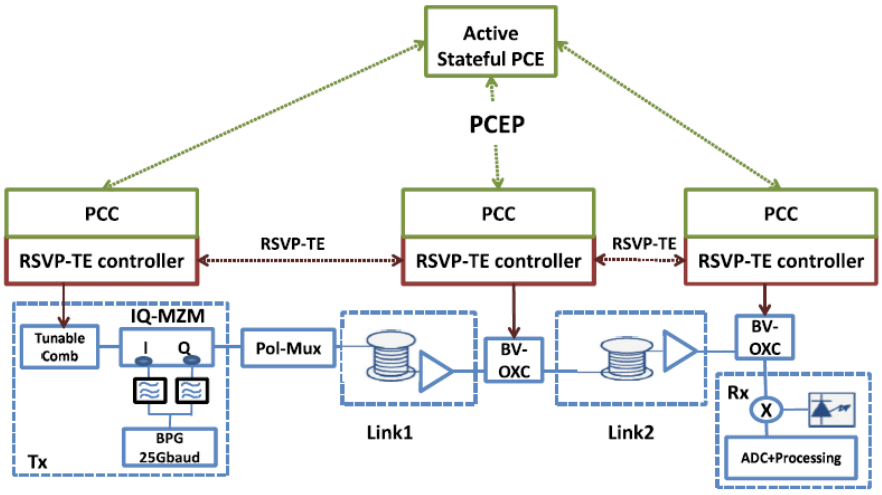

Figure 43: Elastic operations and defragmentation: joint experimental testbed

Source-independent shifting

Differently from end-to-end push-pull, for which the frequency shift is done by the laser that generates a carrier (at the source), with the source independent push-pull technique (SIPP), the frequency shift is achieved only in a path segment, between an intermediate node equipped with a PPLN and the destination node, by shifting in frequency one of the two pumps (P2), at the node where frequency conversion takes place. Details of SIPP procedures and its mechanism (including the PPLN and the pumps to perform signal frequency conversion and shifting signals) are shown in Figure 44 and are fully explained in [28]. In particular, the links interested in the defragmentation process are the ones downstream to node i. In order to enable the SIPP in all the traversed links, the super-channel has to enter the PPLN at the source node. SIPP is particularly suitable for super-

channels because the converted sub-carriers are shifted in frequency in a solid way only by tuning fP2, without the need to move the laser of each sub-carrier.

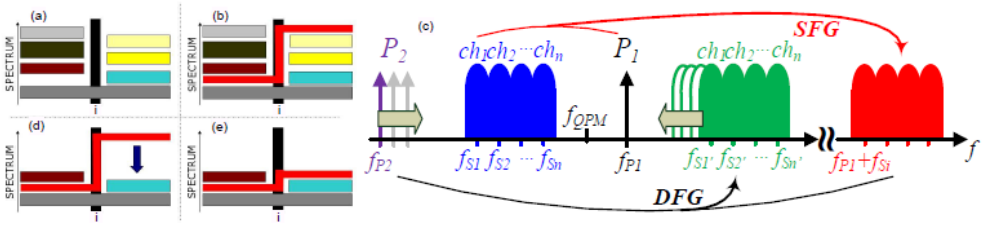

Figure 44: Concept of source-independent push-pull (SIPP)

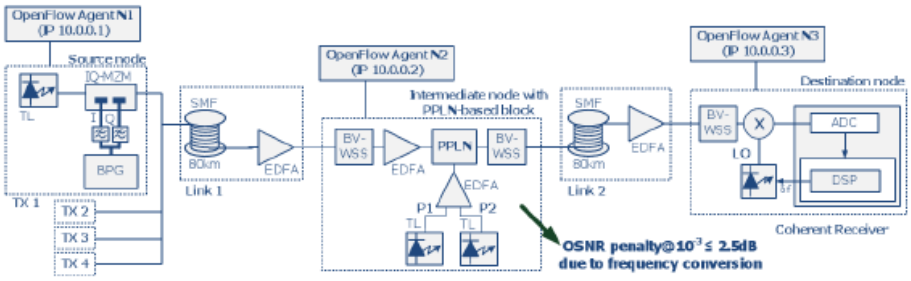

Figure 45: Testbed for SIPP

The testbed is reported in Figure 45. OpenFlow Controller and OpenFlow agents (co-located at the source N1, the intermediate node N2 performing conversion, and the destination N3) are responsible for the entire procedure control. The data plane is composed of a transmitter at N1, a link, an intermediate N2 emulated by the PPLN-based block and BV-WSSs, a second link, and N3. Sub-carriers of the 200-Gb/s super-channel are obtained with four 25-GHz-spaced 100-kHz linewidth TLSs at fS1=193.06875 THz, fS2=193.09375 THz, fS3=193.11875 THz and fS4=193.14375 THz, respectively. Nyquist transmission is achieved with electrical filtering. The signal launch power into the fibre spools was 0 dBm per sub-carrier and 15 dBm at the PPLN input. Coherent detection is applied.

3.12.2 Attained results

End-to-end shifting

Figure 46 reports the spectrum of the tunable comb generator, reaching an output power uniformity of 0.39 dB and an extinction-ratio higher than 30 dB. Although the linewidth measurement resolution of the comb-lines is limited by the analyzer, a linewidth value of about 150 kHz was measured for all the carriers with a heterodyne technique. Power uniformity and stability during laser tuning is of key importance for hitless defragmentation. To assess comb tunability, the feeder laser was tuned to both longer and shorter wavelengths over a 15-nm span, without bias adjustment. A power peak variation between the generated lines less than 0.8 dB was demonstrated while moving the comb central frequency from 1,545 to 1,560 nm. As mentioned above, the comb is modulated through an IQ-MZM and polarization multiplexed providing 100 Gb/s for each channel. The overall capacity of the comb is 400 Gb/s over a spectrum portion of 100 GHz (see Figure 47).

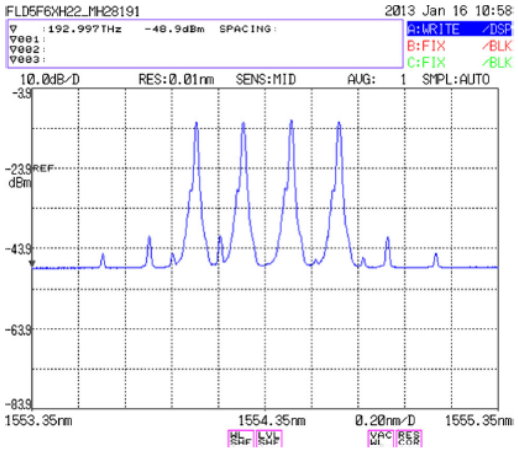

Figure 46: Tunable comb laser

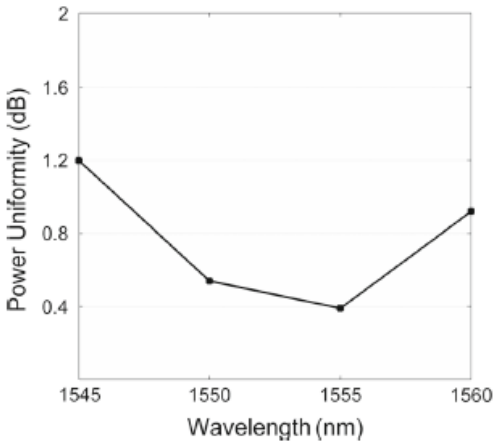

Figure 47: Tunable comb: power stability over tuning

The joint data-control plane experimental evaluation is now reported as follows. A request for elastic operation of an established 100-Gb/s LSP is considered in this evaluation. Figure 48 illustrates the initial spectrum allocation in solid lines. Thus, to increase the LSP bitrate to 200 Gb/s, the allocated spectrum has to be doubled and a shift of the adjacent superchannel is required. Specifically, upon receiving the PCReq message, event (1) in Figure 48 and Figure 49, the PCE returns the set of actions required to perform the elastic operation. In particular, the EL-SPRESSO algorithm returns the action list within 3ms. As a result, the 400-Gb/s superchannel is shifted by 100 GHz. Figure 49 captures the relevant control messages, collected at the PCE used to complete the process. A PCUpd message (2) is sent to the superchannel ingress node to trigger the superchannel shifting, which is realized with the RSVP-TE make-before-break mechanism (i.e., filter broadening, channel shifting, filter tightening). After broadening the BV-OXC filter, the comb laser source at the transmitter is retuned: 80 frequency steps are applied, each providing a shifting of δ = 1.25 GHz. At the receiver, coherent detection is exploited and the shift is followed by automatically retuning the local oscillator, according to the locally estimated frequency offset. Due to the off-line processing of the utilized receiver, the signal spectral shift is performed with a finite number of frequency steps (each step is completed in few milliseconds). However, hitless continuous spectral shift has been successfully demonstrated. Figure 50 shows both the frequency estimation offset and the BER performance at the receiver for one of the four subcarriers. Off-line processing has been

used; however, the data are captured during superchannel tuning. In fact, as shown in the Figure 50, before starting the tuning, an estimated frequency offset between the data and the local oscillator was very close to 0. During superchannel tuning, on the other hand, the frequency offset assumed an almost constant value of about −1 GHz that has been fixed by the digital PLL used for the local oscillator tracking. At the end of the process, the frequency offset returns to the original value. Since tuning is achieved by just moving the central comb frequency, no residual signal is present in the cleared bandwidth and any channel can subsequently be allocated onto that frequency slot. Once all the shifting operations are concluded (3), the source PCC notifies the PCE with a PCRpt message (4). The PCE then updates its Stateful DB and triggers the elastic operation by sending a PCRep message (5) to increase the LSP bitrate to 200 Gb/s over the newly available spectrum resources. Once the elastic operation is performed (6), the PCC notifies the PCE with a PCNtf message (7).

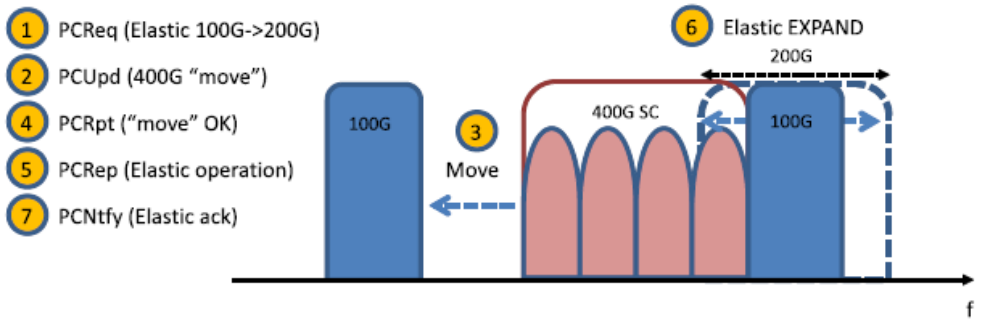

Figure 48: Experiment: sequence of CP procedures

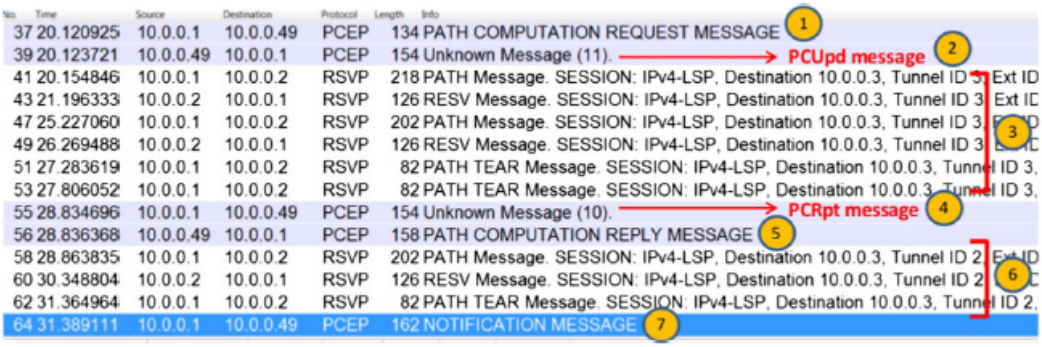

Figure 49: Capture of control plane messages

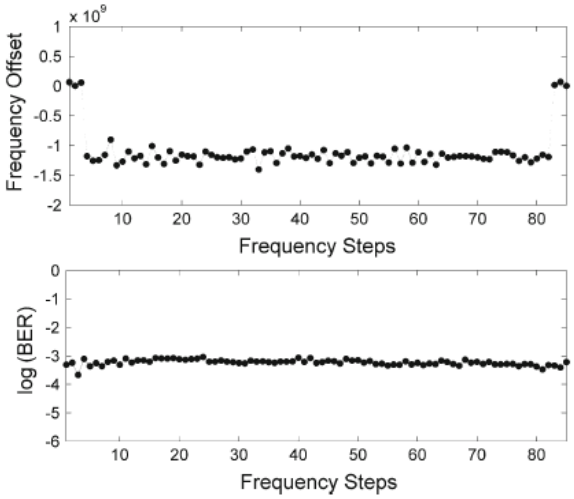

Figure 50: Frequency offset and BER at the coherent receiver during shifting

Source-independent shifting

A 200-Gb/s superchannel that has been previously activated, is frequency converted (shifted) at the PPLN-equipped node. SIPP is thereby demonstrated, by shifting fP2 and achieving an overall super-channel shift of 100 GHz. To this purpose the controller sends FLOW MOD only to N2 (frame 33) and N3 (frame 34). Frame 33 (see Figure 51b) shows the BV-WSS enlarge indication (m=16 slices, 200 GHz wide) and the PUSHPULL object. The OPT PORT MOD (frame 41, Figure 51b) triggering pump laser shift is also expanded, showing the novel proposed LASER SHIFT fields. 80 shifting steps of 1.25 GHz complete the overall shift of 100 GHz which takes around 400 seconds, performing hitless and solid shift of the super-channel. Upon shift termination, the novel proposed OPT PORT ACK message with a positive outcome is generated, thus the controller re-configures the BV-WSSs to the original m=8 slices and centered on n′=-148 (192.175 THz). DSP at the coherent receiver changes the LO nominal frequency, thanks to an estimation of the frequency offset between the sub-carrier and the LO. This way, while the sub-carriers move, according to the P2 tuning, the LO frequency fLO follows the received sub-carrier frequency fSi′. The estimated frequency offset values δf at the receiver, for each acquisition, are shown in the right axis of Figure 51(c). At the beginning, δf is close to zero, and then during SIPP, δf remains almost constant thanks to the feedback compensation with a value of about 1.2 GHz. When the overall shift of 100 GHz has been achieved, δf returns to zero again. The BER values of each shifting step are computed off-line and reported on the left axis of Figure 51(c), demonstrating no performance degradation (and no loss of data) during SIPP operation. To highlight the benefits achieved with solid frequency shift, Figure 51(d) shows the performance degradation (on a central sub-carrier) due to partial sub-carrier overlapping in the back-to-back case. By reducing the carrier frequency separation to 23 GHz (instead of 25 GHz) an OSNR penalty of 3 dB is measured, while the system does not work with 22-GHz separation. This result strongly supports the effectiveness of SIPP, which avoids sub-carrier overlap during the super-channel frequency shift.

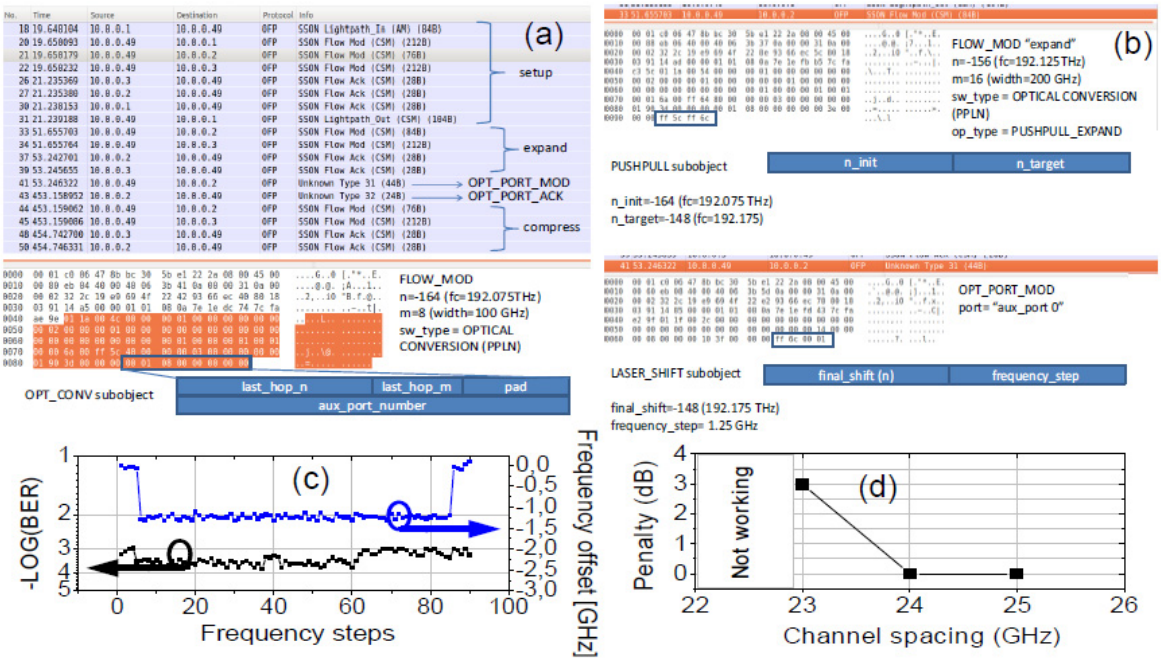

Figure 51: SIPP: Captures and performance

3.12.3 Analysis of the results

End-to-end shifting

The cascade configuration of the tunable comb generation at the Soft-FBVT provides better carrier suppression and power equalization, suitable for both single carriers and superchannels. Moreover, the tuning of the seed TLS laser results in a cohesive tuning of all the sub-carriers.

The obtained results show that thanks to the power stability of the proposed comb source and the correct frequency estimation, no BER degradation is detected during the frequency shift. Simultaneous shifting of four subcarriers composing a 400-Gb/s superchannel was successfully demonstrated, showing power uniformity and stability during the laser tuning, without affecting the BER. The enhanced architecture of the CNIT active stateful PCE provides a multi-actions procedure and sequential multi-step optimization, such as channel shifting to make space for elastic operations.

Source-independent shifting

The proposed defragmentation technique, exploiting PPLN and two pumps, is independent of the source node and can be applied at each intermediate node performing frequency conversion with the same technique. This shifting method is particularly suitable for super-channels, because the frequency shift of a single pump imposes a rigid frequency-shift of all the superchannel subcarriers. This is the main advantage of SIPP with respect to other defragmentation techniques; indeed, SIPP provides a frequency-shift of a super-channel without incurring subcarrier overlapping, which would otherwise generate loss of data.

3.13 E14. Monitoring and Modulation Format/Code Rate Adaptation

The goal of this experiment is to validate proactive restoration and lightpath adaptation by the Soft-FBVT due to QoT degradations occurring in the network. Advanced monitoring of the lightpath QoT (introduced and described in [55]) at the coherent receiver DSP is able to track BER and MSE sampling. Alarm notifications are provided to the control plane, which reacts by properly restoring the path and adjusting the physical parameters of the signal. In particular, modulation format and code rate adaptation are considered as the two main parameters for proactive QoT-enabled restoration. The experiment induces QoT degradations, emulating both a fibre cut and fibre degradations. Extensions at the CP level proposed in WP3 are considered and evaluated by considering an active stateful PCE. Adaptation is evaluated in terms of hitless/not hitless operation, and providing feedback to WP2 and WP3 about the feasibility of the restoration/adaptation procedures.

The WP4 components (as defined in [58]) of the experiment are the CNIT and TEI Soft-FBVT, including the advanced coherent receiver DSP and the CNIT PCE/GMPLS control plane including the active stateful QoT-aware PCE. The experiment has been also reported in [29].

Use-cases	**Building Blocks**				
	Algorithm suite (off-line and on-line)	Performance metrics for network modeling and experiments	BVT and S-BVT	Flexgrid ROADM and BV-OXC	GMPLS and OFP extensions for flexgrid
Optical restoration after fibre breaks	X	X	X	X	X
Optical restoration in IP networks	X		X	X	X

Table 21: Use-cases and Building Blocks associated with E14

3.13.1 Description of the setup

For the restoration/adaptation demonstration, the CNIT active stateful PCE has been utilized in the flexgrid elastic optical network testbed employing the Soft-FBVT, shown in Figure 52. The testbed includes BV-OXCs, also called SSSs, and the Soft-FBVT that can implement up to 1-Tb/s transmission over 200 GHz through seven carriers at up to 160 Gb/s PM-QPSK (40 Gbaud). The transmission relies on the TFP technique through configurable LDPC coding with coherent detection. The control plane includes GMPLS controllers able to configure the number of generated subcarriers, the tunable lasers, the modulation format, and the LDPC code through dedicated Ethernet, USB, and serial interfaces. Moreover, at the destination node, QoT optical parameters computed by the DSP at the receiver are collected every 15 seconds for monitoring purposes. The node controller locally compares the QoT parameter values to predefined threshold values, triggering alarms in the PCE when thresholds are exceeded.

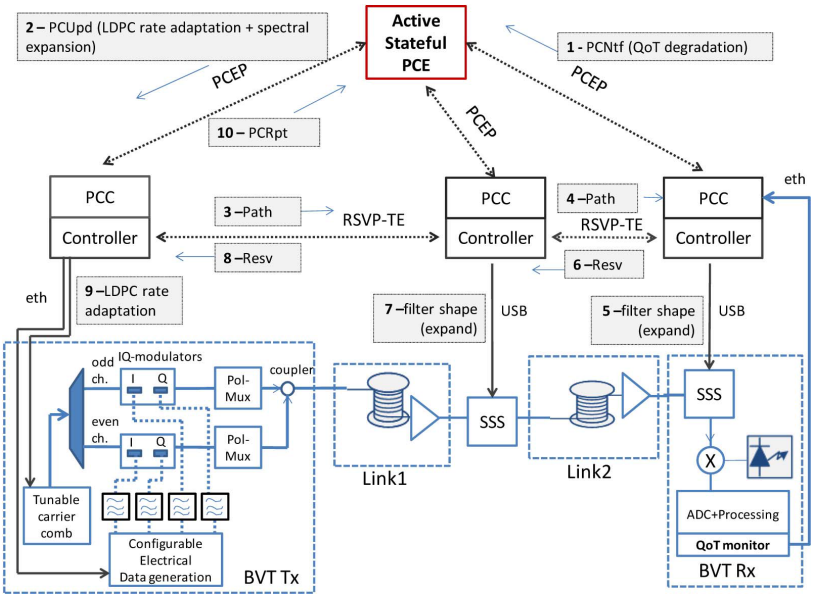

Figure 52: Soft-FBVT Monitoring and code adaptation testbed

3.13.2 Attained results

Adjustments of existing lightpaths can be operated to either cope with requests for higher bit rates, or to deal with degradations in transmission performance. The implemented active stateful PCE described here has been applied to address this latter case. A set of multiple LDPC codes with different overheads are available, e.g., of type 8/9 (8 information bits out of 9 transmitted), with the optimum LDPC code computed by the PCE and set according to the link conditions and the desired reach. As the distance increases, impairments due to OSNR degradation and nonlinear effects also increase, limiting the maximum achievable information rate. Figure 53 shows the net information rate as a function of the desired reach for the considered superchannel. For a distance such as 3,000 km, a low overhead is required (i.e., low redundancy LDPC code such as 9/10 or 8/9 can be used), guaranteeing a 1-Tb/s net information rate. As the distance increases, OSNR degradation and the impact of nonlinear effects require more robust coding (i.e., 5/6 or 3/4), thus reducing the net information rate.

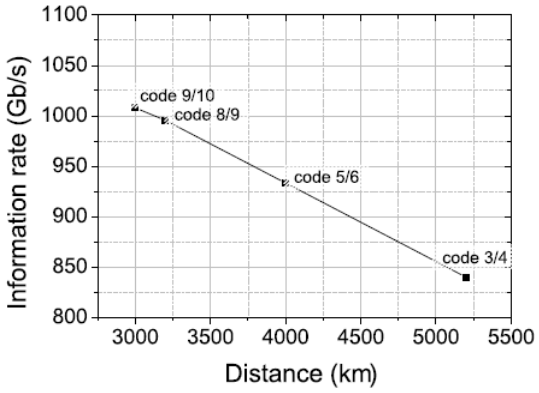

Figure 53: Net information rate for TFP 1-Tb/s superchannel

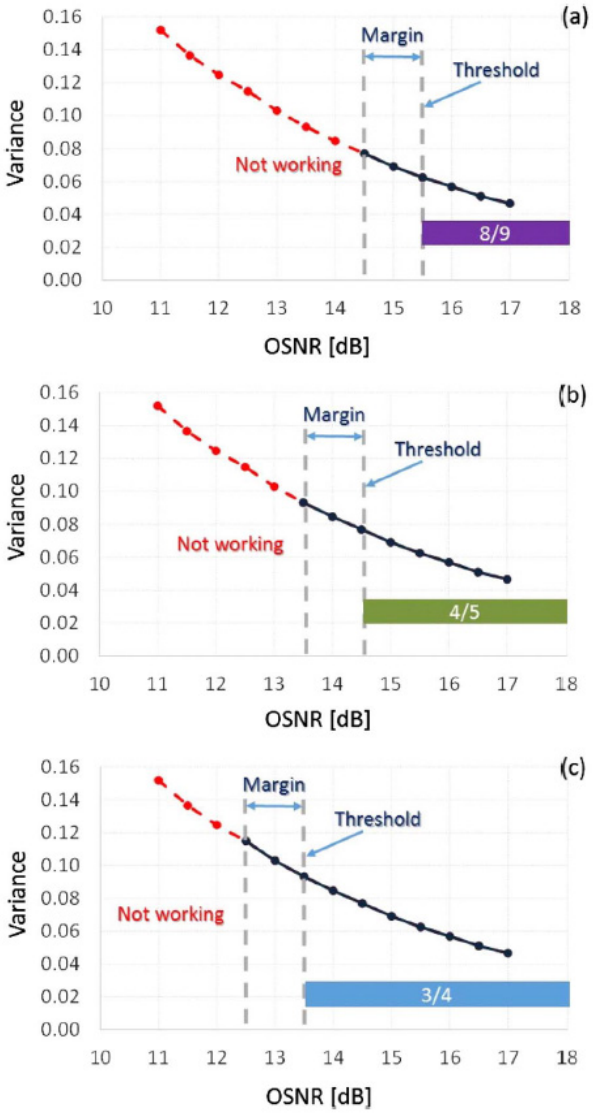

Figure 54: Samples variance for different LDPC code rates

Figure 54(a)-(c) shows the measured variance of the acquired samples as a function of OSNR. Moreover the different sub figures show, for different codes, the OSNR range of use where the applied code can successfully operate (solid line). Note that the variance does not depend on the applied LDPC code. For each code, an OSNR threshold is identified at a certain margin (i.e., 1 dB) from the minimum OSNR required for error-free operation. Monitoring of variances then reveals any OSNR degradation and indicates whether the working-limit condition is approaching for the code in use. In this case, a monitoring system can therefore predict OSNR degradation a good time in advance, before reaching the working-limit condition. If the OSNR degradation exceeds the threshold and remains within the margin (e.g., a variance of 0.07 for 8/9 coding), no post-FEC BER degradation is experienced, but a warning alarm is locally triggered to switch to a more robust code before post-FEC errors start occurring.

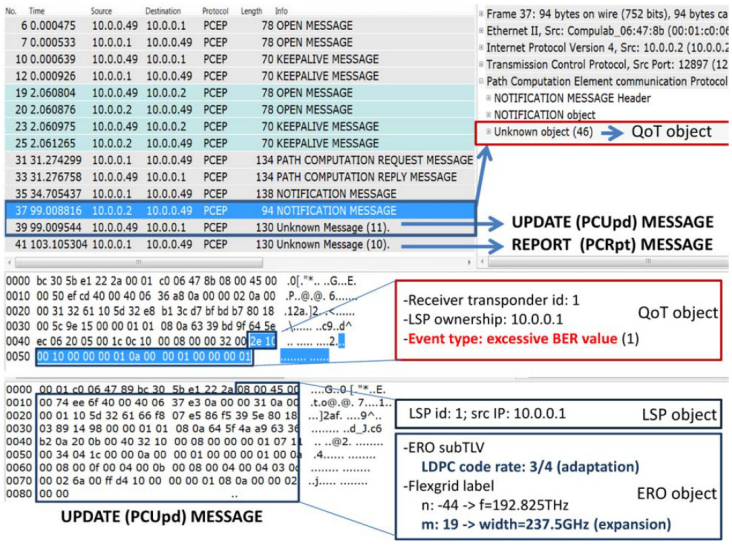

Figure 55: Control plane capture of the adaptation experiment

Figure 55 reports the Wireshark capture of the control plane packets collected at the active stateful PCE (IP address 10.0.0.49) exchanged with source (IP 10.0.0.1) and destination (IP 10.0.0.2) nodes. In addition to the handshake, a 1-Tb/s LSP is computed by the PCE having 8/9 coding and established in the testbed (see PCReq, PCRep, and TE Ntf messages, packets 31, 33, and 35, respectively). After establishing the LSP, OSNR degradation is introduced into the path by increasing the attenuation of a VOA at the input port of the EDFA placed on Link2 of Figure 52. According to the aforementioned predefined policies, a notification message (i.e., PCEP Ntf extended with a novel QoT object, packet 37) is sent to the PCE to notify it of the LSP degradation and trigger the required improvement in transmission robustness. The QoT object identifies the affected LSP and the alarm event; in particular, the QoT alarm indicates an excessive pre-FEC BER value. Based on the information retrieved from the LSP-DB, the PCE modifies the parameters for adapting the LSP, while considering the network resources, modulation format, coding, or combinations of the above. In this experiment, the PCE computes the LDPC coding adaptation from 8/9 to 4/5. To preserve the information rate, an additional carrier is also activated. This requires an increase in the occupied spectrum resources, from 200 to 237.5 GHz. To make room for such an increase, the PCE also has the potential capability to first trigger a necessary network de-fragmentation. To improve transmission robustness, the PCE sends a PCUpd message to increase the reserved spectrum resources of the degraded LSP and apply the code adaptation (packet 39). A novel explicit routing object (ERO) Sub-TLV is enclosed to specify the updated LDPC code at the source node transmitter. The source node runs the RSVP-TE signaling (using a make-before-break mechanism) to adapt the BV-OXC filter configurations along the path. The new coding is then activated in the transmitted data via software configuration of the configurable electrical data generation block of the transmitter. Within the preamble of each data block, a specifically introduced 3-bit field is configured as part of the overhead to communicate to the receiver the applied 4/5 coding. In this way, the receiver becomes aware of the code to apply. It processes the incoming data through the new coding, successfully supporting the more robust transmission, which aims at preventing post-FEC BER degradation. Code adaptation is therefore performed with no disruption to the traffic.

At the end of the procedure, a PCRpt message is sent to the active PCE to inform it about the outcome (packet 41). The time needed to complete the whole adaptation is around 4 seconds. This value is mainly due to the time needed to configure the BV-OXC filters by means of the BV-OXC proprietary software tool.

For the case where the spectrum reservation is not modified, and only the hitless code adaptation procedure is performed, only a few milliseconds are required. Figure 56 reports the collected variance statistics before and after degradation is introduced. The figure also shows the related spectral efficiency of the transmitted data. As degradation occurs, the variance increases above the predefined threshold for code 8/9 (0.06) and spectral efficiency is reduced due to the more robust applied code. After a certain time, the source of degradation is removed (i.e., the VOA gain is reset to the initial value) and the link condition subsequently returns to its initial state. Consequently, the observed variance returns below the predefined threshold for code 8/9. The PCE can then restore the initial 8/9 code, as the higher redundancy of 4/5 is no longer required, thus increasing the spectral efficiency back to its initial value.

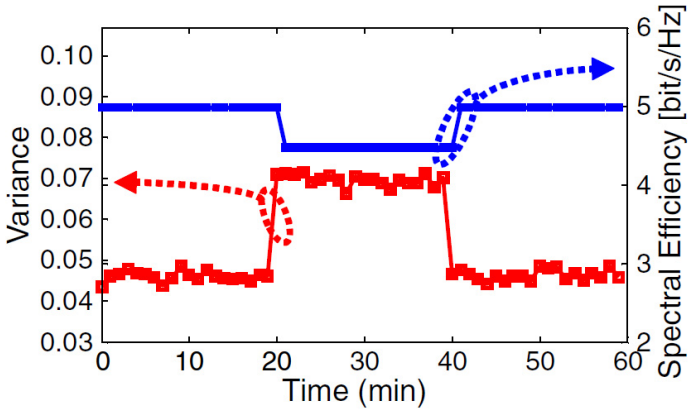

Figure 56: Variance and spectral efficiency measurements

3.13.3 Analysis of the results

In order to enable proactive restoration and adaptation purposes, advanced monitoring functionality of the Soft-FBVT exploiting DSP parameters was first introduced and experimentally demonstrated in a flexgrid optical network testbed including a multicarrier terabit LSP. The DSP parameters were used to detect impairment degradations before the BER was affected. A new dynamic LDPC code adaptation technique was then introduced and validated to dynamically adapt the transmission robustness. Hitless adaptation of the applied LDPC coding was achieved in only a few milliseconds with no traffic disruption.

One of the main conclusions of this experiment is that, unlike modulation format adaptation, code rate adaptation represents the key adaptation procedure to enable QoT robustness. While modulation format adaptation, targeting constant net bit rate, requires re-synchronization and, intrinsically is not hitless, code rate adaptation was demonstrated to be hitless and the adaptation could be driven by the control plane controller (either PCE/GMPLS or SDN controller) through either receiver coherent receiver direct monitoring or alarms. One of the main conclusions is that modulation format adaptation could be employed in use-cases where traffic can be disrupted (e.g., upon failure events), while code rate adaptation is clearly identified as the main hitless adaptation procedure. Therefore, code rate adaptation is suitable for effective QoT-aware restoration purposes,

particularly in the case of minor failure events (e.g., QoT degradations due to device aging).

3.14 E15. Long Term Channel Overlap

The goal of this long-term experiment is to validate the feasibility of a complete overlap of two source-independent optical signals, configured with the same central frequency. The experiment considers two PM-QPSK signals independently generated by two Soft-FBVT transponders with different transmission parameters and received by a single coherent receiver. Control plane extensions consider a multi-level flexgrid label with triple (n,m, overlap level) parameters.

The WP4 components (as defined in [58]) of the experiment are the CNIT and TEI Soft-FBVT and the CNIT PCE/GMPLS control plane. The experiment has been also reported in [30].

Use-cases	Building Blocks			
	Algorithm suite (off-line and on-line)	Performance metrics for network modeling and experiments	BVT and S-BVT	GMPLS and OFP extensions for flexgrid
Resource allocation in EON	X		X	X
Dynamic provisioning including DC interconnection	X	X	X	X

Table 22: Use-cases and Building Blocks associated with E15

3.14.1 Description of the setup

The experimental demonstration is performed on a network testbed shown in Figure 57, where the testbed reproduces a 4-node scenario. The two independent optical signals SA and SB are generated at nodes A and B respectively, having node D as the destination. At node C, where the two signals start overlapping, a simple optical coupler is utilized without the need for any electrical or all-optical processing performed on the signals. Links A-C and B-C are 35 km long, while C-D is composed of a 40 km fibre span. Each optical signal is generated by modulating two lasers with the same nominal frequency fc = 192.750 THz. In particular, at both nodes A and B, two encoded 20-Gb/s electrical signals are applied to the I and Q ports of a double-nested Mach-Zehnder modulator. An LDPC code with configurable rate R is employed, thus achieving a Rx40 Gb/s QPSK signal. In the considered measurements, RA=9/10 (9 bits of information rate out of the transmitted 10 bits) and RB=3/5. The bit rate is further doubled by including a polarization multiplexing (PM) stage. The 80-Gb/s PM-QPSK (gross bit rate) signals are then transmitted through 35 km of standard fibre, thus reaching node C. Different carrier to interference (C/I) power ratios are considered, and the performances for both SA and SB are evaluated with the technique described in the next section. In particular, the SA power at the node A output is set to 0 dBm while the power SB at the node B output is varied to achieve a different C/I ranging from 5 dBm to 11 dBm.

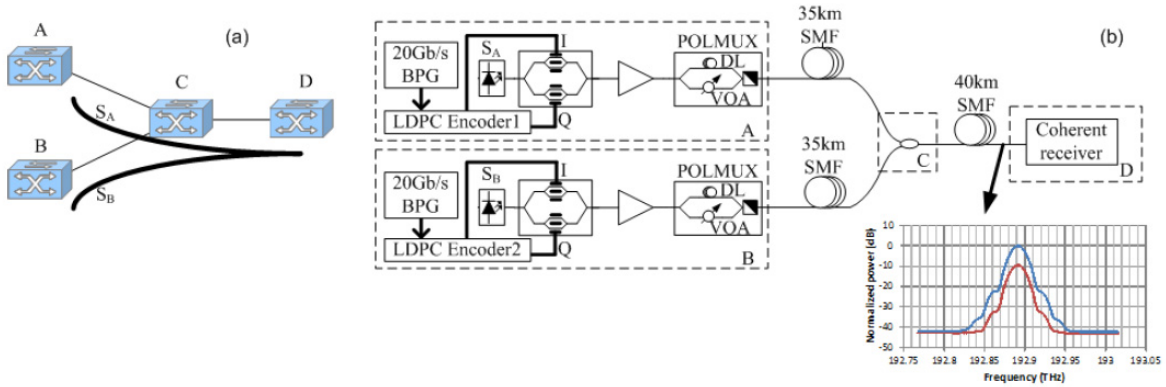

Figure 57: Frequency channel overlap: scenario and testbed

3.14.2 Attained results

In Figure 58, below, the minimum required OSNR for proper detection of both SA and SB is measured for different C/I values. For each point in Figure 58 a bit-error-rate around 10^5 is measured for both the signals. The reported OSNR considers as signal power the contribution coming from both SA and SB. The optimum C/I value that requires the lowest OSNR is 9 dB, while higher OSNRs are needed for different values of C/I. In Figure 57(b) optical spectra at node D are also reported for the case C/I=9 dB.

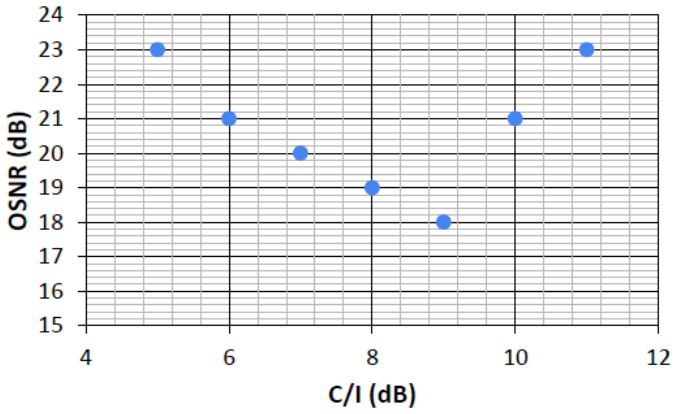

Figure 58: OSNR required for overlap detection

To support the overlapping of optical signals, the basic assumption that a reserved frequency slot results in it being unavailable to other slots has to be revised. Here we propose to adopt a bi-dimensional representation of the frequency spectrum, such that two optical signals can reserve any specific portion of the spectrum. In particular, we propose to extend the current (n;m) representation with a 3-tuple (n; m; k) representation, where k represents the 'layer' of optical signals in the spectrum. In this study, k assumes the values of either 0 or 1. Figure 59 shows the updated flexgrid GMPLS label format, where 3 reserved bits are now utilized to include the k parameter.

The extended control plane has been utilized to perform the provisioning of the two overlapping signals. To this end, four node-collocated GMPLS controllers have been employed. Figure 59 shows the Wireshark capture performed at node C (IP 10.0.0.3) of the RSVP-TE signaling (i.e., Path and Resv messages) triggering the lightpath provisioning. In

particular, frames 4, 8, 10, 12 are referred to the first signal, whose label is assigned by the destination node D (IP 10.0.0.4) and propagated backwards to node C and source node A (IP 10.0.0.1). Similarly, frames 21, 23, 25, 27 are referred to the second signal, when the first signal is already active. The assigned label for both signals, enclosed in the new LABEL object of Resv messages, includes the same central frequency (n=-56, corresponding to 192.750 THz, with a flexible grid featuring 6.25 GHz channel spacing), the same channel width and two different values for the overlap layer (k=0 at frame 10, k=1 at frame 25).

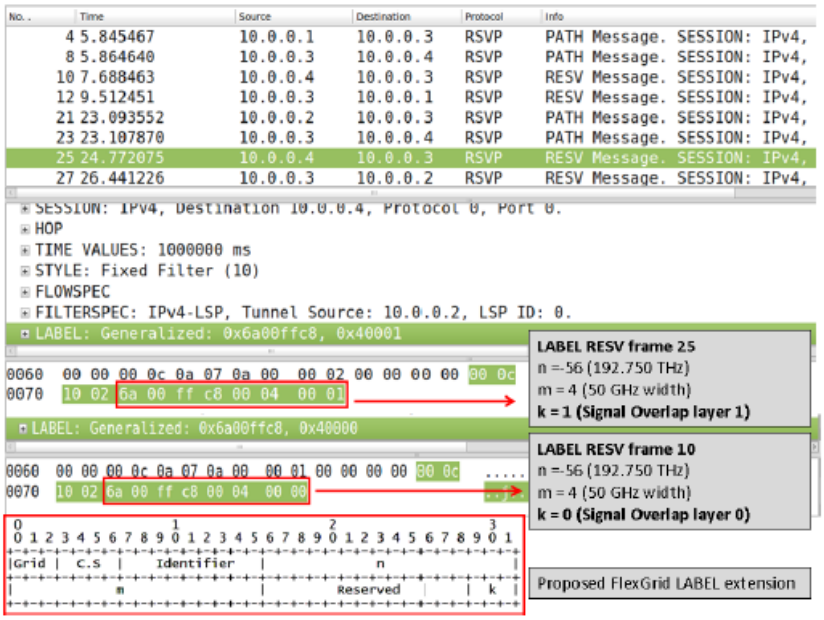

Figure 59: GMPLS capture with extensions supporting overlap

3.14.3 Analysis of the results

Two independent optical signals are established at the same central frequency and featuring complete overlapping. Novel GMPLS-based control plane extensions have also been proposed and successfully implemented. The combined effect of different coding rates and different power levels allows the same coherent receiver to properly detect and rebuild the two signals. This shows the potential of coding in the Soft-FBVT TFP transmission technique. This experiment suggests that a long term scenario with code-division multiplexing techniques could potentially be a future promising research topic for optical transmission in transport networks.

3.15 E16. CNIT/Ericsson - Coriant Transponder Interoperability

The interoperability transponder experiment was carried out in Pisa, CNIT, in collaboration with Coriant. This experiment represents an extension with respect to the results published as invited papers at OFC 2015 [31] and JOCN [33] that were obtained as part of a joint experiment carried out, this time, in Munich at Coriant Lab and again in collaboration with CNIT.

The novelty of this experiment, with respect to the one in Munich, relies on the control plane used to control both transponders (from CNIT and Coriant), which is also a part of the pan-European testbed used for the collaborative experiment published as a post-

deadline paper at the last ECOC 2015 conference [10], where both partners were among the leading authors of the paper.

Use-case	Building Blocks				
	Algorithm suite (off-line and on-line)	Performance metrics for network modeling and experiments	BVT and S-BVT	Flexgrid ROADM and BV-OXC	GMPLS and OFP extensions for flexgrid
Multi-vendor and multi-technology interoperability	X	X	X	X	X

Table 23: Use-case and Building Blocks associated with E16

3.15.1 Description of the setup

The data plane part of the setup consisted of a 4-nodes flexgrid network, a CNIT / Ericsson DSP unit at the transmitter and two different ones (CNIT / Ericsson and Coriant) at the receiver, as part of an optical coherent testbed [10]. The transmitter is able to generate a super-channel with different numbers of carriers and capacities (i.e. 1 carrier for 100G, 3 carriers for 400G, and 7 carriers for 1T). At 1 Tb/s, we adopted PM-16QAM Nyquist-shaped signals shaped by a roll-off = 0.05 and symbol rate = 23GBd. A 64-GSa/s DAC was used with digital pre-emphasis to compensate for its bandwidth limitations. Subcarrier spacing was set to 25 GHz. The testbed was equipped with an optical re-circulating loop consisting of 2×80km SSMF spans, EDFAs to compensate for the span losses, and a wave-shaper acting as a loop filter to perform gain equalization and suppress accumulated out-of-band ASE noise. After the loop circulation, the desired sub-carrier was selected by filtered and demodulated by employing coherent phase- and polarization-diversity detection, and setting the LO at the nominal wavelength of the selected sub-carrier. The received optical signal was sampled and digitized at 50 GSa/s with a 20-GHz real-time oscilloscope for off-line post-processing and BER measurements.

With regard to the control-plane, this is performed via GMPLS controllers running RSVP-TE and PCEP and dynamically configuring the BV-WSS, transponders (i.e., symbol rate, carriers, frequencies, etc.), and the DSP parameters (i.e., modulation, FEC, etc.). Interoperability between CNIT / Ericsson and Coriant DSPs is achieved by the exchange of novel Transponder Class attributes in BGP-LS and PCEP/RSVP-TE protocols, including the agreed ranges for the physical parameters. Path computation allows transponder-transponder paths only if they belong to the same class.

3.15.2 Attained results

The main results are reported in Fig. 5 of [10]. In particular, we reported the transmission performance of the single-vendor (CNIT / Ericsson) & cross-vendor (CNIT / Ericsson & Coriant) solutions as a graph plotting BER (measured over all seven sub-carriers composing the terabit super-channel) vs. distance. We transmitted a line rate of 1.28 Tb/s that allows a 23% FEC-OH plus 5% framing OH. Under this assumption, the pre-FEC BER threshold (BER_{th}) of 3.4×10^{-2} can be considered for the single-vendor solution, as more powerful data-aided vendor-specific SD-FEC can be adopted. Such FEC provides a transmission distance of ~1250km. If the cross-vendor scenario is considered, with already standardized hard-decision (HD) FEC and common blind DSP processing, the transmission distance is reduced to ~300 km.

3.15.3 Analysis of the results

Several results can be discerned from this experiment. Firstly, we demonstrated multi-vendor error-free transmission with up to 300 km of reach. Secondly, we prove that in the case where SD-FEC is standardized with a BER_{th} ~ 2×10^{-2}, this would already enable error-free distances of the order of 600-700 km, which corresponds to a regional network, and basically covers all possible links in the context of European telecommunication operators. Finally, as reported in [40], we compared this last experiment with the one reported in [31], showing that the performances of the single-vendor and multi-vendor cases are basically identically in the two independent experiments.

3.16 E17. Dynamic Bandwidth Allocation

The goal of this experiment is to investigate the ability of flexgrid networks to dynamically reconfigure in order to accommodate changes in the loads of links. This reconfiguration capability paves the way for new business models, where operators can sell connections that dynamically adapt to the traffic demands of clients. Network reconfiguration could also enable power savings when links are being under-used.

This is an experiment related to the control plane. The objective is to show how the monitoring probes can be integrated with the ANM, and how the OAM Handler can calculate which is the appropriate bandwidth for links, according to the monitoring information. The experiment also shows how the ABNO Controller can reconfigure the network when the OAM Controller sends a bandwidth update command.

Use-cases	Building Blocks		
	Algorithm suite (off-line and on-line)	Performance metrics for network modeling and experiments	Network Orchestrator (ABNO)
Resource allocation in EON	X	X	X
Dynamic provisioning including DC interconnection	X	X	X

Table 24: Use-cases and Building Blocks associated with E17

3.16.1 Description of the setup

Figure 60 shows the setup of the experiment performed at Cisco's testbed in Telefónica I+D. Using NAUDIT's trace playback tool, traffic is injected into a gray interface of the Cisco CRS router. Traffic at that interface is monitored using the probes developed by NAUDIT, particularly the FPGA-accelerated version of the Detect-Pro tool that has been developed in the context of IDEALIST. Detect-Pro creates the flow records, and these records are passed to the OAM Handler where the bandwidth estimation algorithm runs. In the experiment, the FPGA-accelerated Detect-Pro and the OAM Handler run in the same server. Finally, the OAM Handler sends a message using the RESTful API to TID's ABNO Controller, which is in charge of contacting the other elements of the ANM in order to execute the network reconfiguration.

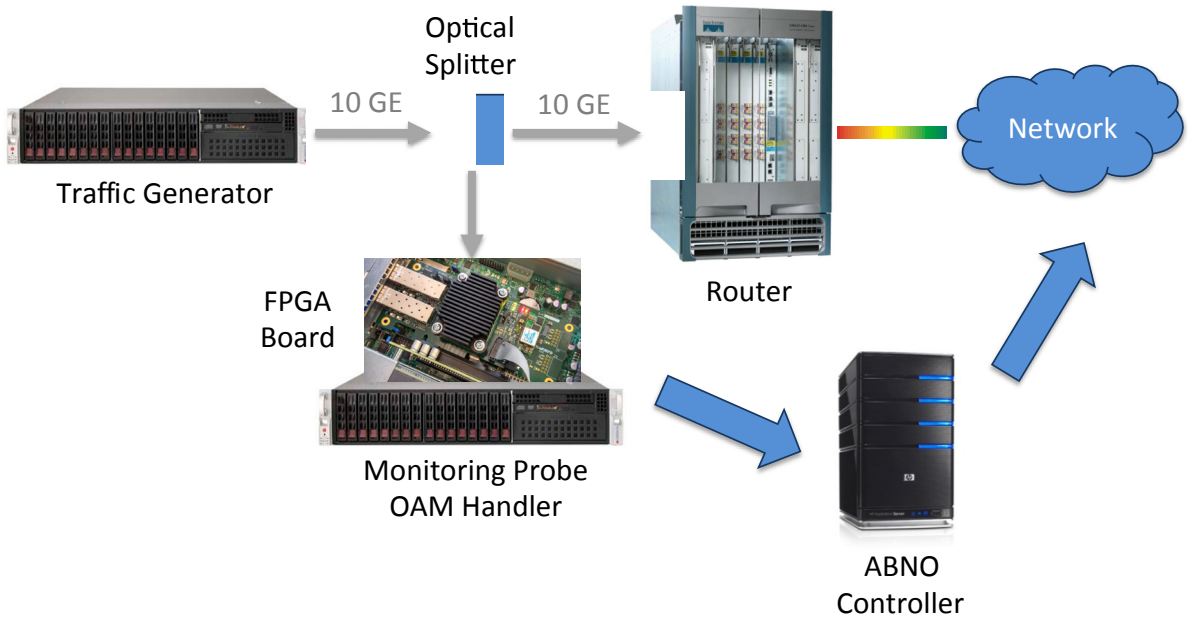

Figure 60: Setup of the Dynamic Bandwidth Allocation experiment

Figure 61 shows a picture of the traffic generator and the monitoring probe in the actual testbed. For the monitoring probe, the hardware-software solution presented in the IDEALIST deliverable D4.3 has been used [58]. To summarize, this solution uses an FPGA board for capturing and preprocessing network traffic. This board (named Kinnic) is depicted in Figure 62. Kinnic is based on a low-cost Xilinx Kintex-7 FPGA in order to create a product at a reasonable price. The remaining processing is done by NAUDIT's Detect-Pro monitoring tool, which creates the flow records. Due to the use of FPGA acceleration, line-rate operation at 10 Gb/s is guaranteed.

Figure 61: Picture of the traffic generator and the monitoring probe in the testbed

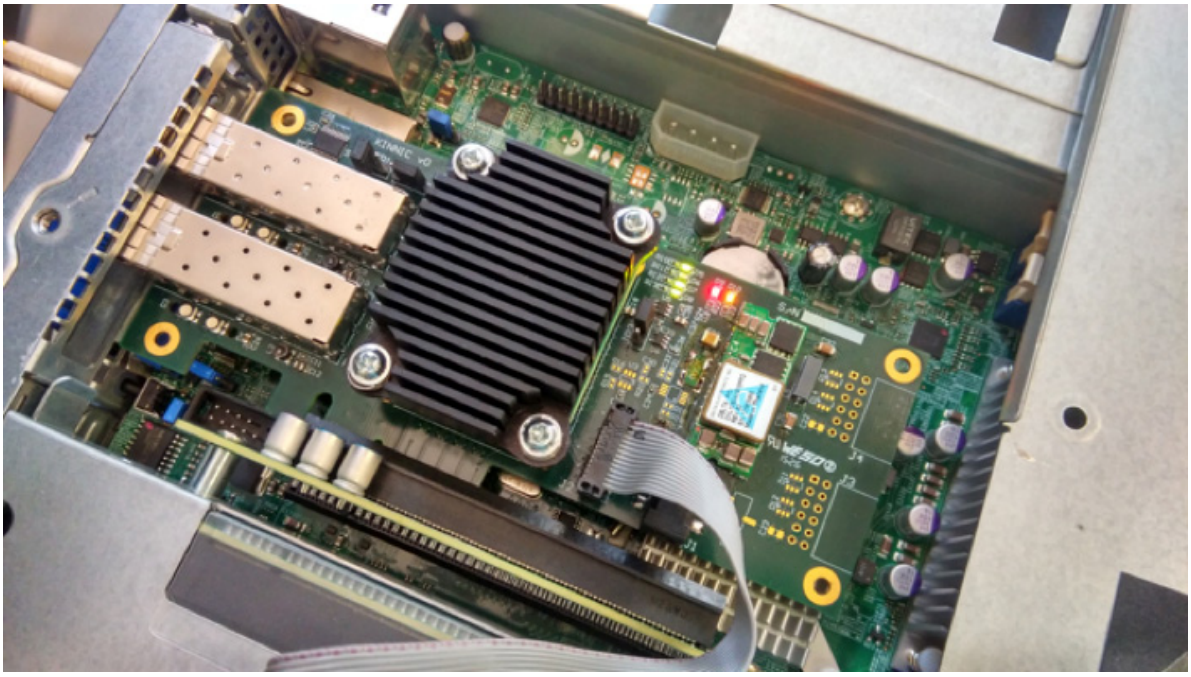

Figure 62: Picture of the Kinnic FPGA board

3.16.2 Attained results

In the experiment, traffic is injected using NAUDIT's 10GE trace player. A synthetic trace has been used, based on a real trace obtained from one of NAUDIT's projects. In this trace, a sudden increase in bandwidth and concurrent flows has been introduced. Figure 63 depicts a capture from the Detect-Pro tool, where the traffic changes can be clearly observed.

Figure 63: Capture from the Detect-Pro tool showing the traffic changes

The Detect-Pro tool exports flow records to the OAM Handler, where the bandwidth estimation algorithm detects the sudden traffic increase. The OAM Handler reacts to this traffic increase by sending a MPLSProvisioning_DBA_WF message to the ABNO Controller via the RESTful interface. Figure 64 shows a Wireshark capture of the messages exchanged between the OAM Handler and the ABNO Controller. This bandwidth change message is received by the ABNO Controller, which starts the network reconfiguration. Similarly, when traffic decreases back to its original level, the same process is repeated again, but this time to reconfigure the network in order to reduce bandwidth. A video showing the complete sequence of operations is available.

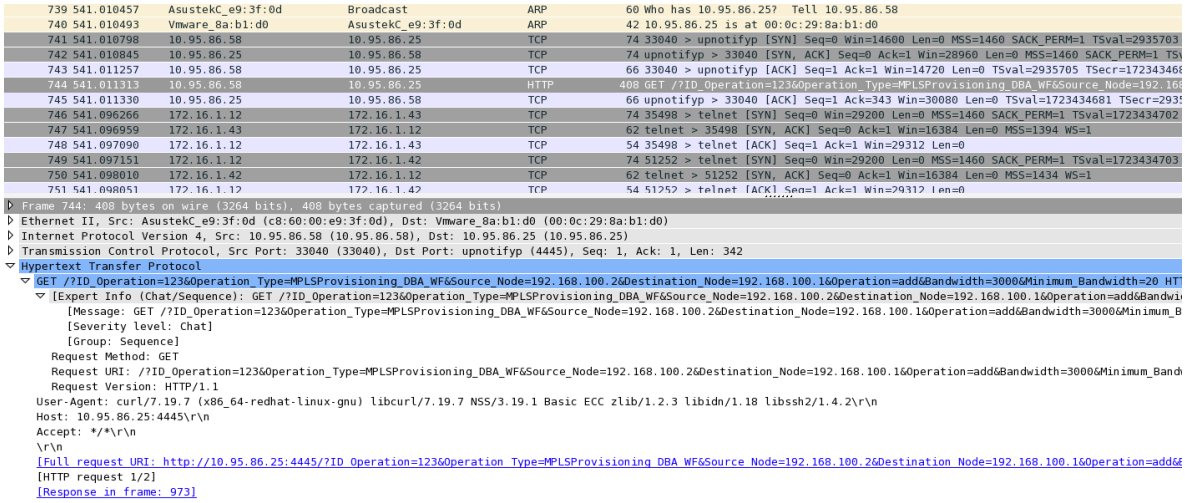

Figure 64: Wireshark capture of a bandwidth update message being sent from the OAM Handler to the ABNO Controller, and its response

3.17 E18. Fixed-Grid/Flexgrid Data Plane Interoperability Experiment

This experiment focuses on the demonstration of interoperability between a flexgrid network domain and a legacy fixed-grid network domain. This demonstration leverages the availability of real-time BVTs and EXCs (Section 3.6) to enable operational compatibility between these types of networks.

Use-case	Building Blocks		
	Performance metrics for network modeling and experiments	BVT and S-BVT	Flexgrid ROADM and BV-OXC
Multi-vendor and multi-technology interoperability	X	X	X

Table 25: Use-case and Building Blocks associated with E18

3.17.1 Description of the setup

Figure 65 presents the flexgrid and fixed-grid optical testbed. In the flexgrid optical network, three AoD nodes are employed. In this network, Node A is connected to Node B by employing 100 km of SSMF and one EDFA. Node A is also linked to Node C via a 50-km optical fibre spool, and Node C is connected to Node B by means of a 75-km optical fibre link. In the fixed grid network, three nodes are used and on each node a WSS-based ROADM (ADVA FSP 3000) with a fixed 100-GHz grid is utilized. For interoperability, the flexgrid optical network is interconnected to the fixed-grid network via a 50-km fibre. In the fixed-grid network, under different configurations, either one or several WSSs are employed in each node for demonstration.

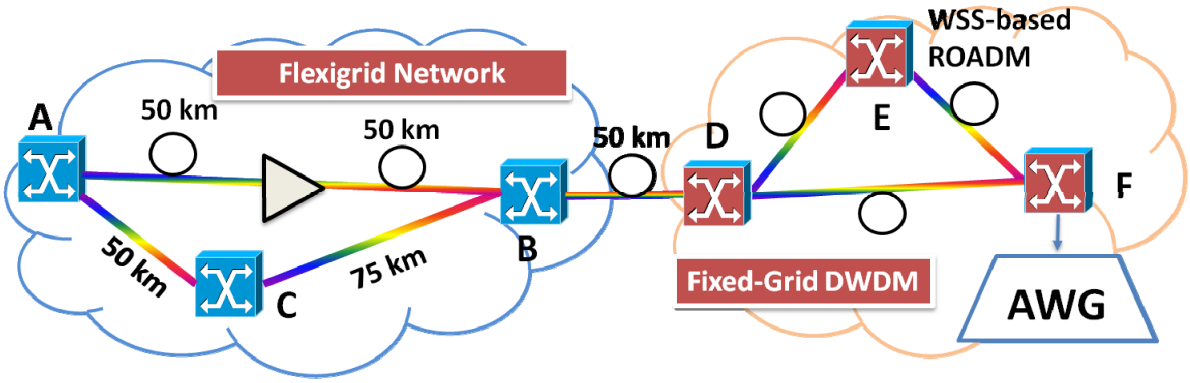

Figure 65: Experimental testbed for interoperability between fixed-grid and flexgrid optical networks

3.17.2 Attained results and analysis

A link from Node A to Node F was setup through nodes B, D and E (Figure 65). To enable compatibility between the two networks and maximize the link capacity, the channel slot is set to 112.5 GHz in the flexgrid network, and 100 GHz in the fixed-grid network, with the centre wavelength at 1548.5 nm. The accumulated filter profiles were tested for the channel with a centre wavelength at 1548.5 nm. Figure 66 shows the obtained filter profiles at different nodes. It can be clearly observed from Figure 66 that the severe filtering effect in the fixed-grid network will affect channels close to the filter edge, and also that after transmission through successive nodes, the filtering effect creates a narrower spectrum width available for the signal transmission.

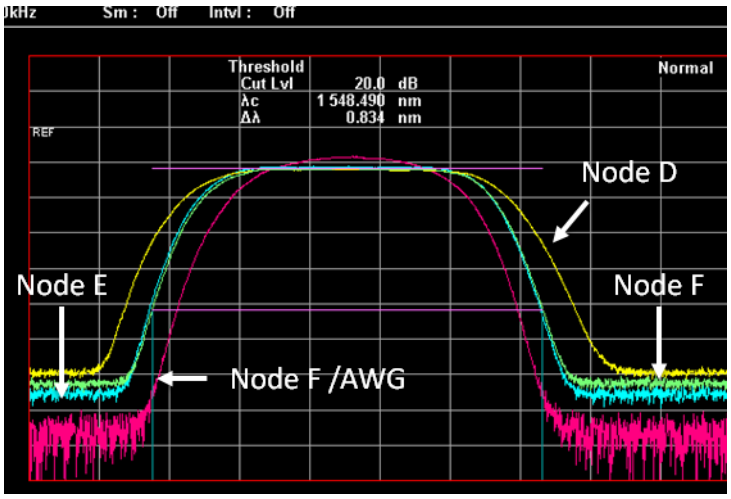

Figure 66: The accumulated filter profiles

To maximize the link capacity, three optical signals, each occupying 37.5 GHz of bandwidth, were launched into the aforementioned link created between the flexgrid and fixed-grid networks. The setup of the transmitters in Node A is shown in Figure 67(a). The centre channel signal is a fixed 28Gbaud QPSK signal, while the other two channels are generated by two BVTs (Section 3.6). With these BVTs, the baud rate can change from 2.67 Gbaud up to 26.7 Gbaud with a step size of ~2.67 Gbaud, to deliver a variable bitrate from 10.7 Gbit/s up to 107 Gbit/s on a PDM-QPSK optical format.

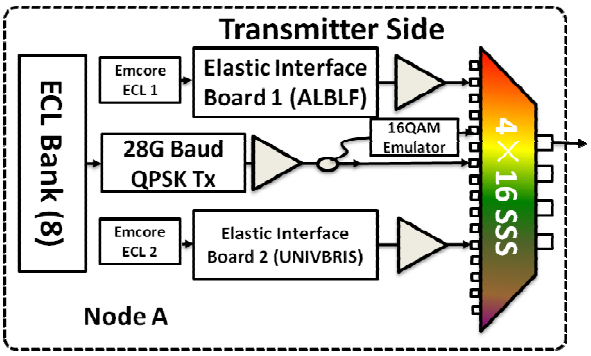

(a)

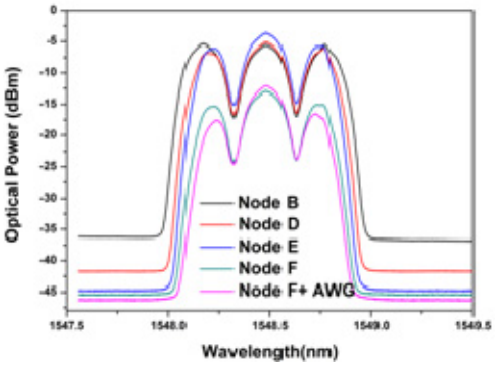

(b)

Figure 67: a) BVT and b) Spectrum of three signals generated by the BVTs (side signals) and fixed transmitter (centre signal)

In phase 1 of this experiment, the two signals created from the BVT (side signals, Figure 67b) operated at full capacity (26.7 Gbaud). Due to the accumulated filtering effect within the fixed-grid network, the tested BERs of the two side signals rapidly increased. Figure 67(b) shows the spectra of the three signals used in the experiment to transmit within the fixed-grid optical network. The filtering effect of the WSS inside the fixed-grid network degrades the two signals in the side bands severely. However, due to the baud rate/bandwidth variable feature of the BVT, the two side channels can adjust their baud rate and therefore reduce their occupied bandwidth to improve the filter tolerance. Therefore, the subsequent phases (phase 2, 3, etc.) are aimed at reducing the baud rate/bandwidth to achieve a better BER transmission performance for the selected signals.

Figure 68 shows the BER performance of one signal created by the BVT (left spectrum in Figure 68b) at different nodes with different baud rates. It can be clearly observed in Figure 68(b) that the BER of this signal increases when it is configured with full capacity (107 Gb/s or 26.7 Gbaud). Figure 68 also shows that at node F, the BER value increases to $1x10^{-3}$. Thus this signal is not able to be retrieved after transmission through the AWG (used for the demultiplex operation) since typical FEC thresholds will not be able to cope with the recovery of such a degraded signal.

In order to combat the filtering effect, the baud rate of the BVT is adjusted to 25 Gbaud. Based on this adjustment, the BER performance recovers to a similar range of the reference signal (centre channel), which does not suffer from any such filtering effect. If we further decrease the baud rate to about 21 Gbaud, the BER performance of this side channel signal further improves to a lowest BER level of $2x10^{-6}$, when passing through Node D, and to a lowest BER of $3x10^{-4}$, when passing through Node F and the AWG used for demultiplexing.

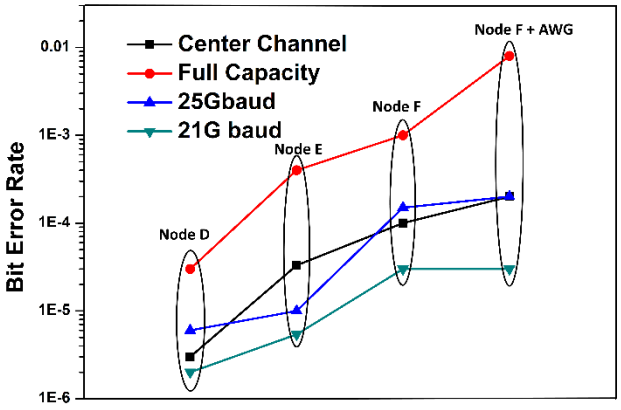

Figure 68: BER performance of a side channel signal with different baudrates. The centre channel signal at 28-Gbaud PM-QPSK is used as a reference to the side channel signal

3.18 E19. Field trial with Orange Telecom (in collaboration with the EU project SASER)

This field trial between Coriant and Orange Telecom has set new world records for optical transmission capacity and distance using state-of-the-art modulation technology in a multi-terabit field trial. The results of this experiment have been published as a post-deadline paper at OECC 2015 [34]. This field trial was conducted in cooperation with the Celtic-Plus SASER project.

Use-case	Building Blocks			
	Algorithm suite (off-line and on-line)	Performance metrics for network modeling and experiments	BVT and S-BVT	Flexgrid ROADM and BV-OXC
Ultra-high capacity and long-reach transmission	X	X	X	X

Table 26: Use-case and Building Blocks associated with E19

3.18.1 Description of the setup

We demonstrated the successful transmission of 24 Tb/s (16QAM), 32 Tb/s (32QAM), and 38.4 Tb/s (64QAM) over a 762-km G.652 fibre link. The telecommunications infrastructure is part of the Orange transport network connecting Lyon and Marseille. The link was equipped with EDFAs and novel Raman amplifiers.

Throughout the course of the field trial, Coriant, Orange and other partners worked closely to successfully implement a wide variety of test scenarios aligned to current and future optical transmission applications. These test scenarios included a mix of transmission speeds and modulation formats, such as QPSK, 8QAM, 16QAM, 32QAM, and 64QAM. The flexi-rate applications demonstrated during the field trial were enabled by prototype technologies developed within the IDEALIST project.

3.18.2 Attained results

The completed multi-terabit field trial showcased the latest advances in ultra-high-capacity optical communications technologies being investigated within the IDEALIST project. More precisely, we broke several world transmission records by exploiting advanced technology research carried out at Coriant. The trial marked the first-ever demonstration of terabit super-channel transmission across a live network in France, as well as the first-ever field demonstration of full flexi-rate and flexgrid transmission – ranging from QPSK to 64QAM. A first-ever demonstration of C-band transmission capacity of 24 Tb/s using 16QAM and 38.4 Tb/s using 64QAM in a live networking environment was carried out. Orange and Coriant also achieved a record-setting transmission reach of 762 kilometres using 32QAM at a capacity of 32 Tb/s, and 64QAM at a capacity of 38.4 Tb/s in the same live environment. These results are of significant importance for the following two reasons: (I) the achieved distance for 32QAM is more than twice as large as compare to any previous field records for this modulation format; and (II) it represents the first-ever regional transmission over installed fibre for 64QAM. These achievements represent an important milestone in the research and development of highly scalable, spectrally-efficient optical networking technologies optimized for future network growth.

3.18.3 Analysis of the results

With the achieved results, we have surpassed previous industry records. In particular, this was obtained by providing error-free super-channel transmission speeds and distances through the use of advanced high-order modulation techniques, next-generation DSP algorithms and FEC codes developed and investigated within this project. Also, advanced optical system features and Coriant's next-generation flexi-rate prototype technologies were part of the field trial, which shows that the results gained within this project are creating a firm development foundation to prepare for the next generation of products.

In terms of spectral efficiencies, we achieved for the 24-Tb/s (24x1Tb/s for PM-16QAM), 32-Tb/s (32x1Tb/s for PM-32QAM), and 38.4-Tb/s (32x1.2Tb/s for PM-64QAM) super-channels, spectral efficiencies that were 5 b/s/Hz, 6.67 b/s/Hz, and 8 b/s/Hz, respectively.

3.19 E20. Field trial between Coriant and TeliaSonera International Carrier over Pan-European optical network

We evaluated high-order modulation formats jointly with advanced DSP techniques (at both sides of the transponder) to achieve record transmission. The analyses were conducted in the context of metro, regional and long-haul systems, and we considered transmission over different types of optical fibres, using lumped or distributed amplification schemes.

Use-cases	Building Blocks			
	Algorithm suite (off-line and on-line)	Performance metrics for network modeling and experiments	BVT and S-BVT	Flexgrid ROADM and BV-OXC
Ultra-high capacity and long-reach transmission	X	X	X	X

Table 27: Use-cases and Building Blocks associated with E20

3.19.1 Description of the setup

We conducted a long-haul experiment over multiple spans across 1634 km of deployed fibre routes between Paris, Luxembourg, and Frankfurt. The link is part of a pan-European optical network belonging to TeliaSonera International Carrier (TSIC). The link represented a popular network scenario, being based purely on SSMF and EDFA-only amplification. The trial was implemented on TSIC's existing Coriant® hiT 7300 Multi-Haul Transport Platforms [35]. The 400G flexi-rate trial used a new Coriant CloudWave™ Optics [36] prototype, a versatile suite of software-programmable photonic layer technologies that brings a new level of flexibility, efficiency, and scalability to next-generation optical transmission networks. In order to be able to engineer the trial and the BVT prototype, the research within the IDEALIST project on BVT, modulation formats and physical effects has been a key contribution.

3.19.2 Attained results

The field trial featured the successful transmission of three different software-programmable modulation formats – quadrature phase shift keying (QPSK), 8QAM, and 16QAM – over the complete distance of 1634 kilometres each, as well as a variety of line-side transmission speeds (100G, 200G, 300G, 400G) in a mix of capacity and reach application test scenarios.

3.19.3 Analysis of the results

This trial represents an industry-first demonstration of cutting-edge flexi-rate technology that promises to significantly advance the state of optical layer flexibility. With optical transmission speeds up to 400G, we showcased high-capacity high-order modulation formats for metro, regional and long-haul optical systems with a real-time BVT. Overall, this is a successful field trial demonstration of an innovative flexi-rate technology that supports the dynamic and cost-efficient provisioning of optical transmission speeds up to 400G per channel based on application-specific bit-rate, reach, and modulation requirements, and a proving ground for the research done within IDEALIST.

3.20 E21. High capacity high order modulation formats field trials

This experiment is planned to validate in a field-trial environment the investigations described in E20. The field trial has the goal of testing the IDEALIST high-order modulation format solutions in a real DWDM system configuration, focusing on interoperability of existing and commercially-available coherent 40-Gb/s and 100-Gb/s channels with photonic integrated high-capacity channels provided by the project.

Use-cases	Building Blocks			
	Algorithm suite (off-line and on-line)	Performance metrics for network modeling and experiments	BVT and S-BVT	Flexgrid ROADM and BV-OXC
Ultra-high capacity and long-reach transmission	X	X	X	X
Multi-vendor and multi-technology interoperability	X	X	X	X

Table 28: Use-cases and Building Blocks associated with E21

3.20.1 Description of the setup

The field trial will be done by inserting the IDEALIST high-order modulation format solutions as multi-flow transmitters of a DWDM system employing G.652 fibres installed in a regional Telecom Italia network. The interoperability trial will be helpful in evaluating network migration scenarios towards higher-capacity coherent systems, and share the benefits of the new technologies, besides providing clearer ideas of their potentialities and limits.

Some fibre pairs in the Telecom Italia domestic metro regional network will be devoted to the experiments. Each pair starts in TILAB's "Optical Transmission Lab" and ends around 40 km away, in Chivasso (Figure 69). Some network exchanges are located in between; intra-exchange optical interconnections were made with optical patch-cords into the network exchange distribution optical patch panels.

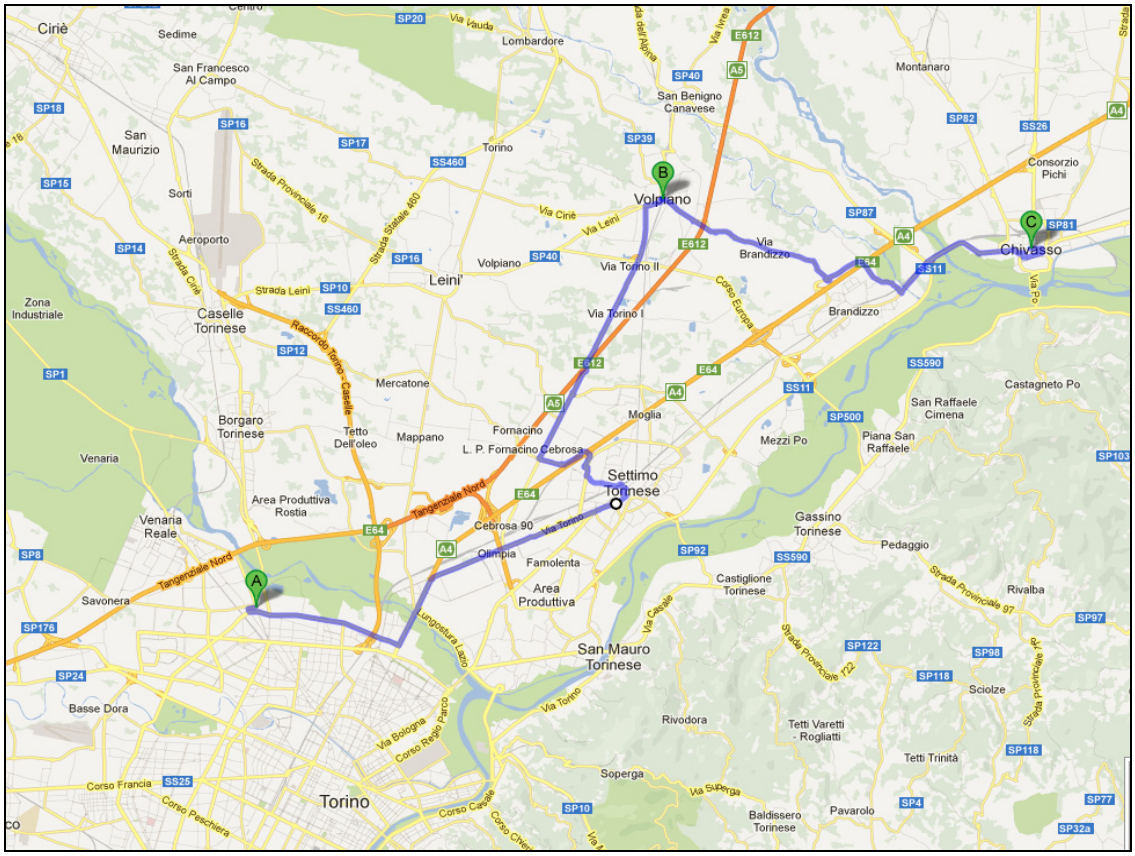

Figure 69: Geographical map with network exchange sites (Torino, Settimo, Volpiano, Chivasso)

Optical interconnections have been set up in the Torino Stampalia, Torino Stura, Settimo, Volpiano network exchanges for the trial period. The overall link is thus composed of five sections: the first one, 3 km long, starts at the TILAB premises and reaches the Torino Stampalia network exchange. Afterwards, a 4-km span leads to Torino Stura, then Settimo, which is 6.7 km away. The last two sections are each respectively 11.4 km and 15 km in length, from Settimo to Volpiano, and from Volpiano to Chivasso (Table 29). In order to obtain a fibre span starting and terminating in TILAB, a hardware physical loop is performed at the Chivasso site: a certain number of 80 km spans will be available for the trial, each of them starting and terminating in TILAB.

TORINO STAMPALIA	TORINO STURA	3.996
TORINO STURA	SETTIMO	6.75
SETTIMO	VOLPIANO	11.435
VOLPIANO	CHIVASSO	14.944
		37.125

Table 29: Span length [km]

In order to concatenate the spans and realize a transmission link, in-line amplifiers are necessary (Figure 70): maximum link length is 640 km, with eight spans. If needed, the transmission link length can be reduced by concatenating a lower number of spans.

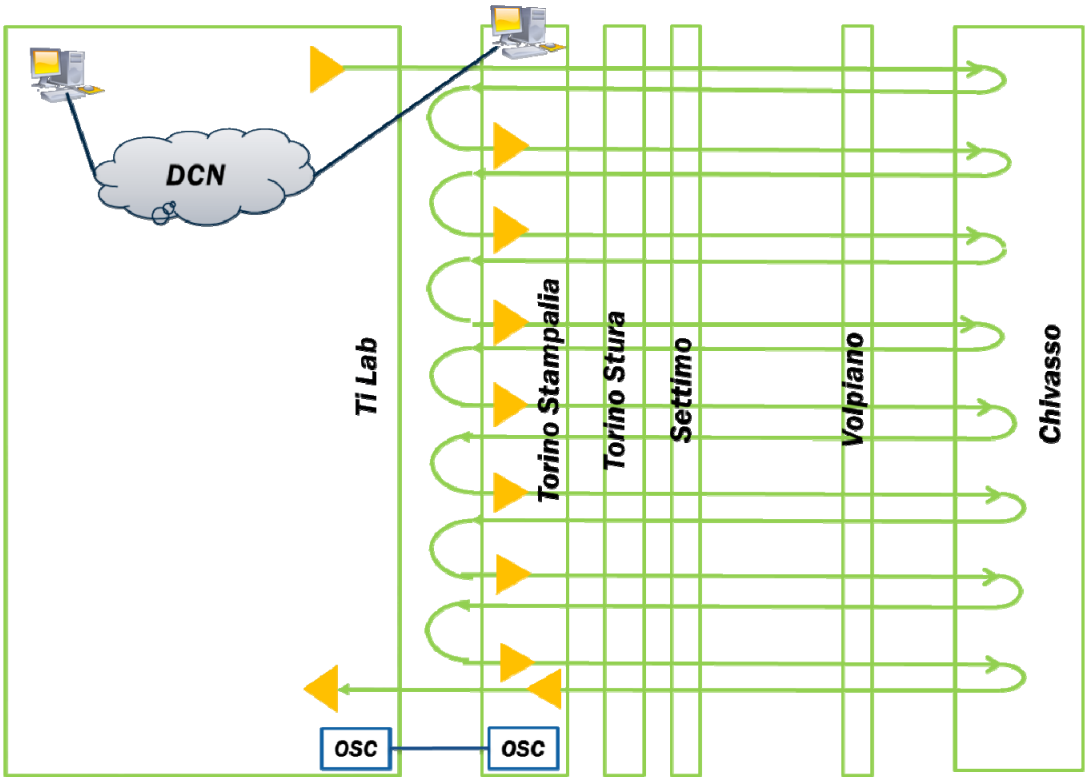

Figure 70: Transmission link set-up

In a typical setup, dual-stage amplifiers with maximum gain from 25 to 30 dB have to be employed; each amplifier has to operate in the constant output power regime, and the power control mode should be reconfigurable by software. An on-board OSA card dedicated to each amplifier grants accurate monitoring and alarm reporting of the power per channel. OSA measurements from the optical amplifier monitoring ports provide useful information about channel power equalization, OSNR evolution, and nonlinear spectral distortion; these measurements being very important for the case where channels at different baud-rates, with different modulation formats and spectral shapes are being transmitted.

The CD of the link was measured by the nonintrusive monitoring of some 40G and 100G coherent optical interfaces with live traffic. The total link CD value was around 9500 ps/nm, measured around 1550 nm, corresponding to an average CD of 16.6 ps/nm/km. The measured value of the total link DGD was around 1.5 ps.

With respect to the transmission aspect, Coriant will transmit different types of channels over the link, starting with DP-QPSK up to DP-128QAM, either in a single carrier configuration or in a super-channel. The field-trial aims at testing the algorithms and hardware components developed over the entire course of the IDEALIST project in a realistic metro / regional environment, such as the one provided by Telecom Italia in Torino. This field-trial is seen as an evolution of the previous one carried out jointly with another EU project and described in Section 3.18.

3.20.2 Expected results

We expect to show ultra-high capacity transmission by employing a wide range of high-order modulation formats. Moreover, typical upgrade scenarios will be tested by varying the

symbol rate, modulation formats, and FEC overhead. We plan transmission over the entire C-band, thus achieving or improving upon the results obtained in Section 3.18; but under completely different link conditions. In fact, in contrast to the experiment as described in Section 3.18, we will not be utilising Raman amplifiers and the fibre attenuation loss will be significant larger. The planned date of the experiment is within the last two weeks of November 2015. Results will only be available in time for the project's Final Audit.

3.21 E22. Multi-layer use-cases with ANM

The ANM is based on the ABNO architecture as proposed in the IETF as a framework that enables network automation and programmability thanks to the utilization of standard protocols and components. This work represents the first experimental demonstration based on two multi-layer use-cases: the Automatic IP Link Provisioning use-case, and the MPLS Service use-case.

Use-cases	Building Blocks			
	Algorithm suite (off-line and on-line)	Flexgrid ROADM and BV-OXC	GMPLS and OFP extensions for flexgrid	Network Orchestrator (ABNO)
IP over optical control	X	X	X	X
Dynamic provisioning including DC interconnection	X	X	X	X

Table 30: Use-cases and Building Blocks associated with E22

3.21.1 Description of the setup

We have used three Juniper MX-240 routers, four ADVA FSP 3000 optical nodes and an emulated GMPLS CP domain developed in Telefónica I+D, as shown in the following figure:

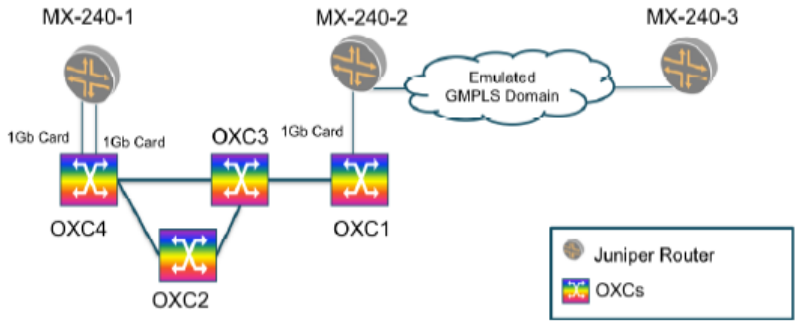

Figure 71: Testbed set-up

The Telefónica I+D control plane testbed is composed of GMPLS nodes run with internally-developed software, with the protocol suite released in github [60]. The experimental setup is built with emulated nodes, which run on an Ubuntu server Linux distribution. Each emulated node implements a GMPLS stack (including RSVP, OSPFv2 and PCEP) and a Flexible Node emulator. Each GMPLS controller is a virtual machine, and all are running a server with two processors comprising an Intel Xeon E5-2630 2.30GHz, 6 cores each, and

192 GB RAM. The GMPLS control plane stack and Flexible Node emulator are developed using Java 1.6. Note that there is no hardware associated with this domain, only an emulation of the nodes. The figure below presents the optical mesh of Telefónica in Spain of the emulated control plane using the Network Library [61].

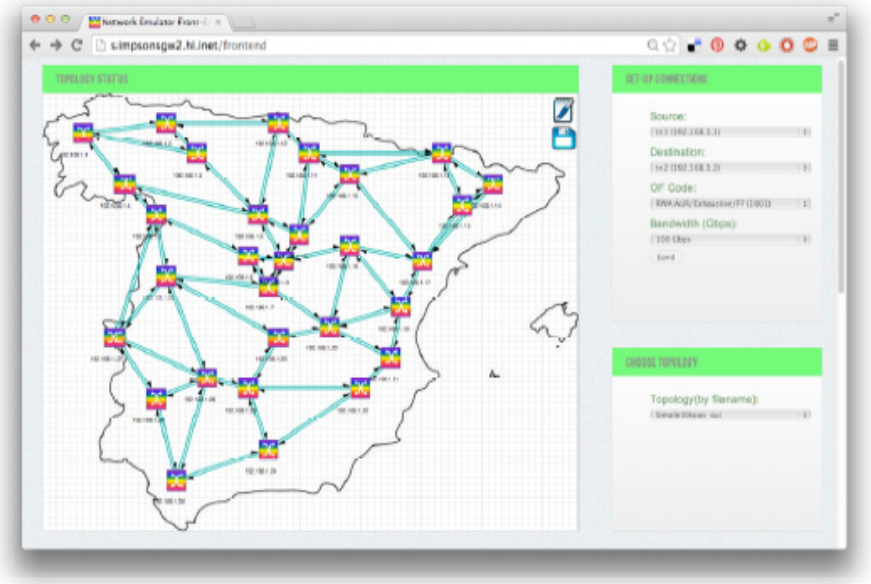

Figure 72: The optical mesh of Telefónica in Spain of the emulated control plane

Using the GUI, link connections can be created, deleted, and the optical paths can be analyzed. Moreover, varying topologies can be selected using the GUI, so that different networks can be tested with the control plane implementation.

3.21.2 Attained results

The following figure shows the PCEP and HTTP messages exchange for the IP Link provisioning use-case. Some messages (like the KeepAlive and Open messages, and the dialogue with the Policy Manager and TM) are omitted to improve readability. As can be seen, the interactions between the main modules of the architecture are done using PCEP messaging. The ABNO sends a PCInitiate message to the VNTM, and the VNTM to the Provisioning Manager, as they have to initiate a new connection in the network. On the other hand, the message to compute the optical path to the L0 PCE is a PCERequest message. We have assumed for this test to use a stateless PCE in the optical layer.

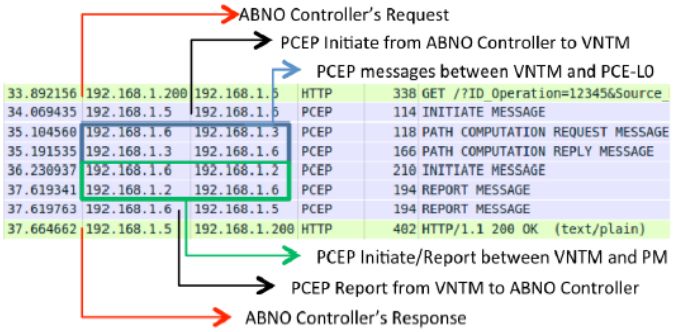

Figure 73: Message flow in the IP Link provisioning use-case

Similarly, the next figure shows the PCEP and HTTP traces for the MPLS Service workflow, which is longer than the previous use-case, because there is an initial interaction with the L3 PCE, which detects that there is not enough bandwidth in the MPLS layer. The ABNO therefore requests a connection between the two end-points for a new IP Link. This request from the ABNO to the VNTM launches a similar process to that of the previous use-case.

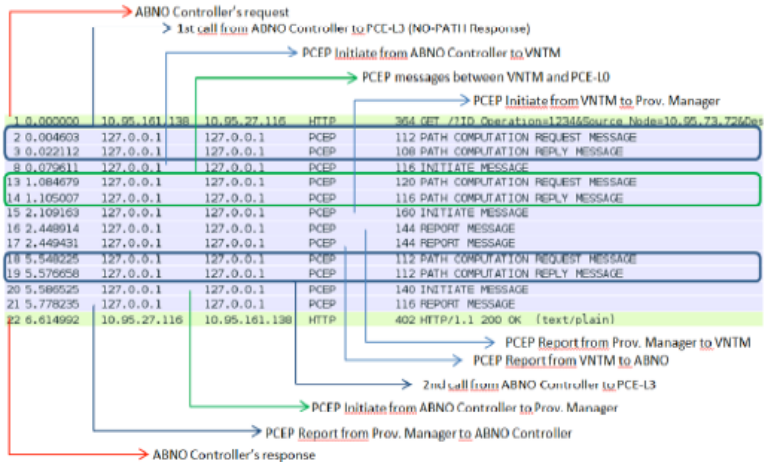

Figure 74: Message flow in the MPLS Service provisioning use-case

3.21.3 Analysis of the results

The ANM architecture enables automated and simplified network service provisioning through different network segments (metro, core, data centre, etc.) and technologies (IP/MPLS, optical, OpenFlow, etc.). Due to its modular nature, the ABNO architecture can be developed as an open platform rather than as monolithic software. The ABNO architecture is based on standard elements and protocols, and most of its components are not as such linked to physical devices and their possible specific parameters. This work validates the ability for the ANM to not only support flexgrid scenarios, but also multi-layer use-cases.

3.22 E23. IPoDWDM Hybrid control plane tests

The goal of these tests is to prove the IPoDWDM network solution based on Hybrid Control plane. The tests covered function from a simple circuit set-up to a complex service provisioning with re-optimization. The tests have been performed on the beta-version SW released and has the goal to show the new Control Hybrid control plane features that are the building blocks of the Cisco SDN architecture.

This plan, including test cases, has be jointly reviewed, approved and performed by TID and Cisco in Madrid Labs. The test bench, the test procedures and the test results could be matter of new White Papers and standard proposals (in IETF, OIF, BBF, etc.).

Use-cases	**Building Blocks**				
	Algorithm suite (off-line and on-line)	Performance metrics for network modeling and	Planning Tools for EON	Flexgrid ROADM and BV-OXC	GMPLS and OFP extensions for flexgrid

		experiments			
Resource allocation in EON	X			X	X
Optical restoration after fibre breaks	X			X	X
Optical restoration in IP networks	X			X	X
IP over Optical planning	X		X	X	X
IP over Optical control	X	X		X	X
Dynamic provisioning including DC interconnection	X	X		X	X
Dynamic re-optimization after link failure repairs	X			X	X

Table 31: Use-cases and Building Blocks associated with E23

3.22.1 Description of the test setups

The following network (Figure 75), designed with the CTP planner, has been used for all the phases of feature tests.

The Cisco testbed is based on a simple optical network connecting two routers CRS-3 4-Slot, one of them with two 100GE colored interfaces and six 10GE interfaces, and the other one with one 100GE colored interface and six 10G interfaces (and extra 100GE colored interface may be added to show LOGO features).

The optical network is based on colorless, directionless, flexgrid ROADMs and can be simply managed by the TL-1 or the Craft Terminal. Although Cisco has the EMS/NMS functions, we think this is not significant for the tests we propose.

Connected to the IP and optical Network, other than the Craft Terminal there is the Hybrid Control Plane (MATE/WAE) able to control either the IP and the Optical Network.

MATE, at the moment, uses traditional interfaces (TL-1, CORBA, CLI, SNMP, XML) to retrieve the network topology and to provision services. MATE can be considered as a building block of the SDN solution Cisco is working on. In the case of CORBA interface, the information is coded as YANG models. The MATE evolution (WAE) will use more standard interfaces like NETCONF/YANG either to interface the IP and the Optical network.

The optical part of the set-up is composed by 3 multi-degree ROADM nodes, simulating a simplified mesh topology as shown in Figure 75:

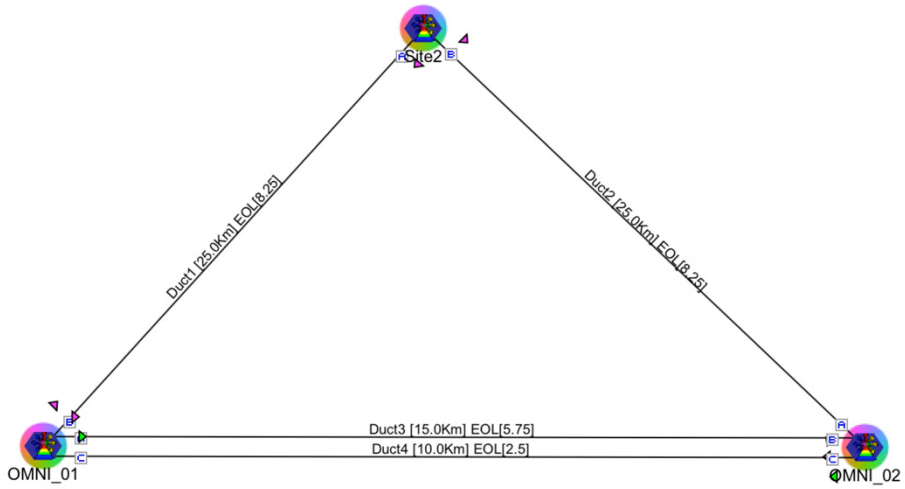

Figure 75: CTP - DWDM Network Design

Figure 75 shows the layout of the network as it has been designed using Cisco CTP, translating into the design tool the required lab topology shown in Figure 76:

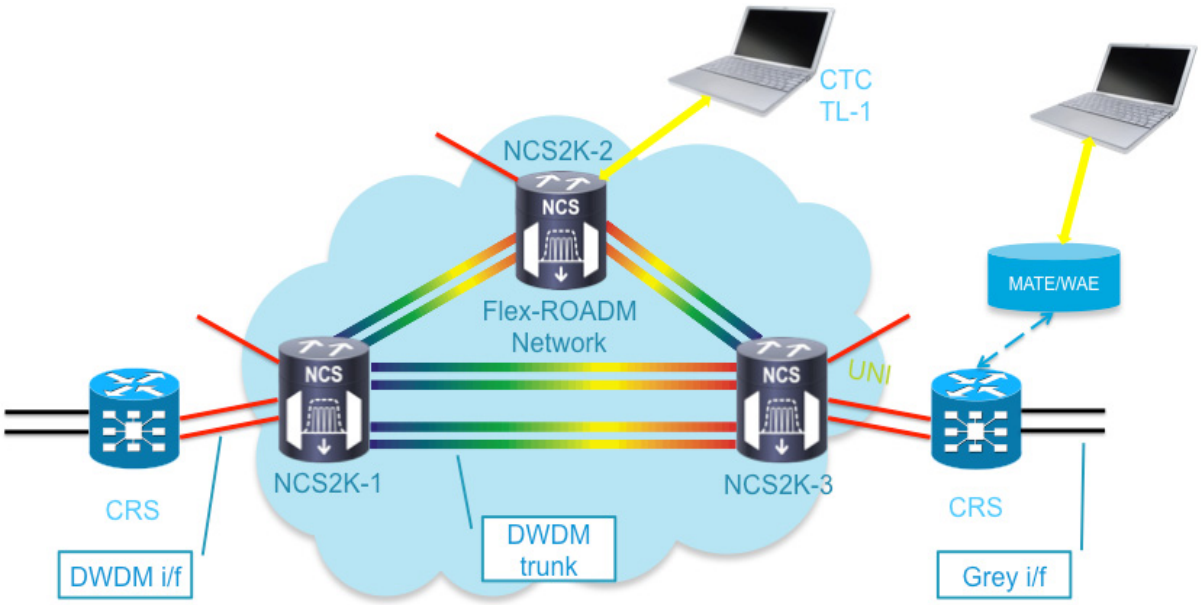

Figure 76: IPoDWDM Lab. Topology

The testbed will include two core routers, each with 2 100G flexible DWDM interfaces and a number of grey 10GE interfaces to get traffic into the network. The testbed will also include 3 flex-spectrum ROADMs, each capable of connecting to additional transponders. The ROADMs will be connected via multiple DWDM trunks as shown in the figure to allow for diverse routing of lightpaths. Some changes to the exact makeup of the testbed are possible, but the overall approach driving its design and functionality will stay as explained.

Each node is built using Cisco NG-ROADM unit, namely the NCS2K-16-WXC-FS= unit. This is the basic building block to build multi-degree ROADM nodes, supporting omni-directional (aka directionless) and colorless switching. The technology used in this unit supports FlexSpectrum providing the capability of managing an arbitrary set of continuous

portions (also called frequency slot) of the optical spectrum, delimited by programmable "start" and "stop" frequencies.

Two of the nodes (OMNI_01 and OMNI_02 in Figure 75) are interconnected with a dual fibre to provide multiple path to reach any destination and therefore test MLR capabilities.

As stated all the ROADM nodes support both omnidirectional and colorless switching.

The nodes will be managed by the Cisco EMS and will run GMPLS. In addition, they can be controlled via CLI or XML (for routers) and TL-1 or CORBA (for ROADMs). This allows out-of-the-box IDEALIST developed control planes, SDN controllers or management systems to control and manage them. Cisco will supply documentation to allow other partners to understand how to interfaces with the NEs.

3.22.2 Test Coverage

The features that will be covered in this document are the followings:

PHASE 1

- Optical Circuit set-up, tear-down via TL-1 / Craft Terminal (using GMPLS)
- Optical Circuit set-up, tear-down via CLI and UNI signaling to GMPLS
- Optical Path diversity option based on Optical LSP-Id
- Shortest path and/or Optical Impairments (LOGO) routing (when only full coherent interfaces are running)
- Dynamic restoration at optical level w/ and w/o Lambda re-provisioning.
- **25 Total Tests** done successfully covering PHASE 1. There is not test description as related on GMPLS only

PHASE 2

- Optical Path diversity based on SRLG
- Multilayer Optical Restoration (MLR-O)
- Hybrid Control Plane (MATE/WAE + GMPLS)
    - IP and Optical Network topology retrieved by MATE/WAE
    - Service Design (IP + Optical) done by MATE
    - Service Deployment (IP + Optical network) done by MATE
    - Restoration driven by GMPLS
    - Circuit/Service re-optimization done my MATE
- Test description for PHASE 2 is reported below.

3.22.2.1 IP and Optical Topology retrieved by MATE

Test 26

MATE is able to retrieve the network topology connecting:

- To the IP nodes via CLI and SNMP
- To the DWDM nodes using an XML interface exporting the YANG models

The possibility to retrieve the network topology via BGP-LS will be supported in a second phase.

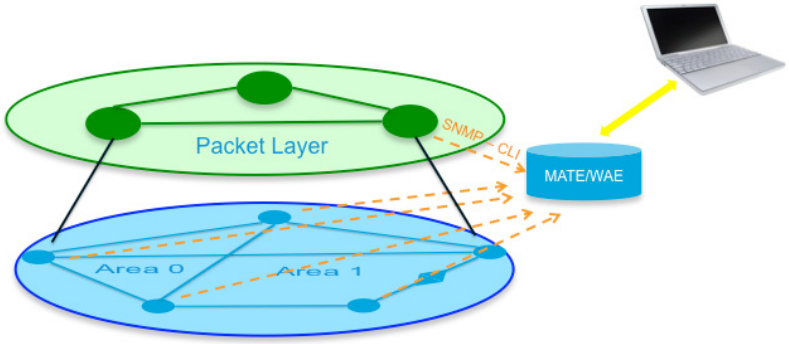

Figure 77: Network Topology discovery

3.22.2.2 Service Design (IP + Optical) done by MATE

Test 27

The provisioning of the service is currently done via CLI and UNI interface.

The PCEP will be implemented in further Phase.

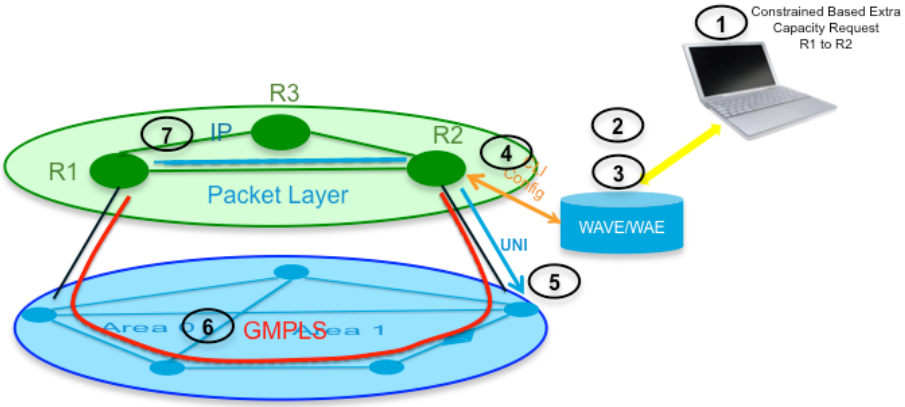

Figure 78: L1-L3 service calculation

1. Start state: the network topology is shown (via CTC or via the MATE GUI)
2. MATE shows the two network layers and their relationship (see Figure 78)
3. A new Service (IP) is required by the operator
4. MATE can show the L3 and L1 circuit in the GUI and as a script

3.22.2.3 Service Deployment (IP + Optical network) done by MATE

Test 28

1. The Operator pushes MATE configuration to the network
2. MATE provisions the L3 (CRS) and L1 (DWDM ERO + Lambda)

3. GMPLS implements the Circuit
4. The traffic goes ON (Traffic analyzer shows 0 errors or packets running)
5. CTC shows the circuit
6. MATE updates the circuit visualization (and the spare ports list)

The deployed circuit is then provisioned in the DWDM layer via UNI interface and the distributed Control Plane (GMPLS).

3.22.2.4 Service Deployment (IP + Optical network) done by MATE with optical path diversity

Test 29

1. A new Service (IP) is required by the operator with Path Diversity
2. MATE can show the L3 and L1 circuit (L1 path = OMNI_01, OMNI_02, OMNI_03)
3. MATE provisions the L3 (CRS) and L1 (DWDM ERO + Lambda)
4. GMPLS implements the Circuit
5. The traffic goes ON
6. CTC shows the circuit
7. MATE updates the circuit visualization (and the Spare ports list)

Following the test 28, the new circuit has been routed on a different link used by the existing circuit.

3.22.2.5 Restoration driven by GMPLS

Test 30

1. Start state: the network topology is shown (via CTC): 2 circuits running
2. MATE is connected to the network and shows the same
3. A fibre cut happens between ONMI_01 and OMNI_02 (L1 path = OMNI_01, OMNI_02, OMNI_03 affected)
4. FRR makes the L3 protections (optional), GMPLS makes the optical restoration (w/ Lambda retuning). Path OMNI_01, OMNI_03 is selected by the GMPLS.
5. The traffic goes ON again on a new Optical path
6. MATE can show the L3 and L1, and New circuit and the DWDM network with the missing span (due fibre cut)

After having set the new circuit a fibre cut is done on the span supporting the circuit.

The GMPLS Restoration reroutes the failed circuit through the path: OMNI_1, OMNI_2 and OMNI_3.

It must be noted that as the failed circuit was set with diversity constraints, the GMPLS selects a 2 hops path instead of the direct path between OMNI_1 and OMNI_3 (as this path is carrying the “diverse” circuit).

3.22.2.6 Circuit/Service re-optimization done my MATE

Test 31

1. The fibre cut is fixed see
2. The fibre fix is shown by MATE
3. The operator makes a network re-optimization using MATE (choosing the best optical path)
4. MATE provisions the new optimized optical circuit
5. CTC shows the circuit
6. MATE updates the circuit visualization

After the fibre is repaired, the operator can work with MATE to re-optimize the optical network and bring back the optical Path to a less expensive route.

Using the MATE GUI it is possible to drive the optical Routing and exclude/include nodes, links and SRLG.

Note in this case that the GMPLS Restoration was set “NOT Revertive” to prevent the GMPLS to bring the Restored Circuit back to nominal path.

3.22.3 Attained results and Test Matrix

All the tests described in previous subsections passed successfully, with the exception that one MATE Network Topology retrievement failed due to a RMI Virtual Machine restart in the Linux server. The issue has been solved re-launching the Virtual Machine.

The following tables contain the mapping between Test Cases and Test Results notes.

The Phase 1 tests were done on the NCS2K Rel.10.02 and CRS XR Rel. 5.1.4.

The Phase 2 tests were done on the NCS2K Rel.10.3, CRS XR Rel.5.3.0 and MATE Rel. 6.1.

Logical ID	Title	Result
Test 1 Test 2 Test 3 Test 4	Circuit set-up, tear-down via TL-1 / Craft Terminal (CTC) using GMPLS	Passed
Test 5 Test 6 Test 7	Optical Circuit set-up, tear-down via CLI and UNI signaling to GMPLS	Passed
Test 8 Test 9 Test 10	Optical Path diversity option based on Optical LSP-Id	Passed
Test 11 Test 12	Shortest path and/or Optical Impairments (LOGO) routing (when only full coherent interfaces are running)	Passed
Test 13 Test 14 Test 15	Optical Path diversity option based on Optical LSP-Id	Passed

Test 16 Test 17 Test 18	Dynamic restoration at optical level with Lambda re-provisioning	Passed
Test 19	Dynamic restoration at optical level with LSP priority	Passed

Table 32: Phase 1 test-cases and reports

Logical ID	Title	Result
Test 20 Test 21 Test 22 Test 23	Optical Path diversity based on SRLG Dynamic restoration at optical level with SRLG XRO path option	Not done
Test 24 Test 25	Multilayer Optical Restoration (MLR-O)	Not done
Test 26	IP and Optical Topology retrieved by MATE	Passed
Test 27	Service Design (IP + Optical) done by MATE	Passed
Test 28	Service Deployment (IP + Optical network) done by MATE	Passed
Test 29	Service Deployment (IP + Optical network) done by MATE with optical path diversity	Passed
Test 30	Restoration driven by GMPLS	Passed
Test 31	Circuit/Service re-optimization done my MATE	Passed

Table 33: Phase 2 test-cases and reports

4 Conclusions, general analysis and final recommendations

IDEALIST WP4 has succeeded at building a pan-European testbed which interconnects all the components developed in the project, both hardware and software. An especial effort, beyond the initial expectancies of the project was made to further integrate the hardware elements. As a result of this, in the laboratories of Pisa and Bristol, the switching elements, S-BVTs, OTN Matrix and control plane were put together to perform the proof of concept of the Multi-Domain Multi-Vendor Elastic Optical Network envisioned by IDEALIST.

The experiments carried out in WP4 validate and measure the performance of the solutions proposed in the project (WP1, WP2 and WP3). The Control and Management plane was tested at large, with numerous experiments showing a robust behavior an unprecedented degree, of interoperability, unusual for research projects. This has allowed that some of the extensions developed in WP3 to advance thoroughly in the standardization process, which extremely values interoperability demonstrations.

4.1 Software-driven flexgrid BVT node

The experimental activities carried out on the Soft-FBVT have achieved all the expected goals and aims of the IDEALIST project. In particular, the architecture of this kind of transponder (as defined in WP2) is able to configure different superchannels with data

rates of up to 1 Tb/s using different modulation formats (mainly PM-QPSK and PM-16QAM) based on the TFP transmission technique enabling LDPC codes.

This technique has been demonstrated to achieve a high spectral efficiency (e.g. 6 bit/s/Hz with a low-order PM-QPSK modulation format), allowing effective packing of the superchannel subcarriers and enabling advanced adaptation functionalities, e.g. distance adaptation with code rate selection, and reliability with code rate adaptation. The result is that a 1 Tb/s superchannel can be conveyed in the 150-200 GHz frequency slot range, depending on the optical reach and the number of traversed nodes.

The high configuration degree of this transponder depends on the configurability of: 1) the baud rate, 2) the tunable lasers, 3) the LDPC code rate, 4) the number of selectable sub-carriers, 5) the modulation format, and 6) the coherent receiver DSP parameters. Multi-wavelength sources enabling sliceability have been employed and successfully tested. Coherent receiver DSP allows real-time monitoring of the received signal, enabling a proactive QoT-aware control plane, as defined in WP3.

This transponder has been validated in a combined data-control plane testbed at the CNIT labs in Pisa, evaluating different use-cases according to the WP1 specifications. Full automatic configuration by means of both PCE/GMPLS and SDN control planes has been achieved. In particular, routing-spectrum-code assignment for provisioning and re-optimization, control-driven hitless shifting, and hitless code adaptation procedures have been validated with extended control messages. Code rate assignment represents a novel output of path computation. Moreover, code rate adaptation was also shown to be the most promising solution in terms of hitless adaptation/restoration due to QoT degradation. The high configurability of the Soft-FBVT has allowed us to propose EON-specific spectrum efficiency techniques, such as differentiated filtering and superfilter techniques.

Finally, the proposed Soft-FBVT has been successfully integrated in the whole IDEALIST project (enabling full interoperability at both the data-plane and control-plane) by means of joint multi-partner testbeds and experiments, including: 1) the PLATON planning tool and backend PCE provided by UPC [20] [17]; 2) the ABNO controller provided by Telefónica [5]; 3) multi-partner distributed control plane, provided by CTTC, TID, TI, CNIT [31]; 4) multi-vendor interoperability at the data plane level (CNIT/Ericsson and Coriant) [31]; and 5) the final IDEALIST integrated experiment for joint control-plane and data-plane multi-vendor and multi-domain interoperability [10].

4.2 Metro-core border node

Alcatel-Lucent's involvement during IDEALIST project was focused on multiple tasks. We spent some effort on WP1 to study the use-cases for elastic optical networking. Among this, we were more interested in studying the design, characterization and impact of a bandwidth variable transponder in its literally meaning, i.e. adapting the baud rate to certain conditions to fully benefit from flexgrid systems. We found out that this would be beneficial to mitigate filtering impairments and to save spectrum for a "beginning-of-life" network, i.e. when capacity is not at full load.

In WP2, we therefore focused a large part of our effort on building (from scratch) the first proof-of-concept of a flexible OTU framer and elastic baud rate transmitter which can be used in metro and/or core nodes. This proposition was leveraged the OTN standards proposition for "beyond 100G" evolution; however, we had to scale down to 100G with QPSK signals due to the best-in-class FPGAs whose maximum frequency clock is about 30 GHz. This proof-of-concept, even if at lower speed, perfectly validated the new framer, and beyond that the applications for flexgrid. We also performed integration with the

current, commercial Alcatel-Lucent 1830PSS product for centralized control of both the OTN switch matrix and the FPGA-based prototype for the flexible OTU framer and BVT, and demonstrated fully compatibility with existing products. Extensions for centralized control are of high interest for business needs, as well as the new data plane that has been prototyped. We are now spending more time in building a real-time prototype as adoption towards commercial products speeds up.

During the IDEALIST project lifetime, Alcatel-Lucent also focused on producing record transmission experiments with a non-real-time transceiver, which are much quicker to program and evaluate. This has permited us to investigate new solutions paths, so as to continue as a best-in-class system vendor. This included 1 Tb/s transmission with single-carrier and superchannel Nyquist WDM, as well as novel techniques for advanced signal processing with 8QAM experiments, and the proposing of novel nonlinear mitigation techniques.

4.3 Ultra-high capacity flexgrid node

The knowledge acquired by Coriant during the timeframe of the IDEALIST project on the data-plane research for elastic optical networks will be of fundamental importance for our product definition, as it will positively impact our products not only in terms of features, but also in terms of the awareness of operator needs. Overall, we believe that IDEALIST has been a great success in terms of its results, the joint work, and the usefulness of its outputs for our company and for the scientific community. We therefore now report a final summary of our work, and the connections with the experiments reported in Section 3 of this deliverable.

We dedicated the first year of the project to acquire the basic knowledge for understanding the transmission characteristics of elastic optical networks. In this framework, we assessed the transmission performance by using numerical simulations tools [41][42] and by carrying out our first experiments within a lab environment [45][46]. Between the end of the first year and the first part of the second year, we optimized our testbed by introducing novel advanced algorithms at the transmitter as well as at the receiver [47][48]. This led to a significant number of publications at leading conferences and journals [49][50]. At the end of the second year, we started the first collaboration activities with our partners by carrying out a series of joint experiments whose results have been published [50].

The last year of the project is well summarized by the list of experiments E16, E19, E20, and E21. Here we combined our acquired expertise with the one of numerous partners and conducted the experiments already described in Section 3.

For example, in [34] we broke transmission records in terms of capacity, and we showed for the first time transmission in the field with 64QAM [34][43]. In [10] we significantly contributed to the hero experiment reported in E16. The results of this collaborative experiment have been published in a post-deadline paper at ECOC 2015, and soon will be extended in an invited JLT paper [40]. This last publication also dealt with the topic of interoperability that has been widely covered by us from a data-plane point of view. The previous results on interoperability have been accepted as an invited paper at OFC 2015 [31], and an invited JOCN paper in the same year [33].

Finally we would like to point out the importance of the experiments E20 and E21. In E20 we showed the first-ever field-trial transmission with a real-time BVT, where the modulation formats and the symbol rate can be switched based on the operator requests [44]. In the experiment E21, we are planning a field trial with Telecom Italia to show the first-ever

transmission in the field of high-order modulation-formats transmitted at high symbol-rates and with advanced FEC techniques.

Altogether we can state that Coriant has significantly benefited from the IDEALIST experience in terms of the acquired knowledge. Our next-generation products are being positively influenced, under different aspects, by the expertise we have acquired within IDEALIST. We have also had the opportunity to investigate and consider customer use-cases thanks to the direct interaction with the operators involved in the project. This has helped Coriant to position itself as a thought leader with respect to S-BVT and elastic optical networking, as has been proven by some of our most important experiments which have achieved industry-wide recognition. Finally, as for all the partners involved in the project, Coriant will be positively affected by the recent achievements in the standardization of flexible optical networks.

4.4 Control and management plane

The experimental activities conducted within the IDEALIST project focusing on the control and management planes have been large and exhaustive, fully dealing with the initial challenges and expectations devised at the beginning of the project. In this regard, the number of network scenarios, addressed problems, etc. in the flexgrid optical context where implementations of control-plane solutions are used, is significant and noticeable. This is appreciated through the pool of experiments where control plane functions are used to complete the targeted setup and experiment.

All the implemented control plane solutions used throughout the experiments, encompassing protocol extensions (e.g., GMPLS, SDN OpenFlow, PCEP, BGP-LS) and/or specific control architectures (e.g., hierarchical PCE for multi-domain service provisioning) were adopted from the activities performed in the WP3 context. That is, WP3 provided the framework in which specific control-plane solutions for targeted flexgrid optical problems were explored and discussed, and finally validated in the WP4 experiments. In this regard, the WP4 experiments have adopted WP3 control-plane solutions that are actually being considered as standard implementations within the IETF [51][52][53][54]. This allows us to state the high degree of feasibility of most of the experiments described here, with respect to the control-plane solutions and/or the support that the control-plane provides to other more data-plane oriented experiments.

As already mentioned, the spectrum of control-plane solutions assessed in the IDEALIST project experiments is widespread, covering a number of use-cases and the problems of flexgrid optical infrastructures. In this regard, an implementation of extended GMPLS RSVP-TE signaling and OSPF-TE routing protocols was validated to control the automatic and dynamic provisioning of flexgrid connections [6]. This involved extending the GMPLS control-plane for handling not only the network elements (BV-OXCs) configuration, but also for controlling S-BVTs when creating flexgrid optical super-channels. Similarly, control-plane extensions for GMPLS and PCE were done in [23] and [24], where the centralized SDN control via the enhanced OpenFlow-based protocol for flexgrid optical networks has also been covered. The utilization of both implemented flexgrid distributed GMPLS/PCE and centralized SDN-based control strategies has permitted us to assess the feasible solutions for a set of detected flexgrid network requirements/problems and scenarios. In an aggregated way, such experimental control-plane works covered the following topics: connection elasticity and defragmentation [27][28]; support of multiwavelength transmitter source configuration [25]; proactive restoration and connection adaptation [29]; and, connection re-optimization [18][9].

Special attention was required for the control plane experiments performed in the context of multi-domain service provisioning. To achieve this, it was necessary to integrate a number of control-plane implementations from different partners (i.e., TID, CNIT, TI, and CTTC) to validate the interoperability from a twofold perspective: end-to-end RSVP-TE signaling traversing multiple network domains controlled by different control-plane instances; and the path computation coordination via a hierarchical PCE approach using PCEP and BGP-LS protocols [32]. Last but not least, the IDEALIST control-plane solutions have also been considered (and achieved an important role) when validating the data-plane setups as reported in [10].

In the light of the conducted experiments, the IDEALIST control-plane assessments and validations provide a valuable set of solutions (including completely different control-plane paradigms) that third-party network operators and vendors may leverage when they are planning/designing their control-plane approaches for flexgrid network infrastructures and/or network systems and equipment.

4.5 Network and service interworking

The Adaptive Network Manager has been implemented as an ABNO architecture, which has been standardized within IEFT with the effort of the partners in the consortium. Most of the interfaces are defined in the architecture and they are used as a proof of concept in this project. Within D4.2, we claimed that there were some modules whose interfaces are not already defined. We proposed that HTTP/JSON interfaces were the most suitable implementation because of its reasons: easy development and flexibility for the workflows definition. Thanks to the work in the project, IDEALIST has contributed to the YANG models to support flexgrid scenarios.

To sum up, ANM implementation has demonstrated the most relevant use-cases defined in the project and achieved a high impact in terms of publications (conferences and journals), demonstrations, standardization and industrial transference. During the last year of the project, the activities have been focused on the collaboration between Cisco, Naudit and Telefonica. The tests validate that is feasible to have an ANM in operators networks and that the commercial solutions are closer.

4.6 Data Plane Interoperability

With regards to the data-plane interoperability, the work undertaken within IDEALIST has shown important results. Data-plane interoperability has been demonstrated between different vendors, research institutions, and universities, considering a list of parameters for interoperability as defined in WP2, T2.4.

For instance, CNIT/Ericsson achieved interoperability at the DSP level with Coriant, as mentioned in Section 3.15 [10]. A line rate of 1.28 Tb/s was successfully accomplished with 23% FEC-OH plus 5% framing OH. Thus, a total transmission capacity of ≥1250 km has been achieved for a single vendor solution. If the cross-vendor solution is adopted, with standard hard-decision (HD) FEC and blind DSP processing, the BER_{th} 1×10^{-2} can be considered, reducing the maximum distance to ~300 km. Therefore, the results show that if SD-FEC is standardized, interoperability may strongly improve performance (i.e. optical reach), achieving a similar performance to a single-vendor network. Indeed, proprietary SD-FEC used in the experiment has permitted us to increase the transmission distance with respect to the standard HD-FEC. For this reason, effort is required in the standardization of SD-FEC.

Interoperability between ALU and UNIVBRIS has been also demonstrated within IDEALIST, employing an elastic real-time BVT (designed in WP2, T2.3), which has enabled the transmission of a DP-QPSK signal with a bit-rate within the interval of 2-107 Gb/s. For the case ALU-to-UNIVBRIS, ALU's BVT transmitter was used as well as the DSP of UNIVBRIS at the receiver. Conversely, for the case UNIVBRIS-to-ALU, the S-BVT transmitter of UNIVBRIS was used and the DSP design of ALU. Both cases demonstrated successful back-to-back interoperability with a BER $<1\times10^{-6}$. In addition, a minimum penalty of <2 dB at the FEC level of 1×10^{-3} was observed between the two cases of interoperability, showing the effectiveness of interoperability between different elastic S-BVTs. Furthermore, ALU-to-UNIVBRIS interoperability has been verified for transmission over 175 km of SSMF and two AoD-based nodes [10]. Thus, this interoperability experiment showed the possibility of achieving interoperability in real-time, which was only possible to demonstrate within the IDEALIST framework, due to this type of BVT being available for the demonstration.

In addition to the data-plane interoperability demonstrations, the control-plane demonstration has been undertaken in parallel, as mentioned in the previous section. This means that results from WP3 within IDEALIST were also verified in combination with the results of WP2 and WP4, as well as applying the use-cases studied and proposed in WP1.

Finally, it is important to mention here that these interoperability demonstrations were only possible with the joint work of several partners in the IDEALIST project and the mobility of a significant amount of equipment. Nevertheless, these interactions between the project members have proved beneficial, since the obtained results were accepted at the ECOC'15 conference as a post-deadline paper, and an extension of the results has been documented and submitted as an IEEE journal paper.